T.C.
İSTANBUL UNIVERSITY
INSTITUTE OF GRADUATE STUDIES
IN SCIENCE AND ENGINEERING

Ph.D. THESIS

DETECTION OF SOME NEUROLOGICAL DISORDERS VIA SYNCHRONIZATION ANALYSIS OF ELECTROPHYSIOLOGICAL SIGNALS

Mehmet Akif ÖZÇOBAN

Department of Biomedical Engineering

Biomedical Engineering Programme

SUPERVISOR
Prof. Dr. Aydın AKAN

April, 2018

İSTANBUL

This study was accepted on 27/4/2018 as a Ph. D. thesis in Department of Biomedical Engineering, Biomedical Engineering Programme by the following Committee.

Examining Committee Members

Prof. Dr. Aydın AKAN(Supervisor)
İstanbul University
Faculty of Engineering

Prof. Dr. Mukden UĞUR
Istanbul University
Faculty of Engineering

Assoc. Prof. Dr. Oğuz TAN
Üsküdar University
Faculty of Humanities and Social Sciences

Prof. Dr. Osman Nuri UÇAN
Altınbaş University
School of Engineering and Natural Sciences

Prof. Dr. Mahmut ÜN
Yeni Yüzyıl University
Faculty of Engineering and Architecture

As required by the 9/2 and 22/2 articles of the Graduate Education Regulation which was published in the Official Gazette on 20.04.2016, this graduate thesis is reported as in accordance with criteria determined by the Institute of Graduate Sttudies in Science and Engineering by using the plagiarism software to which İstanbul University is a subscriber.

FOREWORD

I would like to thank to my thesis supervisor Prof.Dr. Aydın AKAN for his support, interest and grants. I have been honoured to work with him and I have learned a lot of from his academic researches and scientific perspective.

I would like to thank Prof.Dr. Thomas KOENIG who is from Bern Psychiatry University and Assoc.Prof.Dr. Michael X COHEN who is from Donders Institute for their scientific reviews.

I also thank my friends Sebahattin BABUR, MSc., Seda MÜFTÜOĞLU, MSc. for their tolerance, patience, support and respect. I would also to thank my family for their supports.

April 2018 Mehmet Akif ÖZÇOBAN

TABLE OF CONTENTS

Page

LIST OF FIGURES

Page

LIST OF TABLES

Page

LIST OF SYMBOLS AND ABBREVIATIONS

Symbol	Explanation
A	: Amplitude
$E_{1(f)}$	: First eigenvalue for ‘f’frequency point
$E_{2(f)}$	: Second eigenvalue for ‘f’frequency point
f	: Frequency
f(x)	: Discriminating function
GFS(f)	: Global Field Synchronization value in ‘f’frequency point
Hz	: Hertz
$ITPC_{(tf)}$	: Intertrial Phase Clustering value for ‘t’ time and ‘f’ frequency
n	: Number of points in vector x
t	: Time
θ	: Phase angle offset
s	: Standart deviation

Abbreviation	Explanation
AD	: Alzheimer Disease
AUC	: Area Under Curve
BAI	: Beck Anxiety Inventory
CNS	: Central Nervous System
CMW	: Complex Morlet Wavelet
CVM	: Cross Validation Method
DC	: Direct current
DFT	: Discrete Fourier Transform
DTFT	: Direct Time Fourier Transform
DVM	: Destek Vektör Makinaları
EEG	: Electroencephalogram
EOG	: Electroencephalogram
FA	: Fractional Anisotropy
FFT	: Fourier Fourier Transform

fMRI	: Functional Magnetic Resonance Imaging
GAS	: Global Alan Senkronizasyonu
HC	: Healthy Control
HDRS-17	: Hamilton Depression Rating Scale
ITPC	: Intertrial Phase Clustering
MCI	: Mild Cognitive Impairment
MR	: Magnetic Resonance
OKB	: Obsesif Kompulsif Bozukluklar
OCD	: Obsessive Compulsive Disorders
PCA	: Principal Component Analysis
PET	: Positron Emission Tomography
ROC	: Receiver Operating Characteristic Curve
SPECT	: Single Photon Emission Computer Tomography
SVM	: Support Vector Machine
Y-BOCs	: Yale-Brown Obsessive Compulsive Scale
TTM	:Trichotillomania

ÖZET

DOKTORA TEZİ

ELEKTROFİZYOLOJİK SİNYALLERİN SENKRONİZASYON ANALİZİ İLE BAZI NÖROLOJİK BOZUKLUKLARIN TESPİTİ

Mehmet Akif ÖZÇOBAN

İstanbul Üniversitesi

Fen Bilimleri Enstitüsü

Biyomedikal Mühendisliği Anabilim Dalı

Danışman: Prof. Dr. Aydın AKAN

Bu tez çalışmasında, Obsesif Kompulsif Bozuklukların (OKB) beyin yapıları, ağları ve fonksiyonel bağlılık üzerindeki etkileri incelenmiştir. 37 adet ilaç tedavisi görmemiş OKB hastası ve 27 adet sağlıklı gönüllüden kaydedilen EEG datasına ait senkronizasyon gücü, Global Alan Senkronizasyonu (GAS) yöntemi ve Bölütlerarası Faz Kümeleme (BAFK) yöntemi ile hesaplanmıştır. GAS yöntemi, bütün kanallar arasındaki senkronizasyon değerini hesaplarken, BAFK yöntemi, her bir kanal için kısa zamansal parçalara bölünmüş data bölütleri arasındaki bu değeri hesaplayabilmek için kullanılmaktadır. Frontal lob için yapılan GAS analizi sonucunda OKB datalarında, delta bandında ($p<0.001$) ve beta-3 bandında ($p<0.013$), bütün kanallar için yapılan analizde ise delta bandında ($p<0.001$), beta-2 bandında ($p<0.0015$) anlamlı senkronizasyon kaybı tespit edilmiştir. BAFK analizleri sonucunda ise O1 kanalı beta-2 bandı ve T6 kanalı teta bandı haricinde bütün kanallarda ve bütün EEG bantlarında OKB datalarında senkronizasyon düşüşü gözlenmiştir. Sonuçlar Destek Vektör Makinaları (DVM) yöntemi ile sınıflandırılmış ve %85'in üzerinde başarılı doğruluk skorları elde edilmiştir. Bu sonuçlara göre OKB'nin senkronizasyon kaybına, fonksiyonel bağlılıkta düşüşe ve bazı bilişsel fonksiyonlarda bozukluğa neden olduğu tespit edilmiştir.

Nisan 2018, 118 sayfa.

Anahtar kelimeler: EEG, Obsesif Kompulsif Bozukluklar (OKB), Faz Senkronizasyonu

SUMMARY

Ph.D. THESIS

DETECTION OF SOME NEUROLOGICAL DISORDERS VIA SYNCHRONIZATION ANALYSIS OF ELECTROPHYSIOLOGICAL SIGNALS

Mehmet Akif ÖZÇOBAN

İstanbul University

Institute of Graduate Studies in Science and Engineering

Department of Biomedical Engineering

Supervisor: Prof. Dr. Aydın AKAN

In this thesis, Obsessive-Compulsive Disorders' (OCD) effects on brain structures, networks and functional connectivity, were examined. Synchronization power of EEG data were recorded from 37 drug naïve OCD patients and 27 healthy volunteers, were computed by Global Field Synchronization (GFS) method and Intertrial Phase Clustering (ITPC) method. GFS method computes the synchronization value between all channels and ITPC method calculates the value between data epochs that were created as shorter temporal parts for each channel. Significantly loss of synchronization was detected in delta band ($p<0.001$) and beta-3 band ($p<0.013$) for results of GFS analysis for Frontal lobe and in delta band ($p<0.001$), beta-2 band ($p<0.0015$) analysis for all channels. Decreased synchronization was observed in all channels and all bands -only except O1 channel in beta-2 band and T6 channel theta band- as a result of ITPC analysis. Results were classified by Support Vector Machine (SVM) method and successful accuracy scores of over 85% were obtained. According to these results, it is detected that OCD causes loss of synchronization, decreased functional connectivity, and impairment in some cognitive functions.

April 2018, 118 pages.

Keywords: EEG, Obsessive Compulsive Disorders (OCD), Phase Synchronization

1. INTRODUCTION

1.1. STATEMENT AND MOTIVATION OF THE THESIS

Obsessive-compulsive disorders (OCD) is a neuropsychiatric disease defined by repetitive, intrusive disturbing thoughts and mental acts and behaviours that are triggered by these thoughts (Abramowitz et al., 2009). In clinical practice, the Electroencephalogram (EEG) methods such as synchronization, complexity analysis etc., is used only for exclusion of the comorbid disease (for instance depression with OCD), which may cause obsessive compulsive symptoms (First and Gibbon, 2004). In diagnostic or therapeutic use of EEG methods is very limited. Diagnosis of OCD is based on neuropsychological tests such as Yale-Brown Obsessive-Compulsive Scale (YBOCs), Hamilton Depression Rating Scale (HDRS-17), Beck Anxiety Inventory (BAI). One of the methods of diagnosing neuropsychiatric diseases using objective criteria is to use the EEG technique. EEG is more advantageous method than expensive and huge neuroimaging methods. EEG provides real-time monitoring, high temporal resolution, precision so that usage of EEG in clinical purpose, will provide objective physiological criteria or biological test, clinical assessment with neuropsychiatric scales are used for diagnosing and tracking level of treatment (Cohen, 2014, Cohen, 2017). This is a major inspiration factor of this study.

Our study was shown that Global Field Synchronization Analysis (GFS) and Intertrial Phase Clustering (ITPC) values may be used as biomarker for OCD and it can be used also for monitoring course of disease and treatment. Phase based synchronization studies is shown that synchronization power is important marker for diagnosis of several neuropsychiatric diseases (Koenig et al., 2001). Furthermore, the results of one of our other study will be published in this year, was found correlation between GFS result and OCD clinical rating scores (Özçoban et al., 2017a). These results indicate that GFS can be a clinically useful and important method for diagnosis of OCD and other disorders comorbid with OCD.

1.2. OBJECTIVES

The main goal of this thesis is examining the OCD effects on brain functions, structures, networks and functional connectivity using measuring phase synchronization level. For this purpose, phase synchronization values of EEG data belong two group (OCD patients and healthy controls (HCs)) afterwards compared with each other. The objectives of the study are causes and responses to following subjects:

- How OCD effects on brain structures?
- Are there any differences between OCD data and HCs data in terms of phase synchronization power?
- Which brain networks are affected by OCD?
- How OCD influences functional connectivity?
- Does OCD cause dysfunction in cognitive functions?
- Is it possible to design a classification system for auto-detection of OCD?
- Is there any difference between GFS and ITPC methods in terms of estimating phase synchrony?

1.3. OBSESSIVE COMPULSIVE DISORDERS AND LITERATURE REVIEW

OCD is described by presence of obsessions, compulsions or most common both of two. Distinctive features of obsessions are; recurrent, intrusive, unwanted ideas, images, impulses, doubts that cause worries and fears. Most common obsessions are: fear of damaging someone, religious worries, sexual thoughts, worry about getting an infection. Compulsions are characterized as recurrent behaviours and mental acts that stimulated by the obsessions and affected individual feels obliged to do. Major compulsive rituals are checking electrical sockets, excessive hand washing, symmetrically ordering goods etc. (Abramowitz et al., 2009, Heyman et al., 2006, Association, 2013).

There are several investigations and hypothesis on neurochemical and genetic origin of the OCD. Investigation on neurochemical mechanism of the OCD, was found out impairment in 5HTT gene that responsible for serotonin transportation and dysfunction

in 5HT2A gene that regulate serotonin receptor (Greenberg et al., 1998). In addition to dysfunction in serotonin production mechanism, some researcher was claim that impairment in glutamate system also effective in OCD (Jefferson et al., 1995).

Neuropathological researches in OCD was detected dysfunction in some brain regions such as caudate nucleus, frontal orbito-striatal area, dorsolateral prefrontal cortex (Rauch and Jenike, 1993, Whiteside et al., 2004), and also evidence has shown white matter abnormalities in frontal site in individuals with OCD. Similar findings about functional abnormality have been reported for brain networks and pathways such as orbito-frontal subcortical circuitry (Saxena and Rauch, 2000), cortico-striato-thalamic circuit (Saxena et al., 2003).

1.4. LITERATURE REVIEW OF METHODS

GFS is a novel method that can compute phase synchronization of whole brain. It can also compute synchronization between multi-channel time series. The method first used for discriminating the schizophrenia patients from HCs. Decreased synchronization and functional dysconnectivity of EEG theta frequency was found. This result was interpreted as memory dysfunction (König et al., 2001). Some studies showed that reduced GFS values for Alzheimer Disease (AD) and negatively correlated with degree of Mild Cognitive Impairment (MCI) (Koenig et al., 2005, Dauwels et al., 2010). Correlation between severity of AD and GFS values were researched and this analysis results suggested that GFS values can be used as biological correlate of cognitive decline in AD patients (Park et al., 2008). GFS also used for researching anaesthetic administration. Decreased phase coupling values was detected with GFS and in Gamma band. This means that GFS is useful tool for anaesthetic administration (Nicolaou and Georgiou, 2013). The method was used for examining sleep stages and high GFS values was detected in NREM and REM sleep. This finding is related to thalamic activity (Achermann et al., 2016). GFS recently used for predicting cognitive impairment and early diagnosing biomarker for AD (Smailovic et al., 2018).

In the literature, the ITPC method may also referred as “phase locking value”, “phase resetting”, “phase coherence”, “cross-trial” instead of “Intertrial”. “Intertrial Phase Clustering” terms were used in thesis because this description of analysis. The method was used in several field for instance; detecting error-related activity in medial prefrontal

cortex (mPFC). Theta phase synchronization between the electrodes which located on mPFC and lateral prefrontal cortex (IPFC) give information about error-related activity (Cavanagh et al., 2009). In a study, the method was used for detecting HFOs that overlapping on N20 wave (Valencia et al., 2006). Autism Spectrum Disorder (ASD) was investigated by the method. A task was used for compared ASD patients and IQ matched controls. It was concluded that processes underlying decision-making and reinforcement learning may be atypical and less efficient in ASD (van Noordt et al., 2017). The method also was used for relationship between Parkinson disease that was suffered by basal ganglia disease and mechanism that was defined large scale interactions between cortical area involves synchronization among phase and amplitude of different rhythms. It was concluded that M1 local field potentials could be used as a control signal for basal ganglia stimulation (De Hemptinne et al., 2013).

2. MATERIALS AND METHODS

This chapter gives background information on the OCD that we are concerned in this thesis. The proposed method involves the detection of OCD by the analysis of EEG signals. Hence, a brief introduction is given on the physiology of the brain and the electrical activity recorded from the brain called EEG signals. We also give data collection method, details about the participants, experiments and procedures used in our research. Experimental procedure, affective stimuli and measurement system used to investigate the physiological and electrophysiological parameters between patients and control subjects are detailed and further explained. This chapter describes the physiological signals that were recorded and analysed.

2.1. BACKGROUND KNOWLEDGE RELATED TO OCD AND EEG SIGNALS

2.1.1. Brain

Brain is a most important and large component of Central Nervous System (CNS) execute and control most of the physiological processes. The brain has two cell types such as neurons and glial. Glial cells play important role for supporting neurons. The glial term was originated from ancient Greek word ‘glue’. This gives information about function of glial that protect unite structure of neurons. The neurons manage, motor endocrine, cognitive functions etc. specialized by location. Main sites and important regions were mentioned following subsection (Bear et al., 2007).

2.1.2. Brain Structures and Their Functions

The cerebrum is the largest primary component of brain. Cerebrum manages the motor functions, cognitive and emotional processes with help of the spine. Cerebrum has four important as details is given in following section.

- **Frontal Lobe:** Frontal lobe is in under forehead region. This site executes motor functions, mental activity (thoughts, decision making) and speech. Motor cortex region is limited with area of frontal lobe. This lobe is signed as number two in Figure 2.1.

- **Parietal Lobe:** Parietal lobe is in top of the back brain and under the parietal bone of skull. This lobe executes processes related somatic sensory system. This lobe is signed as number three in Figure 2.1.

- **Temporal Lobe:** Primary auditory cortex placed in this lobe. This lobe also responsible for perception and memory systems. Damaging of this lobe can likely result is auditorily, and emotional (fear, aggression) dysfunctions. This lobe is signed as number one in Figure 2.1.

- **Occipital Lobe:** Occipital lobe is the smallest lobe of the four lobes and is located at the rear of skull. It executes visual perception system. All the visual stimulus and images are detected by optic nerves and pass through occipital area for evaluation and associating with images seen before. Impairment of occipital lobes can cause visual problems. This lobe is signed as number four in Figure 2.1 (Waxman, 2010).

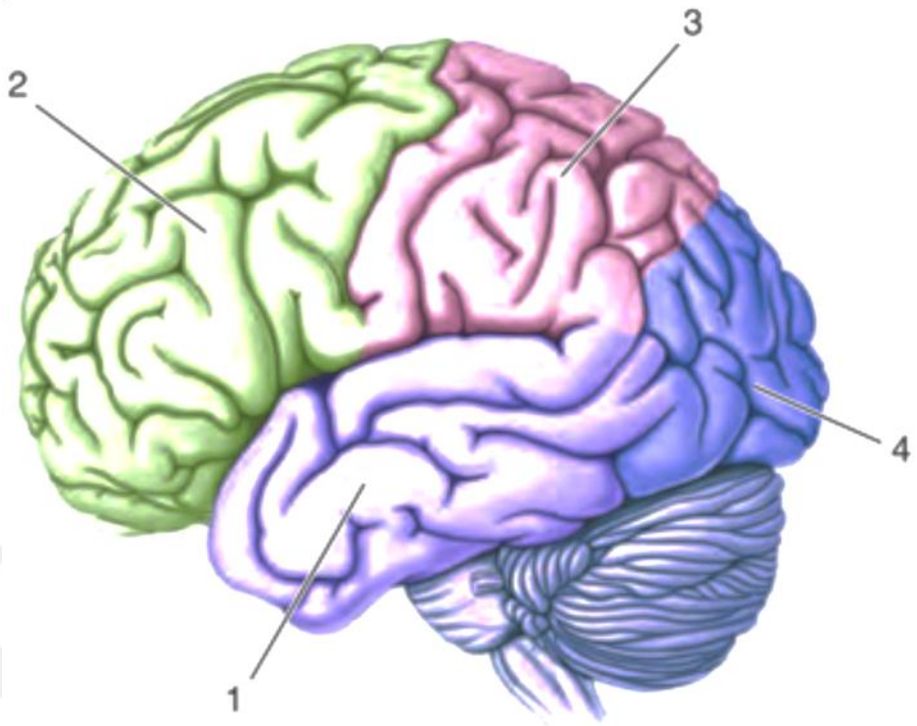

Figure 2.1: Cerebral Lobes [1.]

- **Basal Ganglia:** The basal ganglia contain 4 subcomponents, these are; caudate nucleus, putamen, globus pallidus and subthalamic nucleus. It has several pathways with other brain structures (cerebral cortex, thalamus, brain stem etc.). Some of them are related to motor functions but most of them are related to memorial and cognitive functions (Bear et al., 2007).

- **Orbito-Fronto-Striatal Networks:** The Orbito-Fronto-Striatal Networks (OFSN) are specialized pathways that connect between frontal cortex and basal ganglia (Alexander et al., 1986). OFSN plays important role for emotional and motivational functions (Rolls, 2004, Elliott and Deakin, 2005). Neurological investigations suggested that dysfunctions anywhere in OFNS pathways causes in cognitive functions that learning and decision making (Jones and Mishkin, 1972, Rolls et al., 1994, Clark et al., 2004, Elliott and Deakin, 2005). There were

[1] https://www.slideshare.net/ananthatiger/cerebrum

evidence for supporting OCD causes lesions on cortico-striato-thalamic- networks involving OFSN (Menzies et al., 2008).

2.1.3. EEG

Electrical oscillation records enrolled from scalp show that brain has a continuously and nonlinear electrical activity. This activity is originated by synchronously firing millions of neurons cell (typically for EEG these neurons are cortical pyramid cells) in the brain and named as electroencephalography (EEG). EEG has provided important information about neurophysiological situation of brain. Amplitudes of EEG range between 0-200 μV whereas it is oscillated between 0,5-50 Hz frequencies. Several brain disorders and neural functional dysfunctions brain are detected by examination of EEG signals.

Ag-Ag/Cl electrodes are placed on scalp in accordance with international 10-20 system as shown in Figure 2.2.

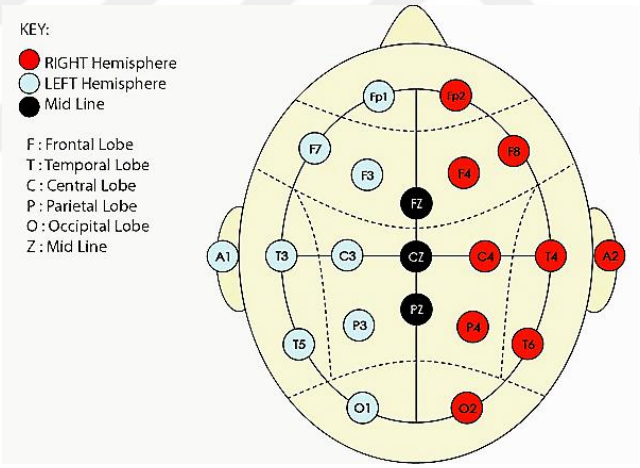

Figure 2.2: Electrode placement in accordance with international 10-20 system[2].

The system is named international 10-20 system because of distance of electrodes 10 percent and 20 percent of inion (neck junction with skull) to nasion (nose junction with eye) distance respectively. In clinical research, usually 8-32 electrode is used. The electrodes are named as channels for EEG system. Signals is obtained by the channels

[2] https://cogsci.stackexchange.com/questions/1553/do-the-jungian-cognitive-functions-processes-really-exist

amplified using amplifier unit located in EEG device. Noise signals that originated from artefact should be filtered.

There are 4 reference setting method for international 10-20 system. These are following next.

- **Sequential montage:** Reference is determined as each channel is differentiated by adjacent channel. For instance, O1-O2 channel represent as voltage difference between both channels.

- **Referential montage:** Usually the ear lobe is selected as the reference point.

- **Average reference montage:** The average of all channels is used as a reference for each channel.

- **Laplacian montage:** One of the channel determined as a reference point according to the weighted average of the channels.

There are five major brain waves oscillate during executive brain functions and cognitive processes. These frequency bands as mentioned below:

Delta Waves (<4 Hertz (Hz)): Delta band primarily associated with deep sleep mode, babies and seriously brain injury. Neuroimaging studies found that delta waves activity was maximum in medial prefrontal cortex and orbitofrontal cortex (Alper et al., 1998, Menzies et al., 2008). According to source localization investigations, EEG activity, potential source of the delta is many subcortical regions such as the common brainstem system (Lambertz and Langhorst, 1998), ventral pallidum (Lavin and Grace, 1996), brain reward system (Nucleus accumbens, medial forebrain bundle, ventral tegmental area) (Lotte, 2008). Delta waves are given as an example in Figure 2.3 (Lotte, 2008).

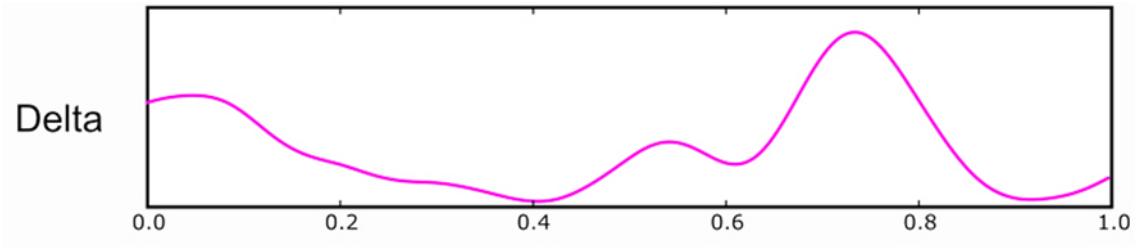

Figure 2.3: Delta waves oscillations.

Theta Waves (4-7 Hz): Generally observed in children's temporal and parietal region and in case of disappointment in adults. Sometimes theta waves emerged in degeneration of brain. Recent investigations on source localization of theta waves indicated that there were several theta oscillation generators more than one in brain. These generation place are limbic (Knyazev, 2012) system, hippocampus (Siapas et al., 2005, Jensen, 2005), midline prefrontal cortex (Hayashi et al., 1987, Mizuki et al., 1980). Theta waves are given as an example in Figure 2.4 (Lotte, 2008).

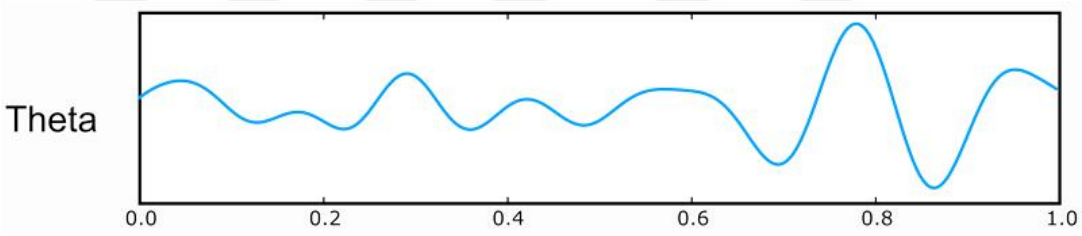

Figure 2.4: Theta waves oscillations.

Alpha Waves (8-13 Hz): Alpha waves usually was visualized in adults that when awake and in a resting state. It is mostly appeared in occipital region but also appear in frontal and parietal region. Several alpha source localization studies demonstrated that alpha oscillations were generated by thalamocortical neurons (Da Silva et al., 1980, Hughes et al., 2004, Lőrincz et al., 2009). Alpha waves are given as an example in Figure 2.5 (Lotte, 2008).

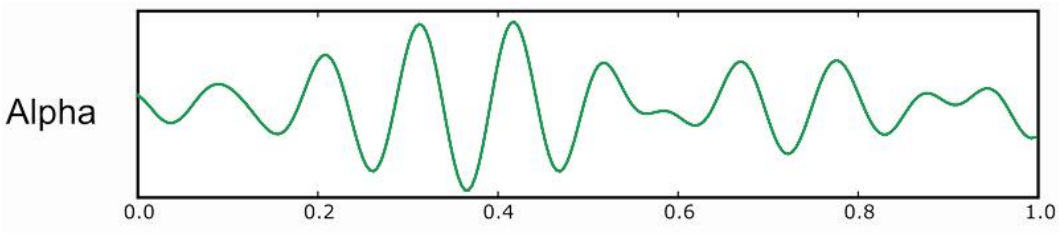

Figure 2.5: Alpha waves oscillations.

Beta Waves (14-30 Hz): Beta oscillations are mostly oscillated in especially parietal and frontal part of cortex. It would be emerged during mental activations. Beta waves are given as an example in Figure 2.6 (Lotte, 2008).

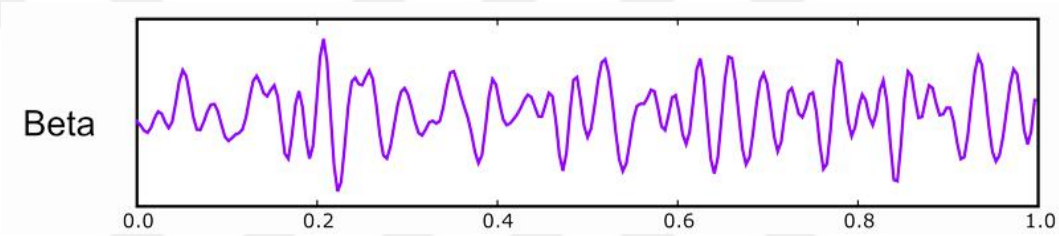

Figure 2.6: Beta waves oscillations.

Gamma Waves (30-80 Hz): Even if power of gamma waves is very low, their oscillations are limited. This wave would be used for verification of brain disorders. The origin of increased EEG frequencies are placed in the frontocentral area (Molina et al., 2003). Gamma waves are given as an example in Figure 2.7 (Lotte, 2008).

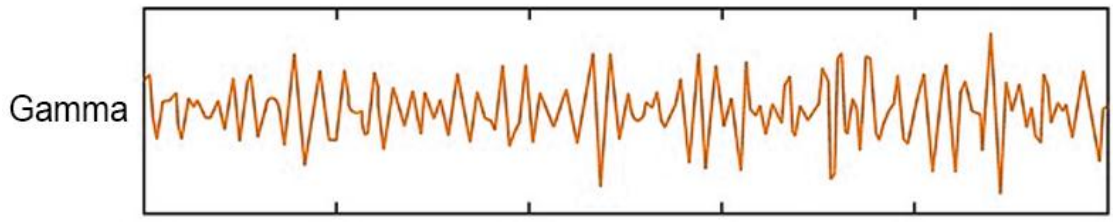

Figure 2.7: Gamma waves oscillations.

2.2. DATA COLLECTION AND PARTICIPANTS

Thirty-seven patients (18 female and 19 male) with OCD and twenty-seven (14 female and 13 male) age and gender matched HCs participated in this study.

The Clinical characteristics and symptom severity scores of the volunteers with OCD in the study are shown in Table 2.1.

Table 2.1: The demographic and clinical characteristics of the patients. (F: female, M: male, o: obsession, c: compulsion, s: score, d1 refer the duration from the appearance of initial symptoms in years and d2 refer the obvious symptoms in months.

Sex	Age	os	cs	Y-BOCs	H-17	BAI	d1	d2
F	26	11	12	23	5	5	2	12
M	28	12	13	25	9	10	5	10
F	28	15	18	23	26	22	5	8
M	42	6	8	14	9	11	2	11
M	48	9	15	24	10	20	18	1
M	23	11	12	23	14	11	5	24
F	22	13	2	15	19	18	11	8
M	29	14	2	16	8	11	11	36
F	31	9	6	15	20	18	6	12
M	22	7	5	12	20	27	2	6
F	33	8	1	14	22	10	15	72
F	28	11	5	16	10	15	2	6
F	24	9	10	19	14	17	11	20
M	28	10	11	21	10	10	12	10
M	23	11	12	23	14	11	5	24
F	32	12	14	34	22	32	4	32
F	32	9	9	18	17	33	16	18
M	27	12	13	26	22	24	7	12
F	33	18	12	30	24	21	5	6
F	32	8	14	16	23	38	8	9
M	29	6	9	25	34	49	9	7
F	21	18	11	29	21	16	3	3
M	19	6	11	17	3	3	2	12
M	40	8	14	22	6	28	8	4
F	34	11	13	24	14	8	10	9
M	21	5	5	10	10	33	6	2
M	18	13	13	26	25	28	3	6
F	29	10	10	20	11	5	16	30
M	27	12	0	12	19	24	7	6
M	36	10	15	25	15	27	12	10
F	24	10	11	21	10	10	8	5
F	33	9	10	25	34	49	9	7
M	27	11	15	26	6	7	2	6
F	18	15	8	23	26	22	6	6
F	39	7	5	12	20	27	19	48
M	36	8	7	7	7	39	12	8
M	20	13	13	26	25	28	5	7

The EEG data were enrolled from voluntary patients and age matched healthy controls at the Uskudar University Neuropsychiatry Health Practice and Research Centre. All the volunteers had been informed about examination processes by neuropsychiatrist physician. Informative form of written consent was signed by all the participants. Helsinki Declaration the ethical principles for medical research involving human subjects, were obeyed, and the thesis research protocol was approved by Uskudar University Clinical Research Ethics Committee.

The neuropsychiatric diagnostic tools used for diagnosis of OCD were the Diagnostic and Statistical Manuel of Mental Disorder (Millon and Davis, 1996), the Y-BOCs is a clinical rating scale consist 10 test items. It is used for determining symptom severity of OCD. Each item has 0 (any symptom) to 4 (extreme symptom) points value. Sum of the total point is with the severity range of 0-40. First five items are related to obsessions and others are using for determining compulsion severity (Goodman et al., 1989). The 17 item HDRS-17 (also known as the Ham-D) is a clinical depression assessment scale, consists of 17 items with Likert scale of either 0 to 4 or 0 to 2. Sum of the point range 0 through 54 (Williams, 1988). HDRS can also detect cognitive deficits, and the BAI score (Beck et al., 1988).

In controls, the inclusion criteria are:

- Non-smoking
- Right-hand use,
- Lacking a history of epilepsy and stroke,
- Not to use medication.

Patients exclusion criteria:

- History of traumatic head injury and brain operation,
- Left-handedness,
- Neurological and bipolar disorders,

- Alcoholics,

- Being medical treated for a while.

2.3. EEG MEASUREMENT PROCEDURE

EEG series were recorded from participants via a Neuroscan Synamps II (Neuroscan Products, Compumedics, USA) recording system including a quick cap in accordance with the international 10-20 electrode placement. The recording room was light controlled and sound attenuated. EEG data were sampled at a frequency of 250 Hz. The analogue-to-digital converter was 16-bit. The impedance values of the Ag/AgCl surface electrodes were maintained at less than 5 kΩ. To remove artefacts originated from eye blinks (EOG signals) or body movements, values were rejected with levels of 50 μVolt peak-to-peak. Both vertical and horizontal bipolar EOG signals were measured by using electrodes, which were placed inferior to the right eye and to the left and right outer acanthi of the eyes. A band pass filter (0.5-70 Hz) was applied to raw data in Scan Edit 4.3 software. Power-line interference of 50 Hz was suppressed by a Notch filter. Finally, muscle artefacts were carefully eliminated by an expert technician.

2.4. TIME AND FREQUENCY DOMAIN ANALYSIS OF EEG

Main time-frequency decomposition techniques for electrophysiological signals is explained as subsections.

2.4.1. Spatial and Temporal Features of EEG

- **Temporal Resolution:** Refers to sampling frequency that was used while recording EEG signals. Usually, it is used among 250 and 1000Hz per second.

- **Temporal Precision:** It can be determined as the certitude of the computation results at each time point. Temporal resolution of EEG method is fairly high whereas temporal precision depends on the analysis and parameter.

- **Temporal Accuracy:** Refers to signals is generated by neurons, measuring real-time and instantaneously pass through to system without delay. Temporal accuracy of EEG is high.

- **Spatial resolution:** Refers to number of channels (electrodes) is used in EEG system and most of the researchers generally use at least 32 channel systems.

Spatial precision is low for EEG, but it can be improved using surface Laplacian or adaptive source space imaging technic filters.

Because of temporal resolution, precision and accuracy is very high, usage of EEG for brain imaging is very advantageous whereas spatial features of EEG lower than another signal processing device such as fMRI, MR etc. (Cohen, 2014). Effects of the parameters on results accuracy is illustrated in Figure 2.8 (Cohen, 2014).

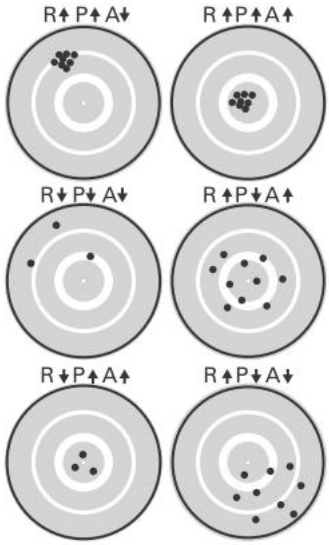

Figure 2.8: Resolution(R), Precision(P), Accuracy(A).

2.5. SIGNAL PROCESSING TECHNIQUES

Some signal processing methods, are used in the study for data analysis, have been discussed in this section. Whole spectral analysis methods were used to determine phase coupling or synchronization of neural oscillations based on acquiring of time varying frequency band features. Almost all of these techniques are based on a mathematical application called the convolution technique. The technique consists of two steps; the first dot product procedure and other is sliding along a kernel through signal. Dot product is the main process of the almost whole time-frequency decomposition analysis methods. The algebraic procedure of the dot product can be explained as multiplying each element in the two vectors point wise and then summing them up so to compute the dot product between two vectors as a number. This number gives information about relationship

between these vectors. One of this two signals are EEG data (time series) are called as time series signal (EEG data, brain image) other part of input signal called as kernel signal (filter, gaussian, wavelet). Kernel is always shorter than signal.

Convolution implementation is backbone of time-frequency domain analysis technics. Its implementation is simple; while the signal is constant position, kernel signal shifted flip forward with dot product processing repeatedly over time points on the time series signal on every step. Before the convolution, both sides of original signal, should be padded with zero as one minus than number of points than kernel. The reason for being 'minus one' is last point of kernel overlap on the first point of original signal. Produced signal that result of convolution onset before original signal and ends after the signal end. Due to this reason produced signal is longer than original signal. In order to remove this excess piece of signal, one half of point number of kernel is chopped than both side of produced signal.

2.5.1. Discrete Fourier Transform

Fourier transform is one of the most important signal processing technic and backbone of the time-frequency domain analysis methods. It has a very common usage area such as science, physics through engineering. Every signal in the nature can be expressed by the combination of some sinusoidal signals. If these sinusoidal waves would be found, several information can be obtained and in this way; chaotic, nonlinear signals can be more understandable and meaningful. In order to make this, sinusoidal waves (kernel) of different frequencies (it will be told later that how many frequencies and waves are needed) should be constructed and computed the complex dot product between signal in first step. The mathematical background of the Fourier transformation is based on complex sinusoidal signals because, execution of Fourier transformation depends on using a signal that consists of two parts; real and imaginary. Complex numbers can be displayed on 2D (two dimensional) polar notation as shown in Figure 2.9.

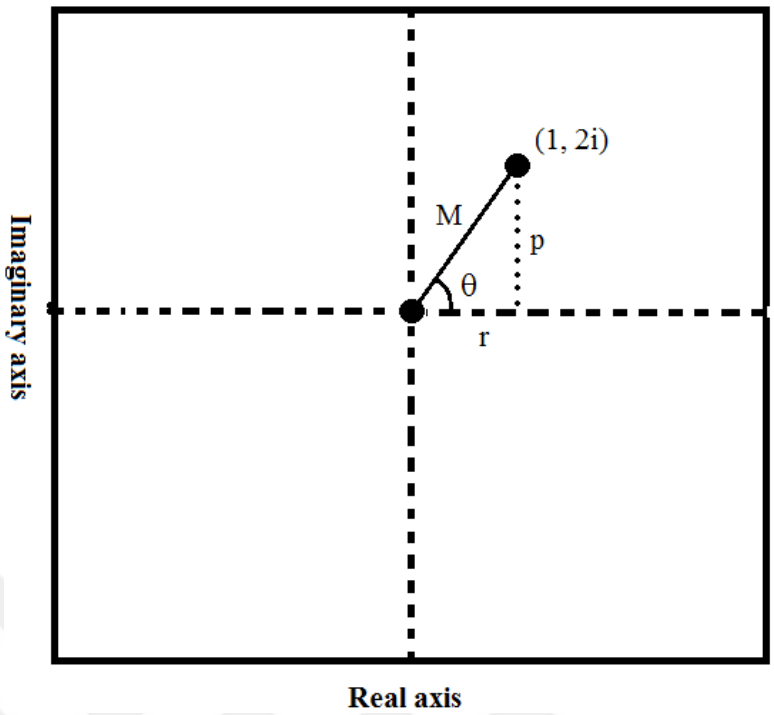

Figure 2.9: A complex number presentation on two dimensional cartesian coordinate system. This provide us information such as: the distance from origin (M), the projection onto the real axis (p), phase angle (θ).

This process also gives us three more pieces of information about signal. Length of vector (magnitude of complex number) was represented by '*M*' provides information about amplitude and power. It can be computed as equation 2.1.

$$M = \sqrt{r^2 + p^2} \tag{2.1}$$

Angle between vector (it is represented by 'θ') and positive real axis ensure phase angle of the signal and projection on real axes gives us some information about time-frequency decomposition. The phase angle can be calculated as equation 2.2.

$$\theta = tan^{-1}\left[\frac{p}{r}\right] \tag{2.2}$$

The phase angle information has been used for getting useful information about such as synchronization value, phase coupling between different brain sites or EEG epochs, functional connectivity among brain structures.

The complex numerical values were obtained as a result of this process, are called Fourier coefficients. The total number of sinusoidal waves to be generated, is determined by the number of data points in the original signal (EEG epoch). The fundamental of Fourier transform mechanism was illustrated as Figure 2.10.

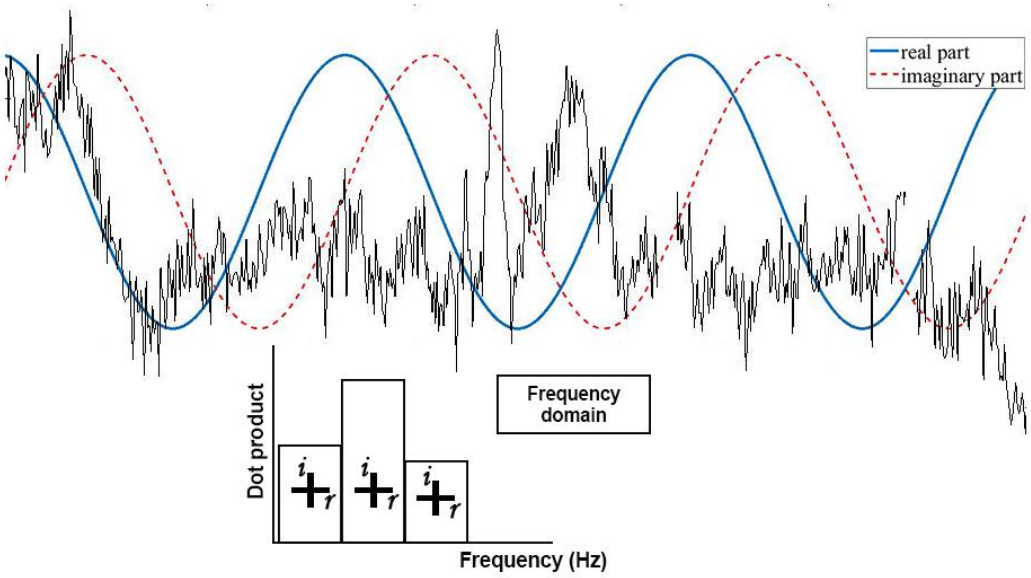

Figure 2.10: Mechanism of Fourier transform.

The Euler formula is used to generate complex sinusoidal waves because all complex waves are three dimensional and contains of 3 different information such as time, real part and imaginary part. The Discrete Fourier Transforms (DFT) of signal '*x(n)'* at frequency 'f_k', can be obtained as follows:

$$X(k) = \sum_{k=0}^{N-1} x(n) e^{-i2\pi fkn/N} \qquad (2.3)$$

where '*N'* is the number of points in signal '*x(n)', 'X(k)'* is the Fourier coefficients computed for normalized frequency sample '$f_k=k/N$' and '$f_k=F_k/F_s$' where 'F_k' is the linear frequency in Hz, and 'F_s' is the sampling frequency used to discretize the signal '*x(n)'* by taking samples from a continuous-time signal '*x(t)'*.

Frequency information of data in Hz can be found using these coefficients after computing the Fourier coefficients. For this purpose, minimum and maximum frequency

points should be determined. Since the frequency in Hz is determined as the number of cycles in a second, minimum frequency occurs in infinite length of time. When this result is fitted to a finite scale, this scale is like linear number line. Fourier transform always starts from zero because the DC component. The Nyquist criterion is used for the computing maximum frequency point. Since a sine wave is always alternate between positive and negative values, it is necessary to take at least two samples from each cycle to digitize an analog sinusoidal wave properly. This means that two points per cycle equivalent to one half of sampling rate of EEG device. Number of frequency steps between the minimum and maximum values also called frequency resolution, depends on the number of total time points of the data. The '*N*' is referring to number of times in the data, '*N/2*' is number of sinusoidal waves that need to be generated for measurement and '+1' is for DC component (mean offset value) (Smith, 1997). The linear number line for computing frequency resolution of Fourier transform is illustrated as Figure 2.11.

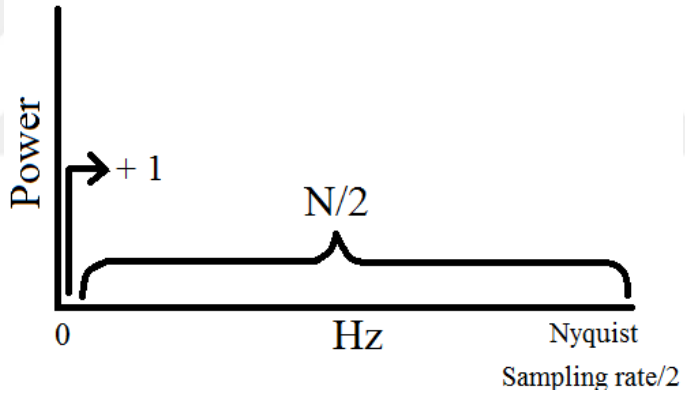

Figure 2.11: Fourier coefficients range from '0' Hz. to the Nyquist frequency.

2.5.2. Fast Fourier Transform and Zero Padding

FFT (Fast Fourier Transform), is an implementation that uses the same algorithm as DFT, but it is faster, more efficient, more elegant and can remove some redundancies. DFT has very much time-consuming procedure so it can be take hours or days. The FFT has developed for accelerating this procedure. There is so many algorithms for computing FFT. Most of them based on construction many sinusoidal in a matrix instead of creating them in a loop.

FFT can be implemented with using '*fft'* function in MATLAB. The function uses three parameters for accurately computing. The first is original data, second is number of result elements, third input determines the number of dimensions were used for analysis.

The frequency resolution of the FFT results is determined by number of data points. It is necessary adding points in data to increase frequency resolution, but the signal might not have any more data. This problem can be resolved with padding zeros on the edge of the signal. This process is called as '*zero padding'* and can be performed with using "*fft"* function in MATLAB software. The Zero padding provides smoother transitions between frequency components with a similar effect on the interpolation process. Zero padding effects on frequency resolution is showed as Figure 2.12.

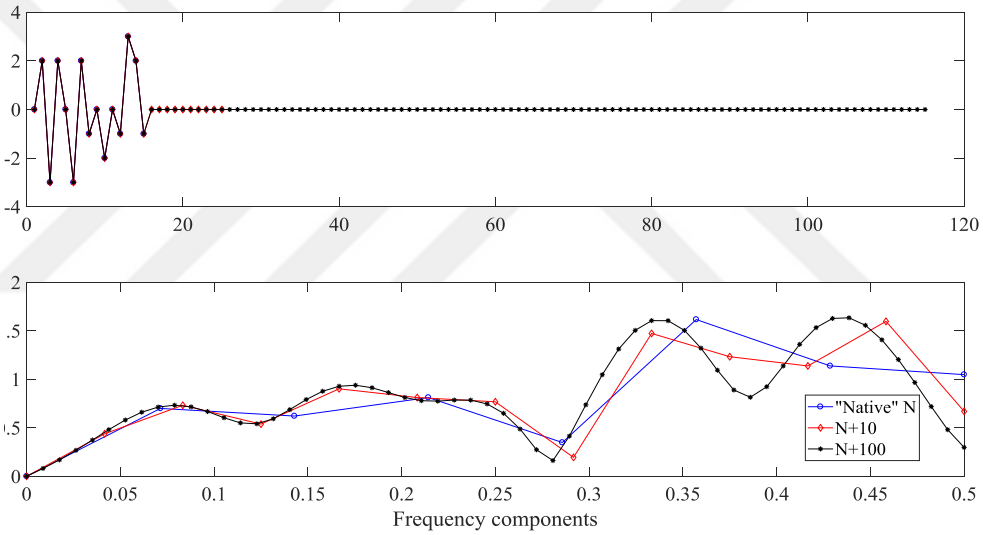

Figure 2.12: Effects of zero padding process on frequency resolution.

2.5.3. Inverse Fast Fourier Transform

Fourier transform is based on obtaining frequency domain from time series. Because there is not any reduction in data the Fourier transform is invertible process. It is possible to get time series from frequency domain. This procedure is called as Inverse Fast Fourier transform (IFFT). Fourier coefficients to scale the sine waves and the sum of scaled sine waves is the time domain.

2.5.4. Frequency Domain Convolution

Convolution in time domain briefly summarized in previous subsections but convolution in frequency domain also very important process. Frequency component of signal and kernel are pointwise multiply and after that Inverse IFFT in applied on results of multiplication. It is yields identical results of time domain convolution. Comparison between time domain convolution and frequency domain convolution are illustrated as Figure 2.13 (Cohen 2014).

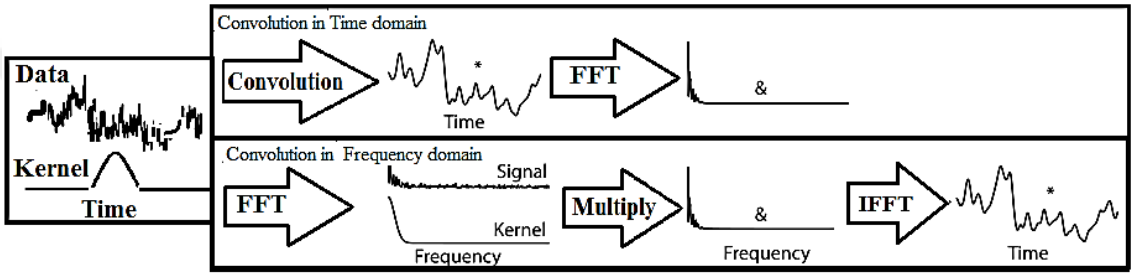

Figure 2.13: Comparison frequency domain convolution and time domain convolution.

2.5.5. Morlet Wavelet and Wavelet Convolution

One of the most important signal processing technic for time-frequency domain analysis is morlet wavelet convolution method. The method can produce successful results on some limitations of the Fourier Transform method. EEG signals are only stationarity in very short time but FFT's assumptions of stationarity required, other limitations are loss of temporal information about frequency components. Because sinusoidal waves have only one frequency component at all time points. For this reason, although frequency precision of the results is good but temporal localization of this frequency is not clear. There are several solution methods to obtain temporal localization information while obtaining frequency components of time series. One of them is determining a time window (boxcar), multiplying with sinusoidal and dot product this result with EEG data. According to this, frequency component obtained will have been at time intervals that limited with length of time window. But using time window has a problem such as it may cause edge artifact two edge of sinusoidal. Gaussian taper is a more convenient for this procedure because its values starts zero then slowly rises after then back to zero.

2.5.5.1. Generating Morlet Wavelet

A Morlet wavelet is created by pointwise multiplication between sinus wave and Gaussian window (bell shaped or normal curve). Frequency value and other variables of Morlet wavelet was determined as follows:

Gaussian time window was created by using following equation.

$$Gaussian_{Curve} = a.e^{-t^2/(2s^2)} \quad (2.4)$$

a: Amplitude

t: Time

s: Standard deviation

The standard deviation parameter determines the width of the wavelet. The ‘s’ parameter can be computed as follows:

$$s = \frac{n}{2\pi f} \quad (2.5)$$

n: number of the wavelet cycle

f: frequency in hertz

‘n’ parameter arranges the balance between temporal resolution and frequency resolution.

A sample Gauss is shown as an example in Figure 2.14. This Gaussian wave is centered at frequency 7 Hertz, number of cycle is 5.

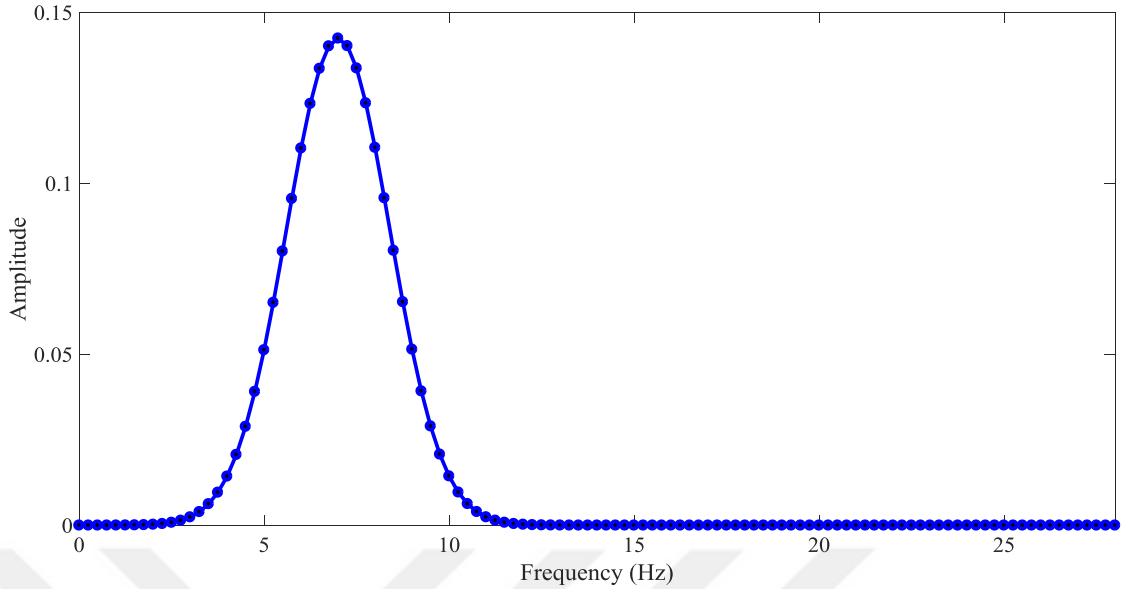

Figure 2.14: Gaussian taper at 7 Hz frequency.

Morlet wavelet convolution between sinusoidal, gaussian taper and convolution results (from top to bottom orderly) is shown in Figure 2.15.

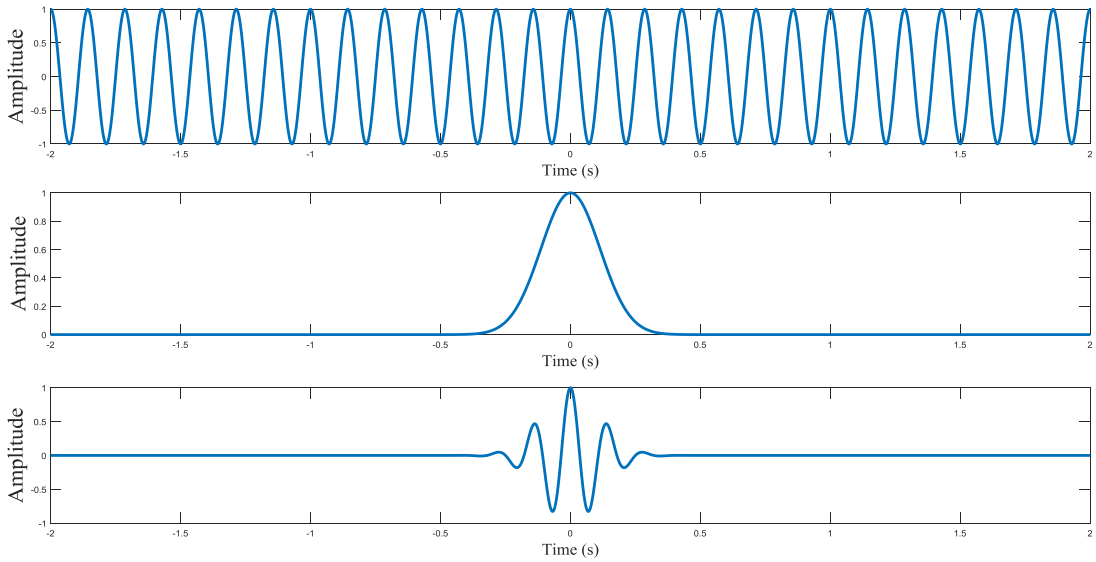

Figure 2.15: Stages of Morlet wavelet creation.

2.5.5.2. Extracting Phase Information Using Complex Morlet Wavelet

Real Morlet wavelet convolution can be used as a band pass filter. It is possible to obtain power and phase information specific to each EEG band by using complex morlet wavelet. A complex wavelet signal is created pointwise multiplication between gaussian shape and sinus signal. It is formulated as equation 2.6.

$$cmw = e^{-t^2/2s^2} . e^{-i2\pi ft} \tag{2.6}$$

The first exponential part of the equation 2.6 is a gaussian wave beside this second exponential is referred as sinusoidal and *'s'* is determined and formulated in equation 2.5. *'f'* variable demonstrate peak value of Morlet Wavelet in frequency domain.

Two parameters are important for creating Morlet wavelet. The first is sinus signal's frequency value in time domain and maximum value of wavelet in frequency domain. Other important point is width of wavelet in frequency domain (it is like gaussian shape). When the width of wavelet increases as the frequency precision will increase but temporal resolution will decrease. Two-dimensional illustration of real part of Morlet wavelet (top) and imaginary part of Morlet wavelet (bottom) is shown as Figure 2.16.

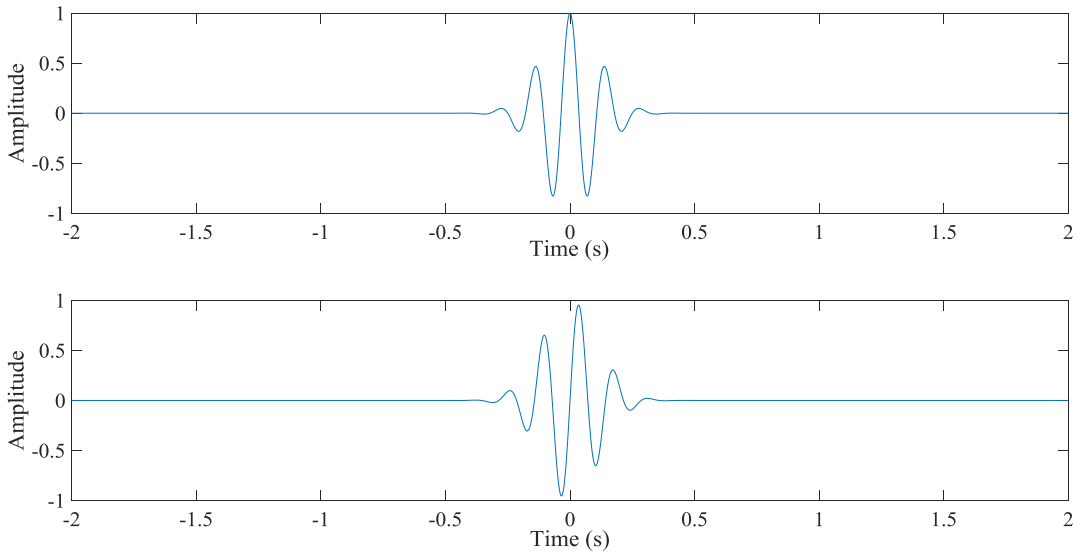

Figure 2.16: Top of the figure shown as real part of complex wavelet.

3D dimensional projection of sum of two signal in Figure 2.16 is illustrated as Figure 2.17.

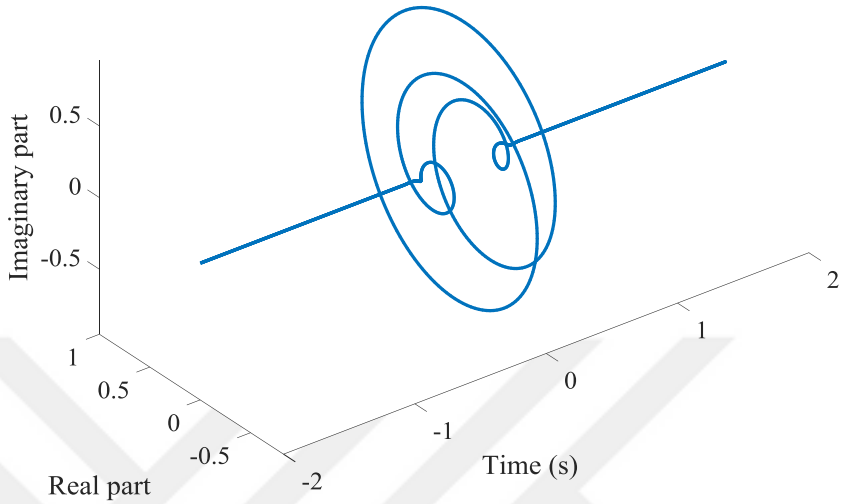

Figure 2.17: 3D time domain representation of a Morlet wavelet.

2.6. PRINCIPAL COMPONENT ANALYSIS

Principal Component Analysis (PCA) is a statistical analysis method, that can be used for obtaining characteristic features of multivariate data set without much loss of information and simplification of the data by dimension reduction. Essential time-frequency decomposition for EEG data, produces output as complex number. Therefore, each output (Fourier coefficient or wavelet convolution results etc.) can be represented on two dimensional cartesian system. This method for computing a single value that symbolize the features belongs to all EEG channels. Each characteristic feature points can be represented on cartesian coordinate system. PCA can be used to extract meaning from such many data and express them more simply. For this purpose, PCA change the direction of cartesian system and transform data according to new axes. First axis, can be called as principal component, refers maximum variance of data and second axis refers next largest variation and perpendicular to first axis. There are many convenience of axis conversion such as describe patterns of variance decrease dimensionality by neglecting dimension in the data have least significant variance, cleaning noise and simplicity.

Computation of this processes and next stages can be done by eigen decomposition method. New axes on cartesian coordinate system is illustrated in Figure 2.18.

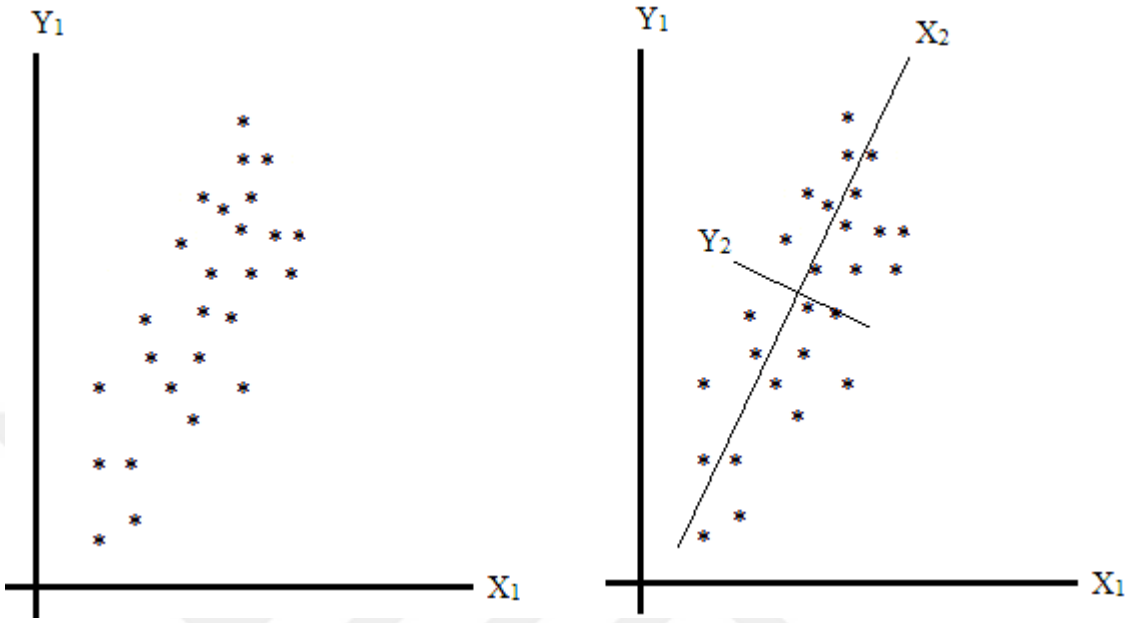

Figure 2.18: Created random data is shown in left panel and same data plotted in PCA space is shown in right panel.

Generally, when any matrices multiply operation with scalar, matrices, direction of resultant vector will be different from first matrices. On the other hand, there is some specific vectors that not transformed their direction by whichever operation is applied. These vectors are called as "*eigenvector*" and the vector's values are termed as "*eigenvalues*". Eigen decomposition analysis of any matrices means that finding its eigenvectors and eigenvalues. Eigenvectors is never changing direction so that they have characteristic identity like as biometric parameters.

In the first stage of PCA application, mean value of data is computed and subtracted from all elements of data. Subsequently covariance matrices should be constructed. Since the data is two dimensional, the covariance matrices always will have two rows and two columns. In third step of the process, eigenvectors of covariance matrices should be computed. These eigenvectors determine drawing a new axis of best fit line that goes

through middle of data points. The last step, eigenvector should be transposed and multiply with mean adjusted data transposed (Cohen, 2017).

2.7. GLOBAL FIELD SYNCHRONIZATION METHOD

GFS method that determines phase-based synchronization level of multichannel EEG oscillations. GFS computes single value between ‘0’ (poor phase degree) and ‘1’ (common phase) for not only all channels but also specific lobe such as temporal, frontal, parietal, occipital. The method can measure phase coupling degree for any frequency point so that it can be performed for all EEG band separately EEG band. GFS values was computed on EEG frequency bands such as delta (0-4 Hz), theta (4-7 Hz), alfa 1 (8-10 Hz), alfa 2 (10-13 Hz), beta 1 (13-18 Hz), beta 2 (18-22 Hz), beta 3 (22-30 Hz) within each subject. GFS results can be evaluated as functional connectivity so that it can be interpreted for functional connectivity of global brain networks.

Methodology of GFS is started by segmenting 3-minutes records are split into 4 second segments. Each segment was called as epoch or trial. Sampling rate of EEG device is 250 Hz so that one of each epoch has 1000-time points. Afterward each epoch transformed in frequency domain with using FFT. According to FFT Dipole Approximation that was improved by (Lehmann and C., 1990), complex fourier coefficients that was obtained by result of frequency transformation process, can be displayed on cartesian system. This plane is called as sine-cosine diagram. Each point was placed on sine-cosine diagram represent a channel at a selected frequency. Scattering map of points give information about synchronization power. More scattered points are interpreted as decreased phase synchronization and scattered as straight line is shown more predominant synchronization. Ellipsoid scattering of points on sine-cosine diagram, is related the real axis components of the points and it means that these signals not produced by single underlying mechanism. To determine how constellation of points close to best straight

line, PCA method is given all the inputs. Two eigenvalues are computed with PCA. The GFS value computation formula is shown in equation 2.7.

$$GFS(f) = \frac{|E_{1(f)} - E_{2(f)}|}{E_{1(f)} + E_{2(f)}} \quad (2.7)$$

2.8. INTERTRIAL PHASE CLUSTERING METHOD

ITPC is a phase synchronization analysis method. It is also named different terms such as "phase locking value", "phase locking factor", "phase coherence", "inter trial phase coherence". After the frequency components of signal was obtained, these complex numbers were placed and displayed on polar plane as unit length vector. ITPC is used to compute common phase value of all phase angels. ITPC values are between '0' and '1'.

In the first step of the ITPC processes wavelets are constructed for obtaining frequency components with wavelet convolution. ITPC is computed for each frequency point. Because the phase angle computation, the complex numbers are formed by wavelet convolution, placed on cartesian coordinate system. According to the trigonometry results of arctangent function will be in radians and so that the phase values are on 0 through 2π. When these values placed on polar plane, average of angles are referring to a cyclic measure that is cycling around this polar space and, so it cannot be computed with arithmetic mean method. Example of illustration about an angle values as unit vector on unit circle. Since the length of vectors on unit circle always is one, the vectors that referred an angle value named as unit vector. Phase values can be demonstrated on unit circle as Figure 2.19.

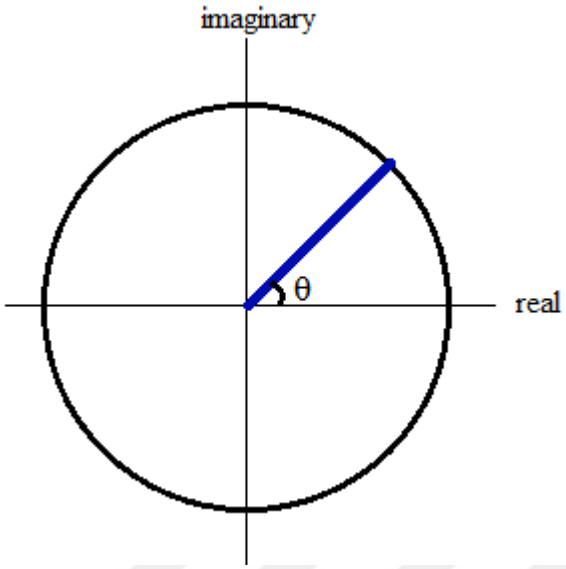

Figure 2.19: Illustration of a phase angel as unit vector on unit circle.

In this stage, the phase angles calculated separately for each part are placed on unit circle as a vector. Afterwards, it is wanted to average vector and find consistency of the phase angle between each of these vectors. In the following example is demonstrated as Figure 2.20, the value of association between two phase angles is calculated by this method. The blue vectors represent average phase values and its lengths referred as degree of phase consistency. The phase synchronization degree increases as the vectors that referred phase angels of EEG epochs, close each other. The common phase increases as the distance

between vectors decreases. An example about computation of phase consistency between two-unit vectors that refer to phase angle, is shown in Figure 2.20 (Cohen, 2014).

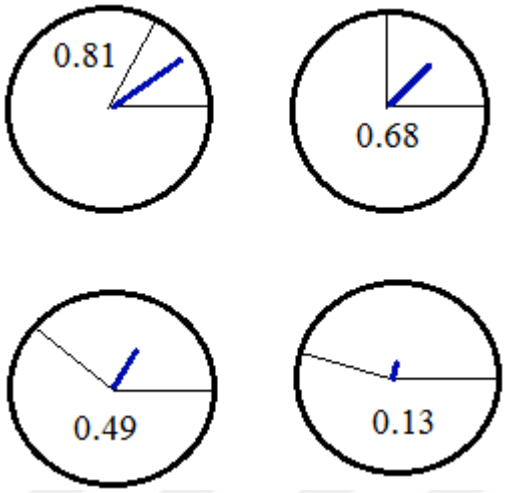

Figure 2.20: Example couple of unit vectors (black) and their averages (blue). The numbers refer the length of average vector, meanwhile ITPC value of the vectors.

ITPC can be mathematically expressed as equation 2.8 (Cohen, 2014).

$$ITPC_{tf} = \left| n^{-1} \sum_{r=1}^{n} e^{-ik_{tfr}} \right| \quad (2.8)$$

'*n*' is determined as number of EEG epochs, '*tf*' is time-frequency point, '*r*' is the one trial and '*k*' referred as phase angle.

Purpose of absolute value is ITPC parameter never will be negative. ITPC computation for 19 trials and average vector is illustrated as Figure 2.21. The average vector is represented by blue line for value of 0,65387. It is same as the length of average vector.

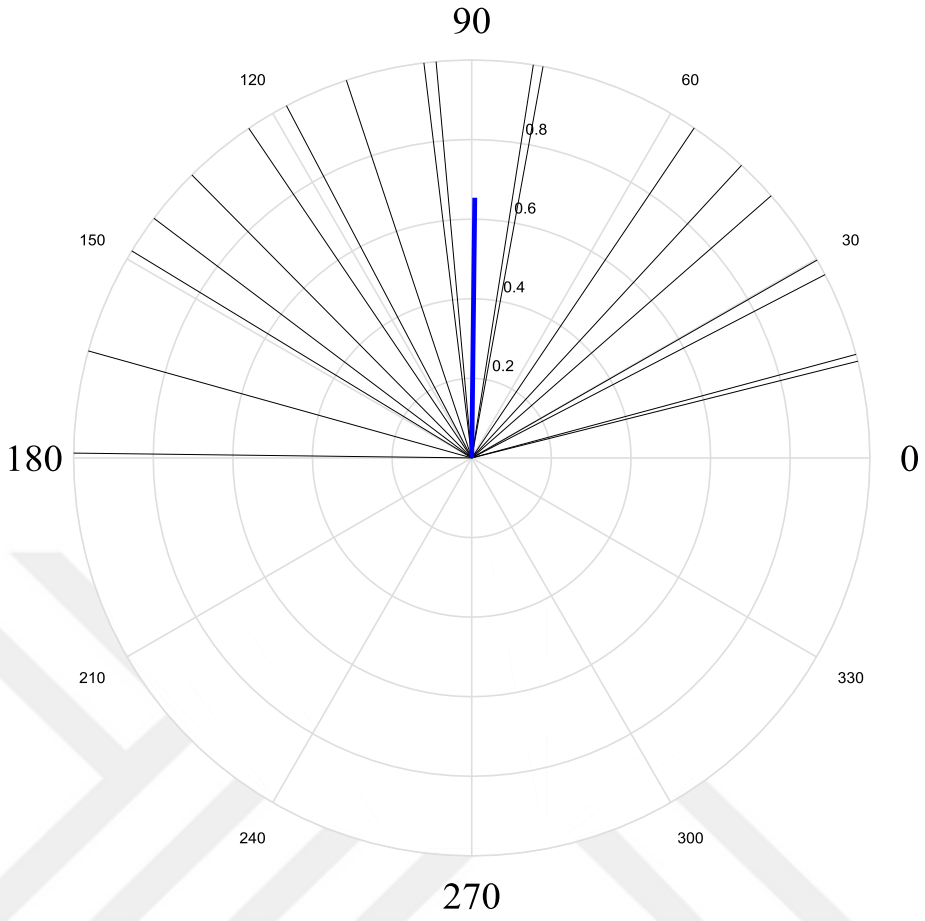

Figure 2.21: ITPC computation for 19 trials.

2.9. CLASSIFICATION OF NEUROBIOLOGIC BIOMARKERS

Several neurophysiological based parameters have been used for determining neurological disorders. These parameters are power spectral values, complexity analysis results and phase synchronization indices, etc. Data enrolled from healthy control and patients then analysed with algorithms that compute the parameters used as a biomarker. Subsequently, biomarkers of patients and healthy are compared between using suitable statistical analysis method. Another way to reinforce the robustness of the results, is classified it with machine learning methods (Goldberg and Holland, 1988).

Machine Learning algorithm to provide humanity talent to computers, and thus machines able to gain new information from their its experience. This ability is named as learning.

Algorithms can improve their estimation performance through more sample. Machine learning algorithms is commonly used in every field in daily life. For example;

- Medical diagnosis such as tumour detection
- For security purposes such as Face recognition
- Computational finance such as; for credit scoring
- Image processing such as motion detection
- Automotive, aerospace, manufacturing, for predictive maintenance
- Natural language processing

Types of machine learning applications is diagrammed as Figure 2.22.

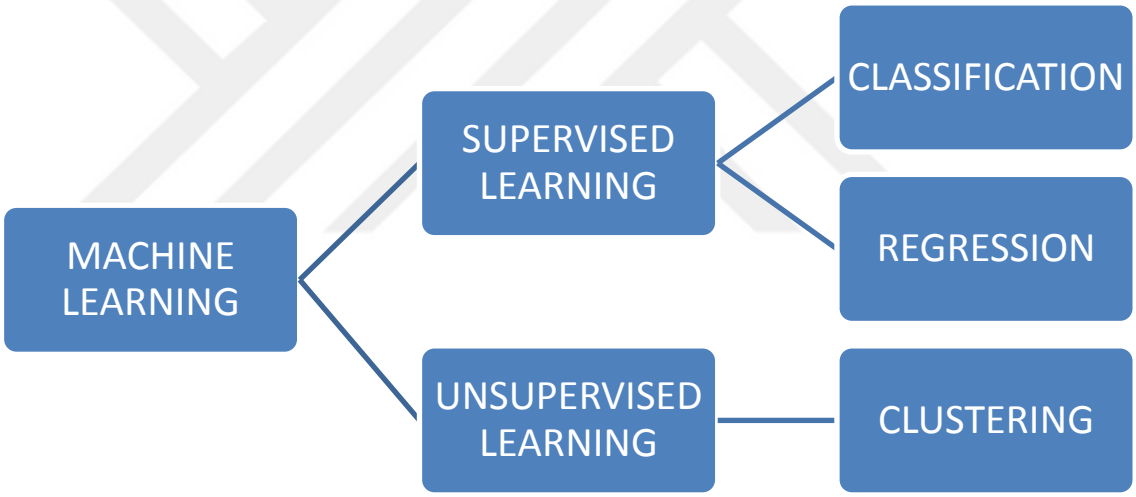

Figure 2.22: Diagram of Machine Learning types.

Supervised machine learning algorithm uses class known data as input and output for learning and creating a classification model. Afterward the model is used to estimate unknown data. Supervised learning used predictive model for producing classification and regression techniques (Shipp et al., 2002). Classification techniques assumes the classes of data points. They determine that whether an e-mail is spam or not, detecting disorders neurophysiological case using EEG data, etc. Unsupervised learning emerges

covered patterns or intrinsic characteristics without label response and include input values. It is generally used for gene sequence analysis, market search (Hofmann, 2001).

2.9.1. Support Vector Machines

The Support Vector Machine (SVM) algorithms was invented by Boser et al, to binary classification (Boser et al., 1992, Vapnik and Vapnik, 1998) as a supervised machine learning algorithm. The place on SVM among the other machine learning algorithms was illustrated in Figure 2.23.

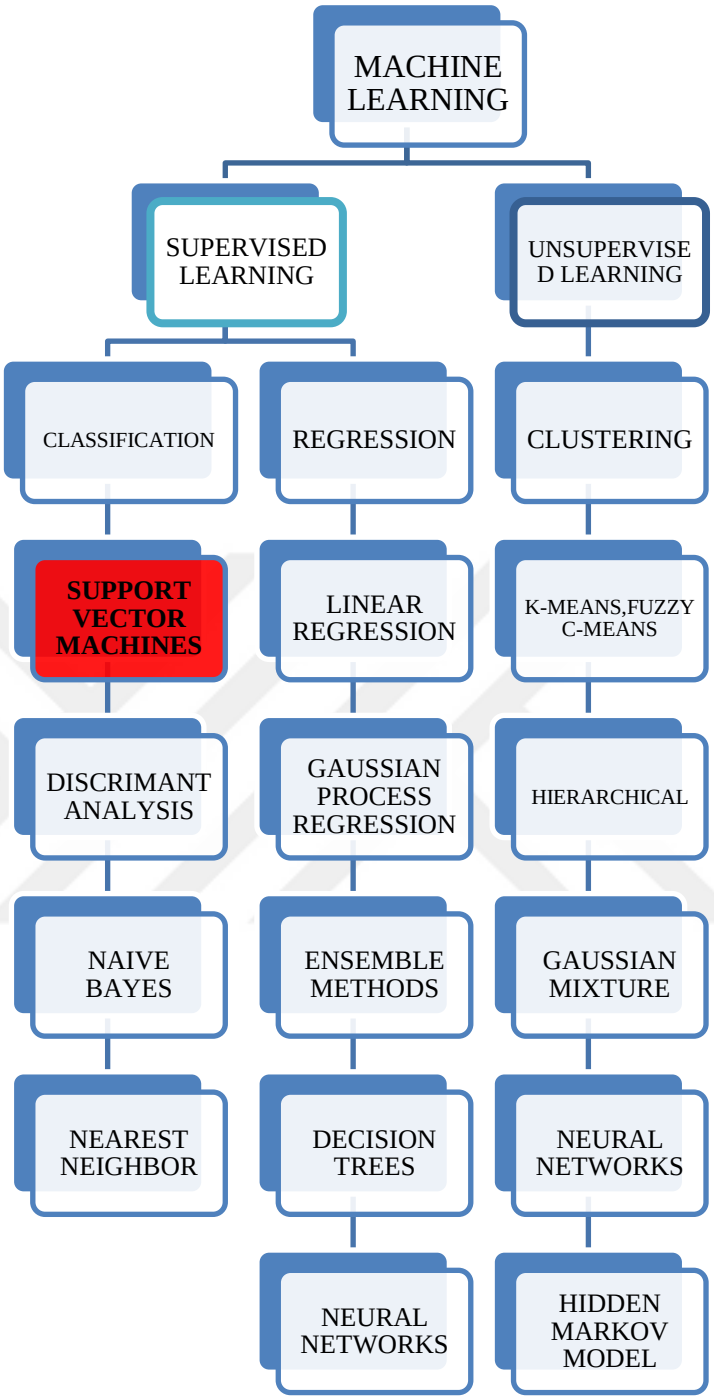

Figure 2.23: SVM is a member of Machine Learning group.

The main advantage of the SVM is solving the classification problem with transformed it to optimization problem. In this way, the number of computation processes will be

reduced and faster resolution can be obtained than other techniques (Osowski et al., 2004).

SVM is a member of linear two class classifiers. Classifying operation of objects in data clusters basically based on labelling the objects as -1 (first class) or 1 (other class). Labelling process is variated as regard to specify of investigation(Friedman et al., 2001). For instance, it can be auto-diagnose system of any disorder, feature belongs to healthy can be labelled as 1 and patients' feature values can be labelled as -1. Main purpose of the SVM is creating an optimal hyperplane (linear decision boundary) that can discriminate the data points that are labelled as various. In other words, maximizing distance between support vectors (Bishop, 2006, Ben-Hur and Weston, 2010). Mathematical explanation of SVM can be summarized as follows; each input point can be shown as 'x_i' and the labels can be referred as 'y_i', 'w' represent normal of hyper plane and weight vector and 'b' is the bias and constant value. A classifier is formed as discriminating function of the form as shown in equation 2.9.

$$f(x) = wx + b \tag{2.9}$$

Geometrical illustration of linear SVM model for two classes and two-dimensional classification, is shown as Figure 2.24.

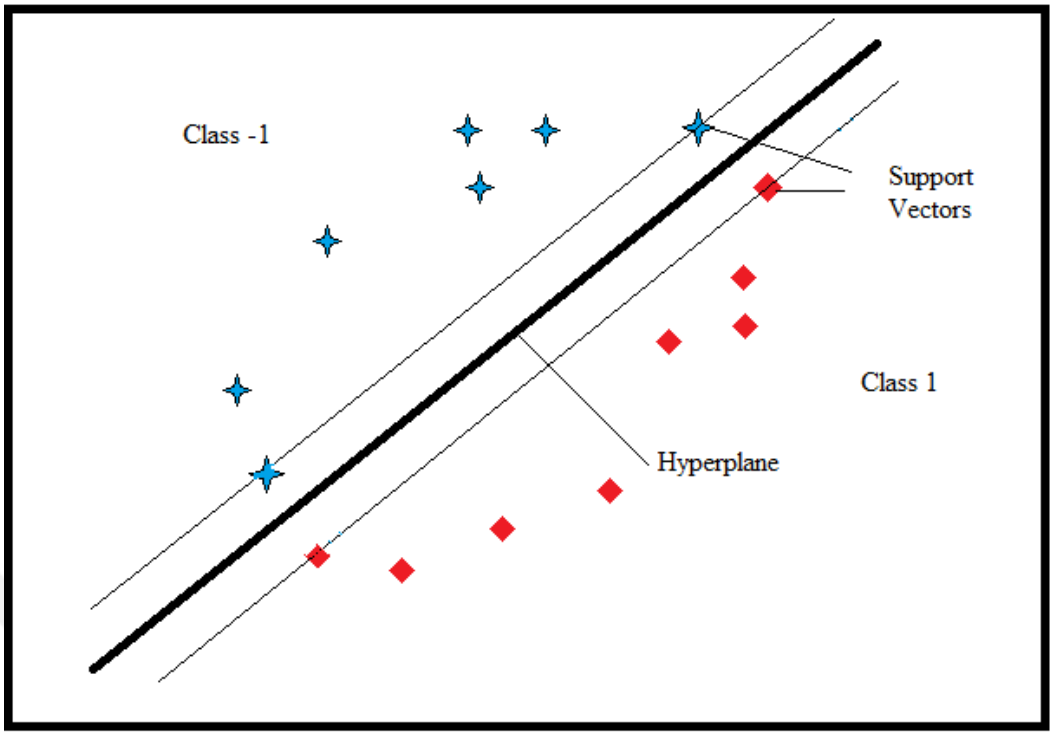

Figure 2.24: Geometric illustration of SVM.

The SVM use a kernel function (such as polynomial, gaussian, etc.) for forming nonlinearly adaptable data into higher dimensions where a linear decision boundary can be found. Two parallel line that intersecting with is named as boundary plane. The bold plane that passing through the center of the boundary planes and equally spaced in both planes is expressed as a hyperplane (Burges, 1998, Soman et al., 2009).

2.9.2. Cross Validation Methods

Cross Validation Methods (CVM) forms several protocols that determine and categorize data cluster as training data and test data (Mosier, 1951). The values in the data cluster are labeled as test or training data by 3 methods; hold-out method, k-fold method and leave-one out method. CVM is also produces objectively selection of training and test data thus increases the classification performance (Browne, 2000). Most of the CVM that implemented in literature are explained below.

2.9.2.1. Hold-out Method

The hold out method is the easiest implementation of CVM. Entire data set are divided into two parts then the values in each part is labeled as a training or test. After the

classification model has been established, it is able to acquire learning with using training data. In the next stage test data asked to classification model for assuming the values' labels. Results of the assumption compared with the real labels and estimated value and consequently classifier performance is determined by this. Because the method has a high variance, performance results are depending on how the division is made. The hold-out method is illustrated as Figure 2.25.

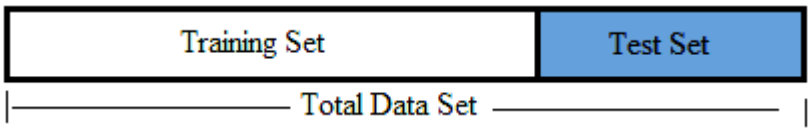

Figure 2.25: Hold-out CVM.

2.9.2.2. K-Fold Cross Validation Method

One of the method is applied for overcome deficiency of hold-out method, is k-fold CVM. In the hold-out method process, data cluster is divided into two equal part and labelled as training data or test data. But to apply k-fold CVM, data should have divided k-piece of subset. Learning process lead k-time iteration and each of the iteration one of the subsets are used for testing and k-1 subsets are used for training. This is advantage, so subsets are randomly selected. Other benefit of the method is all values are used as both training and test. This allows the results to be unaffected by how the data is divided. Because the selected subsets adjacent to each other, this can increase the results. K-fold CVM process is illustrated as Figure 2.26.

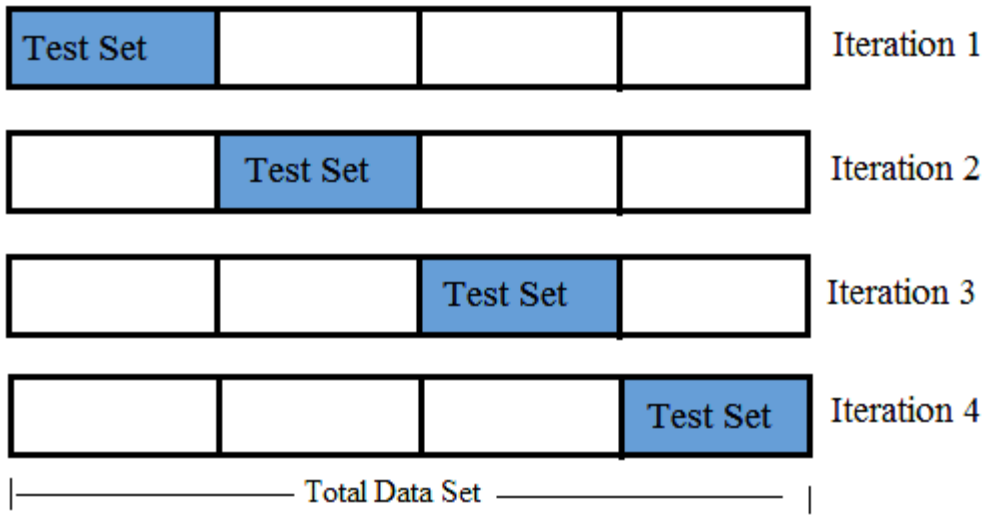

Figure 2.26: K-Fold CVM.

2.9.2.3. Leave-subject-out cross validation

Leave-subject out CVM is also called as leave-one out CVM in literature, is a specialized and innovated type of k-fold CVM. It is performed same as k-fold CVM, but k will always be equal to 1. In this way, the method can overcome effects of subsamples' neighboring on performance scores and the problem that induced from variance excess of the estimator. The estimation results will be more robust since each value in the data set are used as test value. Leave subject-out CVM is operated as Figure 2.27 (Gutierrez-Osuna, 2006).

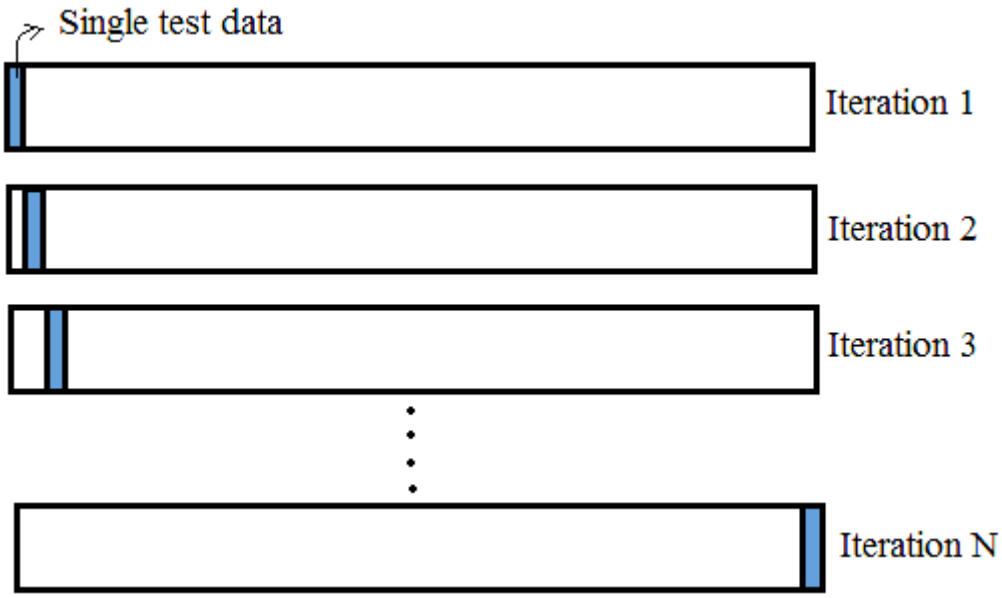

Figure 2.27: Leave-subject out CVM.

3. RESULTS

In this thesis study, 19 channel artefact free EEG records were enrolled from thirty-seven age matched OCD patients and twenty-seven HC volunteers then comparison between in terms of phase synchronization with GFS and ITPC methods. EEG data were recorded for three-minutes. During the records volunteers in light and sound isolated room, in addition to this they are in resting state on comfortable chair and eye closed. Each three-minutes data were separated into four-seconds trials for facilitating analysis. Synchronization values was computed for all EEG frequency bands. EEG bands were selected as follows: Delta (0.0-4.0 Hz), theta (4.0-7.0 Hz), alfa1 (8.0-10.0 Hz), alfa2 (10.0-12.0 Hz), beta1 (12.0-18.0 Hz), beta2 (18.0-21.0 Hz), beta3(21.0-30.0 Hz) (Bear et al., 2007).

In the second stage these values classified with SVM method.

3.1. FEATURE EXTRACTION BY GLOBAL FIELD SYNCHRONIZATION

GFS is a novel method that computes phase synchronization based inter-channels(electrodes) so that it can detect either whole brain or any site (frontal, parietal, etc.) synchronization. In order to compute whole brain synchronization, GFS should be applied all 19 channels. GFS indices will be ‘0’ through ‘1’. The ‘0’ value refers to loss of synchronization and ‘1’ value can be interpreted as prefect synchronization.

3.1.1. GFS Computation for Frontal Lobe

Frontal site of brain is very important for detection and diagnosis of OCD. Several neuroimaging and neurophysiological studies about OCD reported that excessive processing or dysfunction on frontal lobe (Frankel et al., 1986, Wise and Rapoport, 1989, Cummings, 1993). Therefore, synchronization analysis of frontal lobe was investigated by GFS. GFS indices was computed only 6 electrodes that placed on frontal site such as Fp1, Fp2, F7, F3, F4 and F8. According to analysis results, significantly difference was found between HCs and OCD patients in delta ($p<0.001$) and beta 3 ($p<0.005$). Although, similar results were found in also other frequency bands, these were not significantly difference. Independent sample t-test was used for determining significance of

differences. Average GFS values and results of statistical analysis was shown in Table 3.1 and illustrated as Figure 3.1.

Table 3.1: Group mean values and standard deviation of GFS in the Frontal 6 electrodes, bold letter refers statistically significant difference.

Frequency bands	**Delta**	**Theta**	**Alpha 1**	**Alpha 2**	**Beta 1**	**Beta 2**	**Beta 3**
Frequency range in Hz	0.0-4.0	4.0-7.0 Hz	8.0-10.0	10.0-12.0	12.0-18.0	18.0-21.0	21.0-30.0
Patients' GFS value (Frontal)	0.5869	0,5948	0.6085	0.6260	0.5950	0.5990	0.5895
Standart Deviation	0.00782	0.01481	0.03515	0,03616	0.01180	0.01839	0.01738
Control Group's GFS value (Frontal)	0.6166	0.6065	0.6085	0.6131	0.6048	0.6077	0.6038
Standart Deviation	0.01556	0.02797	0.02383	0.03670	0.02353	0.02889	0.02025
p value (2-tailed t test)	**0.0001**	0.124	0.837	0.274	0.133	0.276	**0.026**
p value (1-tailed t test)	**0.00005**	0.0612	0.4185	0.137	0.0665	0.138	**0.013**

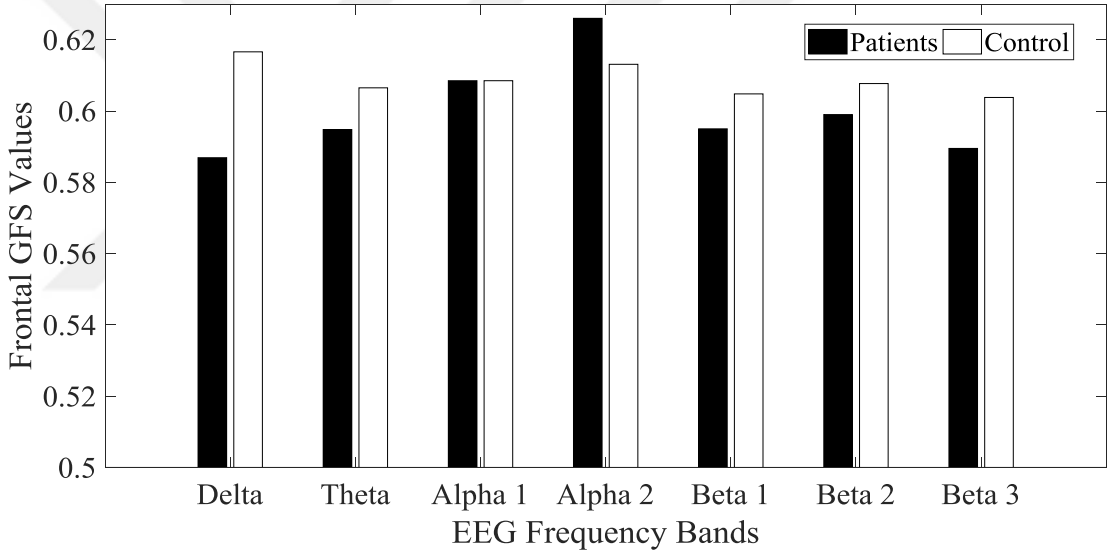

Figure 3.1: GFS analysis and comparison results for frontal channels.

3.1.2. GFS Computation for Whole Brain

The GFS can compute synchronization degree for whole brain. GFS values were for each epoch and after that they were averaged calculated A single value was obtained for each frequency band. Independent sample t-test was used for compared with GFS values belongs to OCD patients and HCs. Mean GFS values and results of statistical analysis was shown in Table 3.2 and illustrated as Figure 3.2. According to table, significantly difference was found in delta band (p=0.001) and beta2 band (p=0.014).

Table 3.2: Group mean values and standard deviation of GFS for whole brain and, bold letter refers statistically significant difference.

Frequency bands	**Delta**	**Theta**	**Alpha 1**	**Alpha 2**	**Beta 1**	**Beta 2**	**Beta 3**
Frequency range in Hz	0.0-4.0	4.0-7.0	8.0-10.0	10.0-12.0	12.0-18.0	18.0-21.0	21.0-30.0
Patients' GFS value (Frontal)	0.4513	0.4719	0.5257	0.5430	0.4880	0.4758	0.4543
Standart Deviation	0.02407	0.03429	0.06504	0,0777	0.03482	0.04896	0.03800
Control Group's GFS value (Frontal)	0.4816	0.4790	0.5201	0.5268	0.4865	0.6249	0.4688
Standart Deviation	0.03273	0.04489	0.06600	0.06499	0.04545	0.01303	0.03525
p value (2-tailed t test)	**0.002**	0.596	0.781	0.458	0.904	**0.028**	0.201
p value (1-tailed t test)	**0.001**	0.298	0.3905	0.229	0.452	**0.014**	0.100

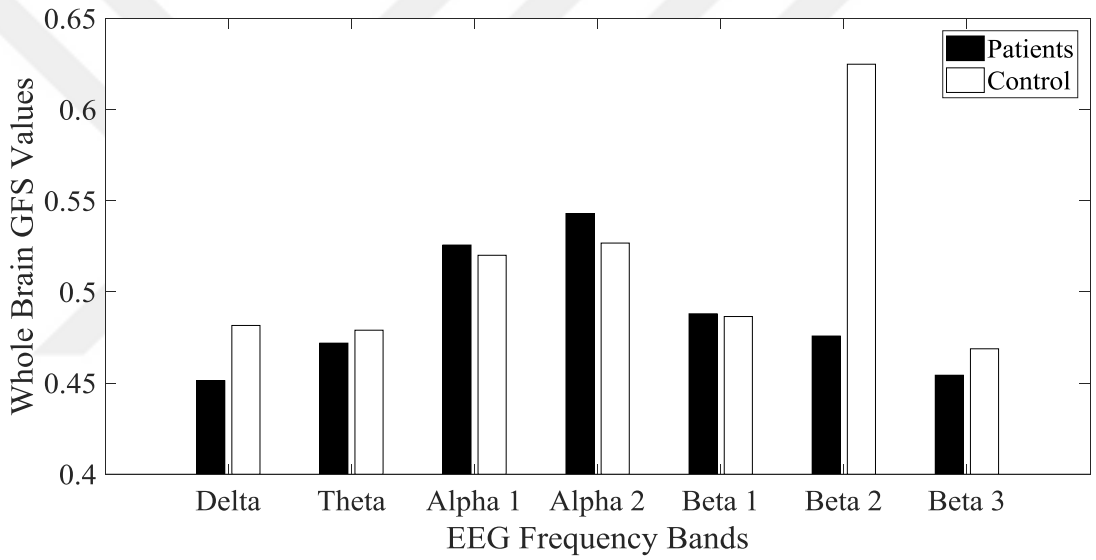

Figure 3.2: GFS analysis and comparison results for all channels.

3.2. FEATURE EXTRACTION BY INTER-TRIAL PHASE CLUSTERING

ITPC method was applied on data that belongs to OCD patients and HCs for comparison. Because the ITPC values is '0' through '1', it will not need normalization process. ITPC values was computed both each channel and each EEG bands such as delta (0.0-4.0 Hz), theta (4.0-7.0 Hz), alfa1 (8.0-10.0 Hz), alfa2 (10.0-12.0 Hz), beta1 (12.0-18.0 Hz), beta2 (18.0-21.0 Hz), beta3 (21.0-30.0 Hz) (Bear et al., 2007). Analysis results have been shown in following subsections, tables and graphics.

3.2.1. Analysis Results of All EEG Channels

Mean values, standard deviations of ITPC values was computed for every EEG band for Fp1 channel. Analysis results of OCD patients' data and HCs' data compared between using independent sample t-test. Significantly difference between OCD and HC data was found in all EEG bands ($p<0.001$). Both two tailed and one tailed results was determined in Table 3.3. and since our hypothesis is that synchronization values of OCD are smaller than healthy controls' values, one tailed t-test is more appropriate for this thesis. The results were shown in Table 3.3. Graphical illustration of results can be shown in Fig. 3.3.

Table 3.3: ITPC synchronization analysis results of Fp1 channel.

Frequency bands	**Delta**	**Theta**	**Alpha 1**	**Alpha 2**	**Beta 1**	**Beta 2**	**Beta 3**
Frequency range in Hz	0.0-4.0	4.0-7.0	8.0-10.0	10.0-12.0	12.0-18.0	18.0-21.0	21.0-30.0
Patients' ITPC mean value	0.1296	0.1305	0.1304	0.1202	0.1302	0.1350	0.1330
Standart Deviation	0.010309	0.00651	0.1119	0.01804	0.1041	0.00636	0.00885
Control Group's ITPC mean value	0.1752	0,173	0.1756	0.1606	0.1655	0.1770	0.1732
Standart Deviation	0.03349	0.03225	0.3307	0.4248	0.02943	0.03426	0.03058
p value (2-tailed t test)	**0.0001**	**0.0001**	**0.0001**	**0.001**	**0.0001**	**0.0001**	**0.0001**
p value (1-tailed t test)	**0.00005**	**0.00005**	**0.00005**	**0.0005**	**0.00005**	**0.00005**	**0.00005**

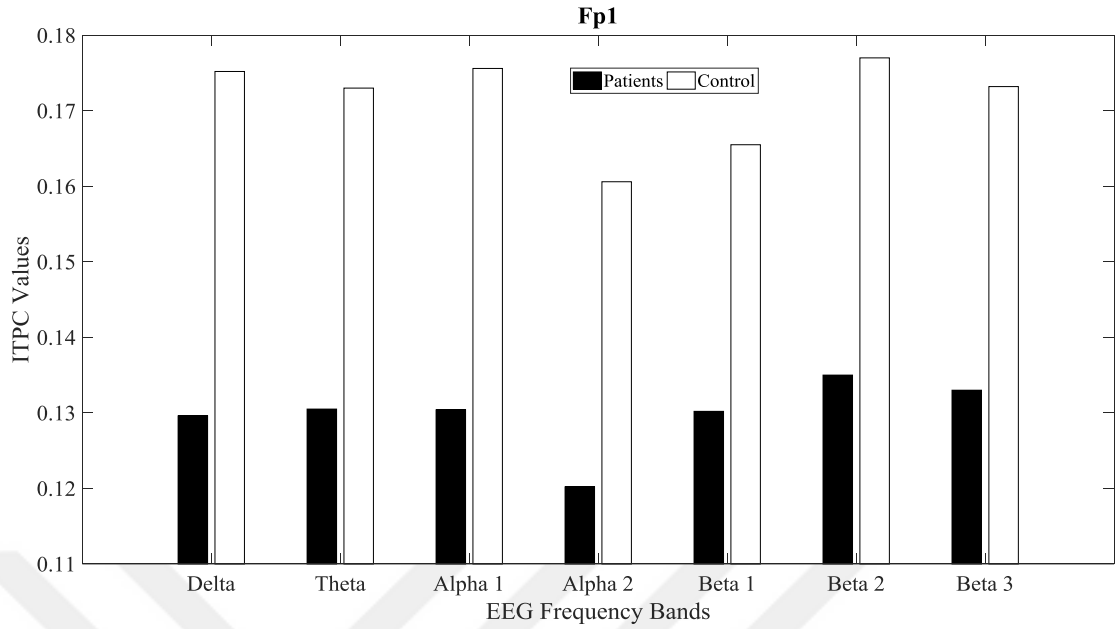

Figure 3.3: Illustration of ITPC analysis results for Fp1 channel.

Main parameters of ITPC values was calculated for every EEG band for F3 channel. Analysis results of OCD patients' data and HCs' data compared between using independent sample t-test. Significantly difference between OCD and HC data was found in all EEG bands ($p<0.001$). The results were shown in Table 3.4. Graphical illustration of results can be shown in Figure 3.4.

Table 3.4: ITPC synchronization analysis results of F3 channel.

Frequency bands	**Delta**	**Theta**	**Alpha 1**	**Alpha 2**	**Beta 1**	**Beta 2**	**Beta 3**
Frequency range in Hz	0.0-4.0	4.0-7.0	8.0-10.0	10.0-12.0	12.0-18.0	18.0-21.0	21.0-30.0
Patients' ITPC value	0.1345	0.1351	0.1344	0.1278	0.1306	0.1334	0.1358
Standart Deviation	0.00973	0.00928	0.01188	0.01912	0.00838	0.00502	0.00690
Control Group's ITPC value	0.1770	0.1787	0.1728	0.1697	0.1662	0.1776	0.1744
Standart Deviation	0.04105	0.03387	0.034686	0.04478	0.02743	0.0300	0.02817
p value (2-tailed t test)	**0,0001**	**0.0001**	**0.0001**	**0.0001**	**0.0001**	**0.0001**	**0.0001**
p value (1-tailed t test)	**0.00005**	**0.00005**	**0.00005**	**0.00005**	**0.00005**	**0.00005**	**0.00005**

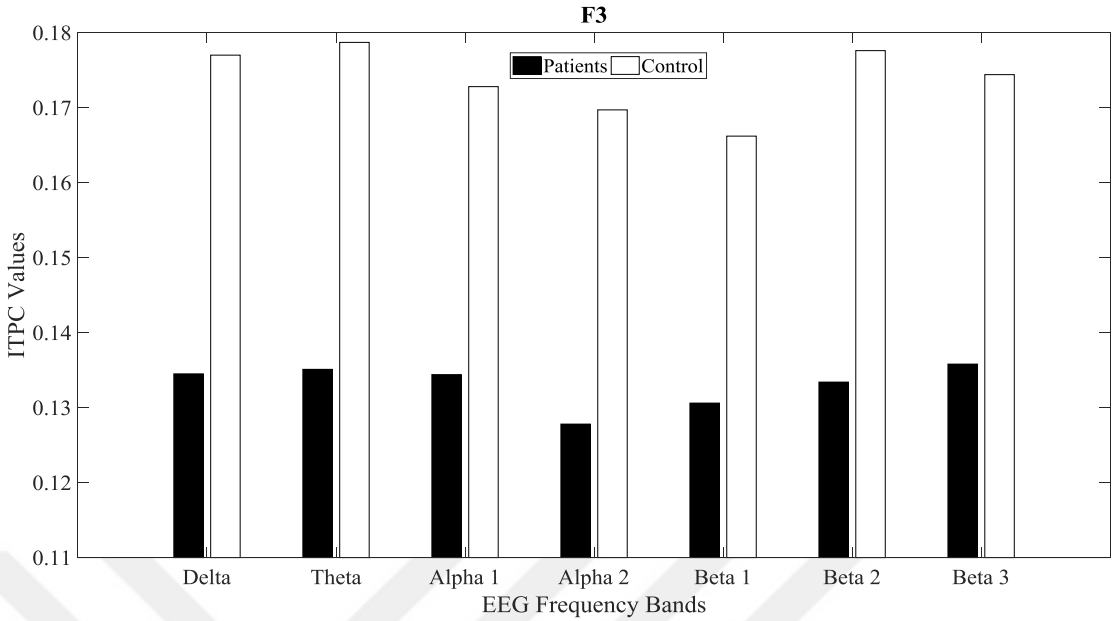

Figure 3.4: Illustration of ITPC analysis results for F3 channel.

Several parameters such as average and standard deviation values of ITPC values was calculated for every EEG band for C3 channel. Analysis results of OCD patients' data and HCs' data compared between using independent sample t-test. Significantly difference between OCD and HCs data was found in all EEG bands ($p<0.05$). The results were shown in Table 3.5. Graphical illustration of results can be shown in Figure 3.5.

Table 3.5: ITPC synchronization analysis results of C3 channel.

Frequency bands	**Delta**	**Theta**	**Alpha 1**	**Alpha 2**	**Beta 1**	**Beta 2**	**Beta 3**
Frequency range in Hz	0.0-4.0	4.0-7.0	8.0-10.0	10.0-12.0	12.0-18.0	18.0-21.0	21.0-30.0
Patients' ITPC value	0.1392	0.1409	0.1308	0.1364	0.1354	0.1404	0.1403
Standart Deviation	0.01597	0.01772	0.01229	0.02144	0.00902	0.00469	0.00390
Control Group's ITPC value	0.1700	0.1689	0.1685	0.1652	0.1631	0.1701	0.1644
Standart Deviation	0.02773	0.03814	0.03264	0.03646	0.03173	0.03666	0.03278
p value (2-tailed t test)	**0.0001**	**0.002**	**0.0001**	**0.002**	**0.0001**	**0.001**	**0.003**
p value (1-tailed t test)	**0.00005**	**0.001**	**0.00005**	**0.001**	**0.00005**	**0.0005**	**0.0015**

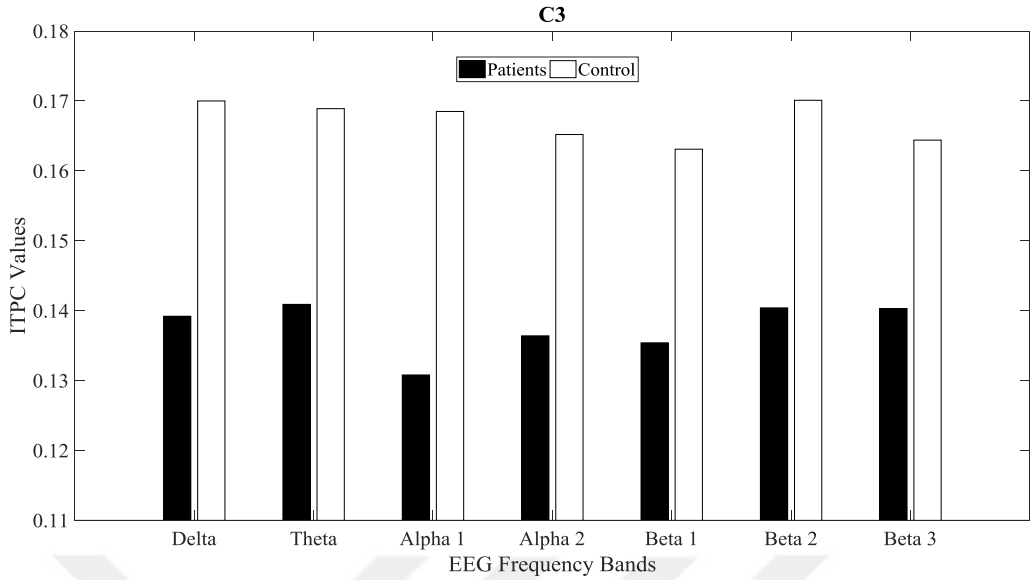

Figure 3.5: Illustration of ITPC analysis results for C3 channel.

Several parameters such as average and standard deviation values of ITPC values was found for every EEG band for P3 channel. Analysis results of OCD patients' data and HCs' data compared between using independent sample t-test. Significantly difference between OCD and HC data was found in all EEG bands ($p<0.05$). The results were shown in Table 3.6. Graphical illustration of results can be shown in Figure 3.6.

Table 3.6: ITPC synchronization analysis results of P3 channel.

Frequency bands	**Delta**	**Theta**	**Alpha 1**	**Alpha 2**	**Beta 1**	**Beta 2**	**Beta 3**
Frequency range in Hz	0.0-4.0	4.0-7.0	8.0-10.0	10.0-12.0	12.0-18.0	18.0-21.0	21.0-30.0
Patients' ITPC value	0.1365	0.1359	0.1359	0.1389	0.1417	0.1386	0.1419
Standart Deviation	0.01402	0.01441	0.02006	0.02149	0.01480	0.00720	0.02064
Control Group's ITPC value	0.1655	0.1573	0.1720	0.1630	0.1603	0.1582	0.1710
Standart Deviation	0.03225	0.03543	0.03375	0.04425	0.03512	0.03693	0.03266
p value (2-tailed t test)	**0.0001**	**0.007**	**0.0001**	**0.0016**	**0.017**	**0.016**	**0.001**
p value (1-tailed t test)	**0.00005**	**0.0035**	**0.00005**	**0.008**	**0.0085**	**0.008**	**0.0005**

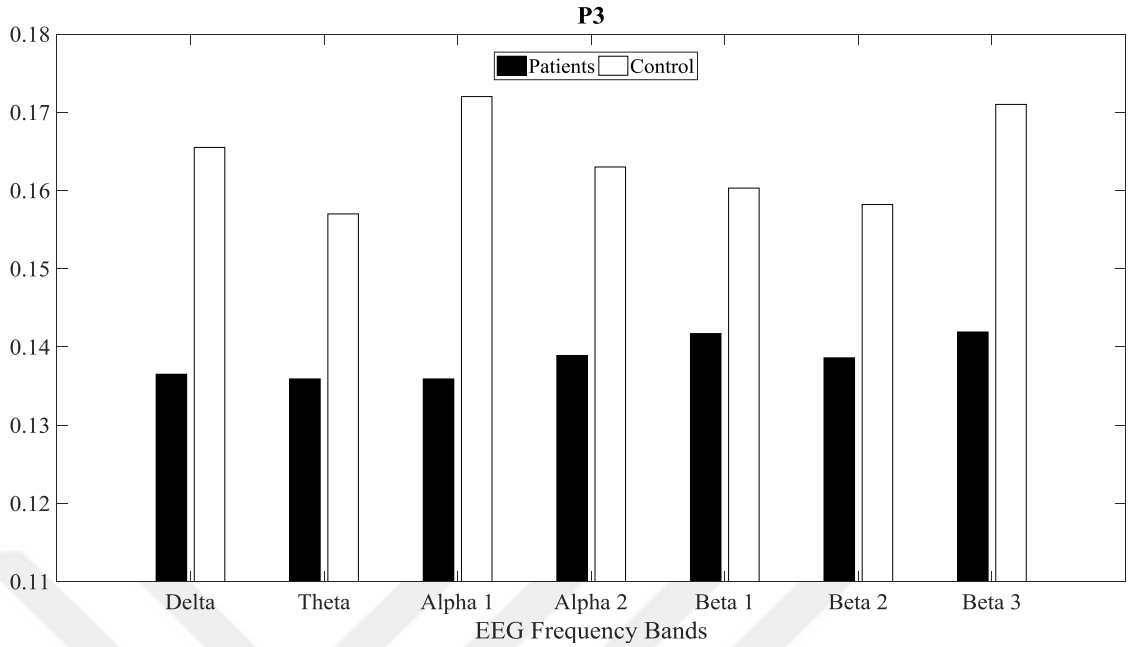

Figure 3.6: Illustration of ITPC analysis results for P3 channel.

Several parameters such as average and standard deviation values of ITPC values was found for every EEG band for O1 channel. Analysis results of OCD patients' data and HCs' data compared between using independent sample t-test. Significantly difference between OCD and HC data was found in delta, theta, alfa1, alfa2, beta1, beta3 bands ($p<0.05$). The results were shown in Table 3.7. Graphical illustration of results can be shown in Figure 3.7.

Table 3.7: ITPC Synchronization Analysis Results of O1 channel.

Frequency bands	**Delta**	**Theta**	**Alpha 1**	**Alpha 2**	**Beta 1**	**Beta 2**	**Beta 3**
Frequency range in Hz	0.0-4.0	4.0-7.0	8.0-10.0	10.0-12.0	12.0-18.0	18.0-21.0	21.0-30.0
Patients' ITPC value	0.1347	0.1311	0.1387	0.1381	0.1413	0.1548	0.1434
Standart Deviation	0.01629	0.01377	0.02048	0.02156	0.00944	0.02563	0.01514
Control Group's ITPC value	0.1738	0.1669	0.1728	0.1587	0.1594	0.1632	0.1709
Standart Deviation	0.03897	0.03845	0.03278	0.03570	0.03591	0,03628	0.03211
p value (2-tailed t test)	**0.0001**	**0.0001**	**0.0001**	**0.019**	**0.019**	0.425	**0.001**
p value (1-tailed t test)	**0.00005**	**0.00005**	**0.00005**	**0.0095**	**0.0095**	0.212	**0.0005**

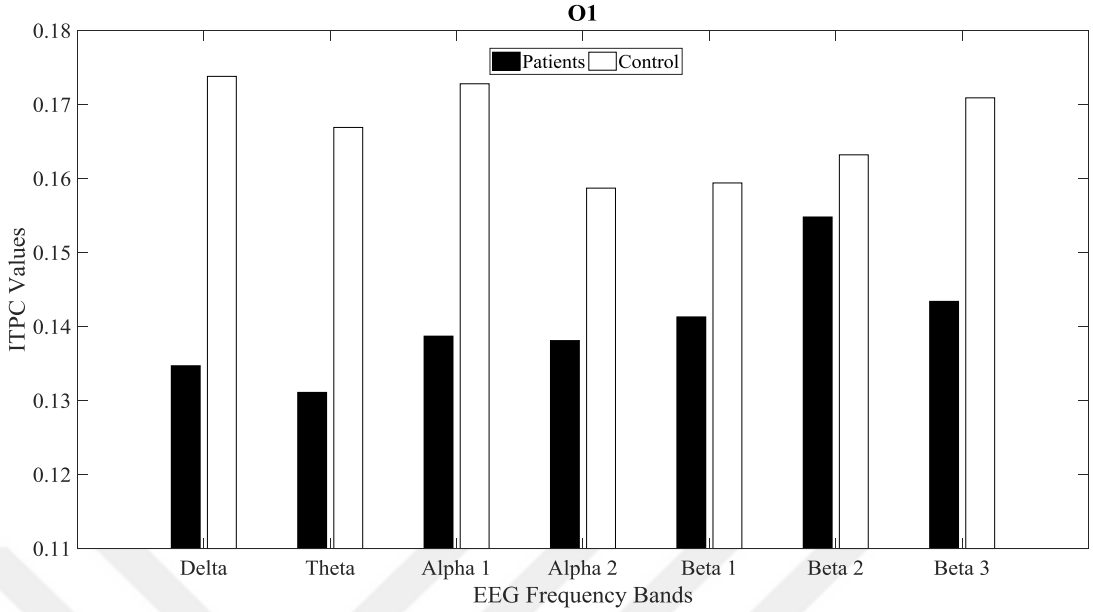

Figure 3.7: Illustration of ITPC analysis results for O1 channel.

Several parameters such as average and standard deviation values of ITPC values was found for every EEG band for F7 channel. Analysis results of OCD patients' data and HCs' data compared between using independent sample t-test. Significantly difference between OCD and HC data was found in all EEG bands ($p<0.03$). The results were shown in Table 3.8. Graphical illustration of results can be shown in Figure 3.8.

Table 3.8: ITPC synchronization analysis results of F7 channel.

Frequency bands	**Delta**	**Theta**	**Alpha 1**	**Alpha 2**	**Beta 1**	**Beta 2**	**Beta 3**
Frequency range in Hz	0.0-4.0	4.0-7.0	8.0-10.0	10.0-12.0	12.0-18.0	18.0-21.0	21.0-30.0
Patients' ITPC value	0.1442	0.1398	0.1412	0.1300	0.1369	0.1410	0.1443
Standart Deviation	0.01072	0.01431	0.01249	0.02386	0.01007	0.01522	0.01498
Control Group's ITPC value	0.1762	0.1758	0.1749	0.1724	0.1682	0.1609	0.1697
Standart Deviation	0.04704	0.03144	0.02928	0.03884	0.03532	0.03780	0.03355
p value (2-tailed t test)	**0.004**	**0.0001**	**0.0001**	**0.0001**	**0.004**	**0.015**	**0.001**
p value (1-tailed t test)	**0.002**	**0.00005**	**0.00005**	**0.00005**	**0.002**	**0.0075**	**0.0005**

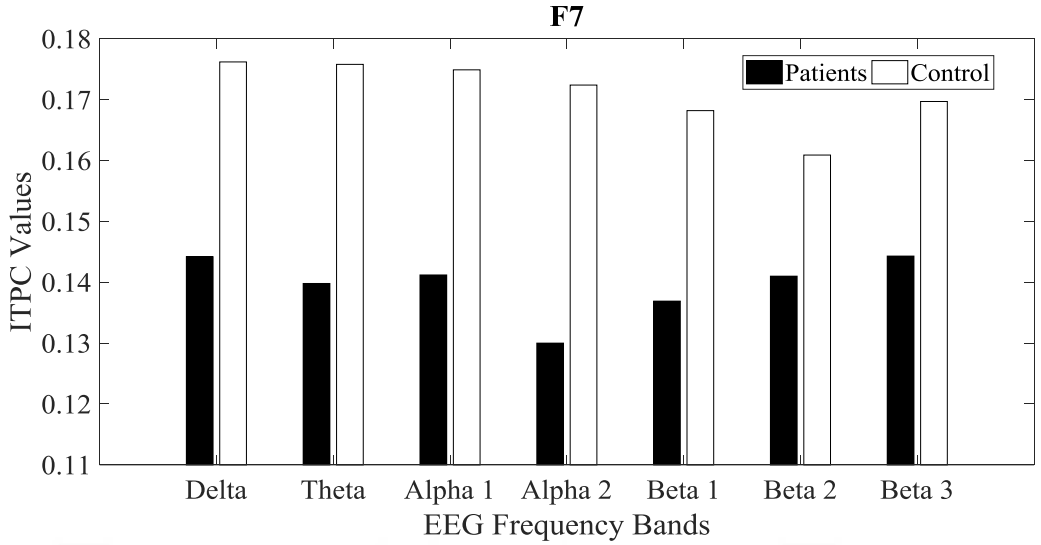

Figure 3.8: Illustration of ITPC analysis results for F7 channel.

Several parameters such as average and standard deviation values of ITPC values was found for every EEG band for T3 channel. Analysis results of OCD patients' data and HCs' data compared between using independent sample t-test. Significantly difference between OCD and HC data was found in all EEG bands ($p<0.0001$). The results were shown in Table 3.9. Graphical illustration of results can be shown in Figure 3.9.

Table 3.9: ITPC synchronization analysis results of T3 channel.

Frequency bands	**Delta**	**Theta**	**Alpha 1**	**Alpha 2**	**Beta 1**	**Beta 2**	**Beta 3**
Frequency range in Hz	0.0-4.0	4.0-7.0	8.0-10.0	10.0-12.0	12.0-18.0	18.0-21.0	21.0-30.0
Patients' ITPC value	0.1399	0.1411	0.1348	0.1308	0.1387	0.1420	0.1361
Standart Deviation	0.01639	0.01735	0.02049	0.01676	0.00980	0.01036	0.01100
Control Group's ITPC value	0.1667	0.1720	0.1704	0.1714	0.1677	0.1697	0.1668
Standart Deviation	0.02955	0.03567	0.03580	0.03507	0.03218	0.03011	0.03279
p value (2-tailed t test)	**0.0001**	**0.0001**	**0.0001**	**0.0001**	**0.0001**	**0.0001**	**0.0001**
p value (1-tailed t test)	**0.00005**	**0.00005**	**0.00005**	**0.00005**	**0.00005**	**0.00005**	**0.00005**

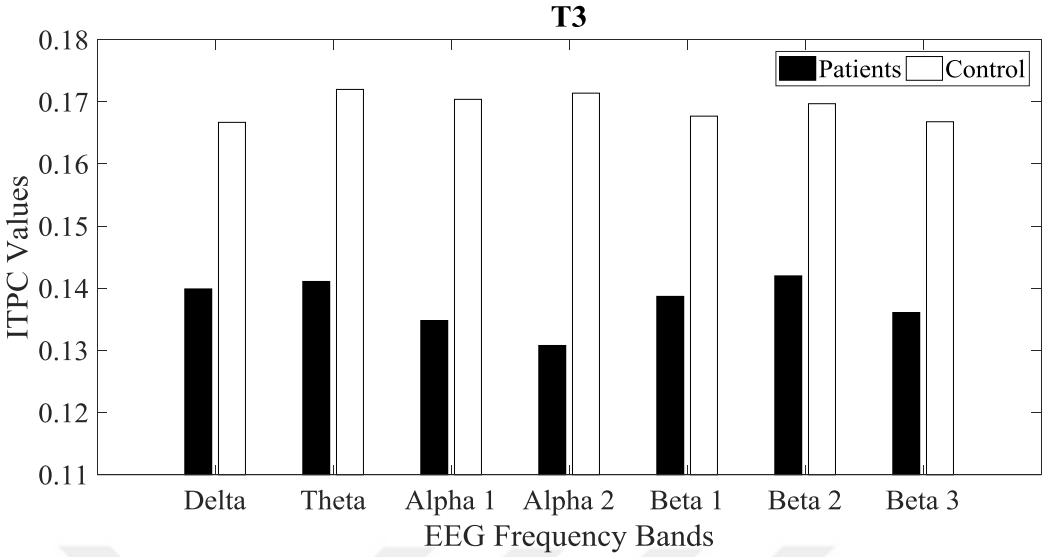

Figure 3.9: Illustration of ITPC analysis results for T3 channel.

Several parameters such as average and standard deviation values of ITPC values was found for every EEG band for T5 channel. Analysis results of OCD patients' data and HCs' data compared between using independent sample t-test. Significantly difference between OCD and HC data was found in all EEG bands ($p<0.05$). The results were shown in Table 3.10. Graphical illustration of results can be shown in Figure 3.10.

Table 3.10: ITPC synchronization analysis results of T5 channel.

Frequency bands	**Delta**	**Theta**	**Alpha 1**	**Alpha 2**	**Beta 1**	**Beta 2**	**Beta 3**
Frequency range in Hz	0.0-4.0	4.0-7.0	8.0-10.0	10.0-12.0	12.0-18.0	18.0-21.0	21.0-30.0
Patients' ITPC value	0.1384	0.1371	0.1370	0.1513	0.1407	0.1416	0.1389
Standart Deviation	0.02270	0.01395	0.01392	0.02021	0.01003	0.00977	0.00867
Control Group's ITPC value	0.1701	0.1765	0.1790	0.1763	0.1724	0.1606	0.1666
Standart Deviation	0.03854	0.03889	0.03442	0.03410	0.03369	0.03744	0.03175
p value (2-tailed t test)	**0.002**	**0.0001**	**0.0001**	**0.008**	**0.0001**	**0.016**	**0.0001**
p value (1-tailed t test)	**0.001**	**0.00005**	**0.00005**	**0.004**	**0.00005**	**0.008**	**0.00005**

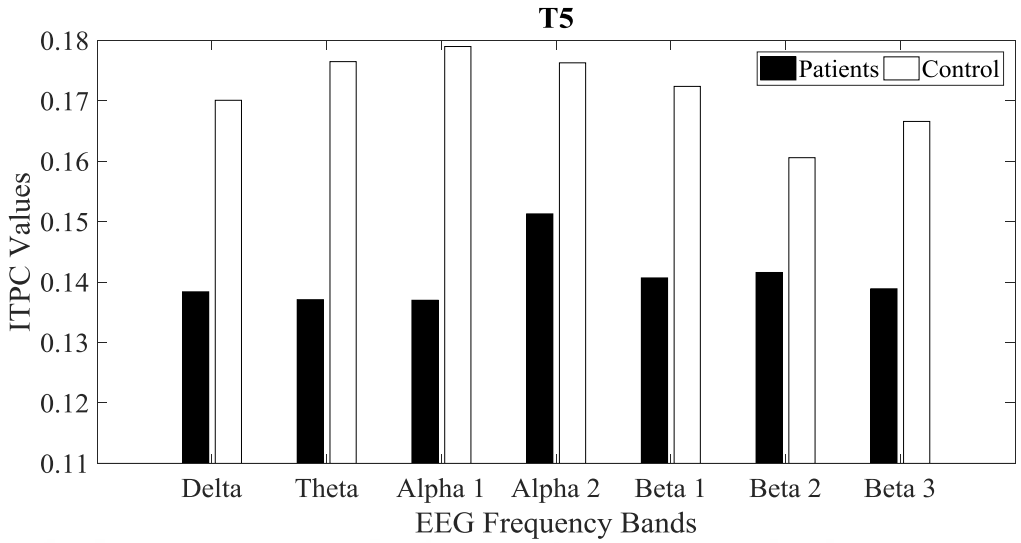

Figure 3.10: Illustration of ITPC analysis results for T5 channel.

Several parameters such as average and standard deviation values of ITPC values was found for every EEG band for Fp2 channel. Analysis results of OCD patients' data and HCs' data compared between using independent sample t-test. Significantly difference between OCD and HC data was found in all EEG bands ($p<0.01$). The results were shown in Table 3.11. Graphical illustration of results can be shown in Figure 3.11.

Table 3.11: ITPC synchronization analysis results of Fp2 channel.

Frequency bands	**Delta**	**Theta**	**Alpha 1**	**Alpha 2**	**Beta 1**	**Beta 2**	**Beta 3**
Frequency range in Hz	0.0-4.0	4.0-7.0	8.0-10.0	10.0-12.0	12.0-18.0	18.0-21.0	21.0-30.0
Patients' ITPC value	0.1301	0.1393	0.1300	0.1170	0.1306	0.1388	0.1366
Standart Deviation	0.01214	0.01577	0.01734	0.01920	0.00927	0.00591	0.01046
Control Group's ITPC value	0.1804	0.1737	0.1727	0.1723	0.1673	0.1774	0.1730
Standart Deviation	0.03483	0.03073	0.03026	0.02693	0.00927	0.03407	0.3016
p value (2-tailed t test)	**0.0001**	**0.0001**	**0.0001**	**0.0001**	**0.0001**	**0.0001**	**0.0001**
p value (1-tailed t test)	**0.00005**	**0.00005**	**0.00005**	**0.00005**	**0.00005**	**0.00005**	**0.00005**

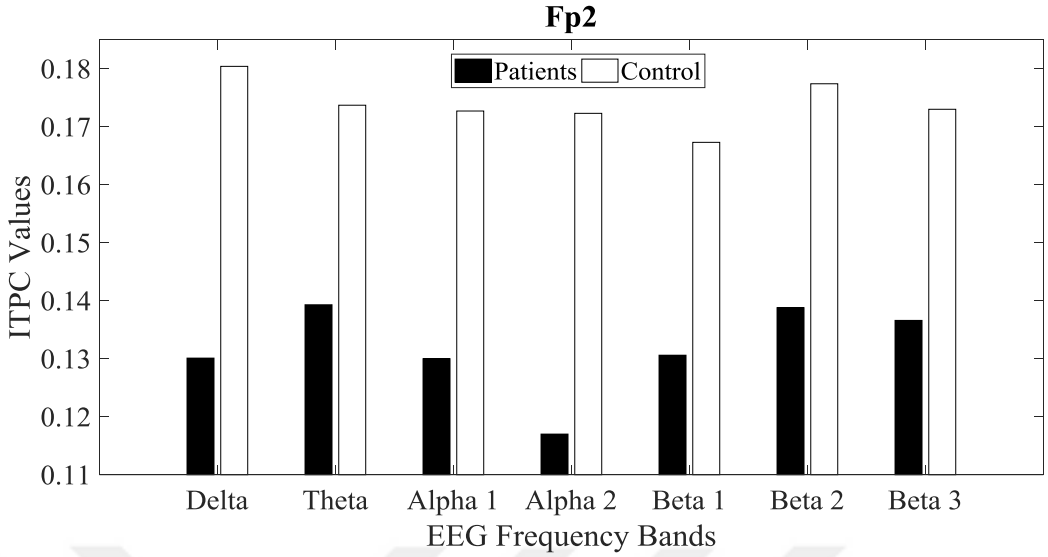

Figure 3.11: Illustration of ITPC analysis results for Fp2 channel.

Several parameters such as average and standard deviation values of ITPC values was found for every EEG band for F4 channel. Analysis results of OCD patients' data and HCs' data compared between using independent sample t-test. Significantly difference between OCD and HC data was found in all EEG bands ($p<0.01$). The results were shown in Table 3.12. Graphical illustration of results can be shown in Figure 3.12.

Table 3.12: ITPC synchronization analysis results of F4 channel.

Frequency bands	**Delta**	**Theta**	**Alpha 1**	**Alpha 2**	**Beta 1**	**Beta 2**	**Beta 3**
Frequency range in Hz	0.0-4.0	4.0-7.0	8.0-10.0	10.0-12.0	12.0-18.0	18.0-21.0	21.0-30.0
Patients' ITPC value	0.1310	0.1351	0.1308	0.1253	0.1337	0.1336	0.1419
Standart Deviation	0.00912	0.00971	0.01391	0.01680	0.00905	0.00798	0.00999
Control Group's ITPC value	0.1722	0.1734	0.1741	0.1714	0.1690	0.1773	0.1681
Standart Deviation	0.03665	0.02954	0.02892	0.02920	0.03118	0.03528	0.03070
p value (2-tailed t test)	**0.0001**	**0.0001**	**0.0001**	**0.0001**	**0.0001**	**0.0001**	**0.0001**
p value (1-tailed t test)	**0.00005**	**0.00005**	**0.00005**	**0.00005**	**0.00005**	**0.00005**	**0.00005**

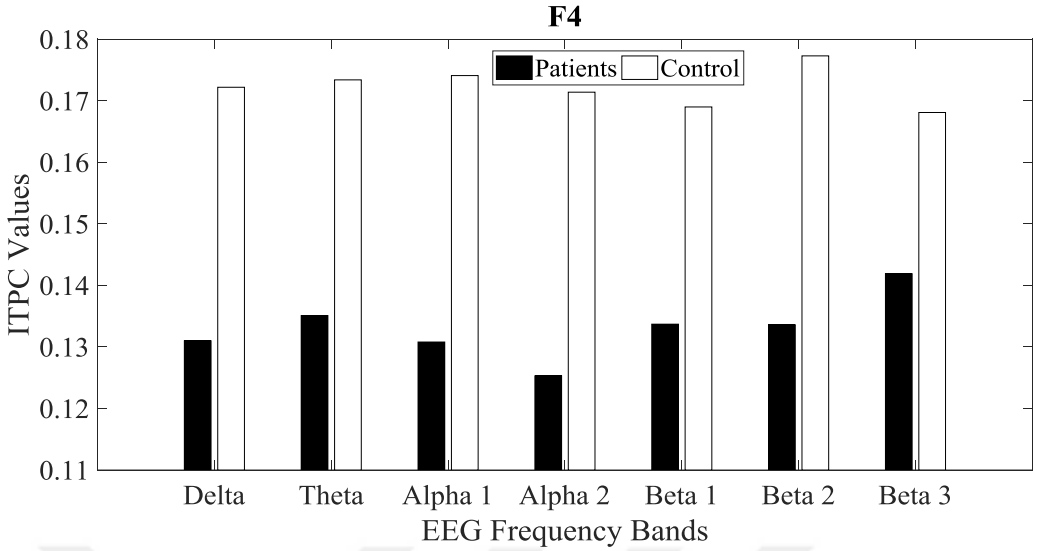

Figure 3.12: Illustration of ITPC analysis results for F4 channel.

Several parameters such as average and standard deviation values of ITPC values was found for every EEG band for C4 channel. Analysis results of OCD patients' data and HCs' data compared between using independent sample t-test. Significantly difference between OCD and HC data was found in all EEG bands ($p<0.01$). The results were shown in Table 3.13. Graphical illustration of results can be shown in Figure 3.13.

Table 3.13: ITPC synchronization analysis results of C4 channel.

Frequency bands	**Delta**	**Theta**	**Alpha 1**	**Alpha 2**	**Beta 1**	**Beta 2**	**Beta 3**
Frequency range in Hz	0.0-4.0	4.0-7.0	8.0-10.0	10.0-12.0	12.0-18.0	18.0-21.0	21.0-30.0
Patients' ITPC value	0.1389	0.1368	0.1309	0.1320	0.1362	0.1386	0.1437
Standart Deviation	0.01406	0.01223	0.01250	0.01685	0.01383	0.01418	0.01366
Control Group's ITPC value	0.1694	0.1664	0.1704	0.1640	0.1668	0.1659	0.1682
Standart Deviation	0.03016	0.02818	0.03743	0.4324	0.03087	0.03011	0.02968
p value (2-tailed t test)	**0.0001**	**0.0001**	**0.0001**	**0.002**	**0.0001**	**0.0001**	**0.001**
p value (1-tailed t test)	**0.00005**	**0.00005**	**0.00005**	**0.001**	**0.00005**	**0.00005**	**0.0005**

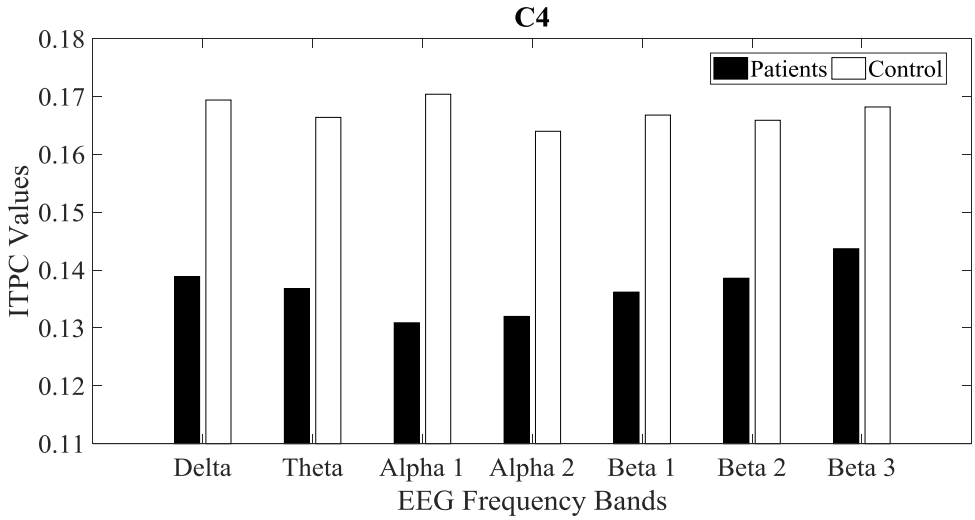

Figure 3.13: Illustration of ITPC analysis results for C4 channel.

Several parameters such as average and standard deviation values of ITPC values was found for every EEG band for P4 channel. Analysis results of OCD patients' data and HCs' data compared between using independent sample t-test. Significantly difference between OCD and HC data was found in all EEG bands ($p<0.01$). The results were shown in Table 3.14. Graphical illustration of results can be shown in Figure 3.14.

Table 3.14: ITPC synchronization analysis results of P4 channel.

Frequency bands	**Delta**	**Theta**	**Alpha 1**	**Alpha 2**	**Beta 1**	**Beta 2**	**Beta 3**
Frequency range in Hz	0.0-4.0	4.0-7.0	8.0-10.0	10.0-12.0	12.0-18.0	18.0-21.0	21.0-30.0
Patients' ITPC value	0.1404	0.1412	0.1315	0.1484	0.1407	0.1462	0.1461
Standart Deviation	0.01416	0.01747	0.01587	0.03145	0.01676	0.02225	0.02121
Control Group's ITPC value	0.1695	0.1648	0.1769	0.1757	0.1721	0.1715	0.1684
Standart Deviation	0.03623	0.03260	0.03285	0.03709	0.03871	0.03811	0.03252
p value (2-tailed t test)	**0.01**	**0.002**	**0.0001**	**0.009**	**0.001**	**0.006**	**0.006**
p value (1-tailed t test)	**0.005**	**0.001**	**0.00005**	**0.0045**	**0.0005**	**0.003**	**0.003**

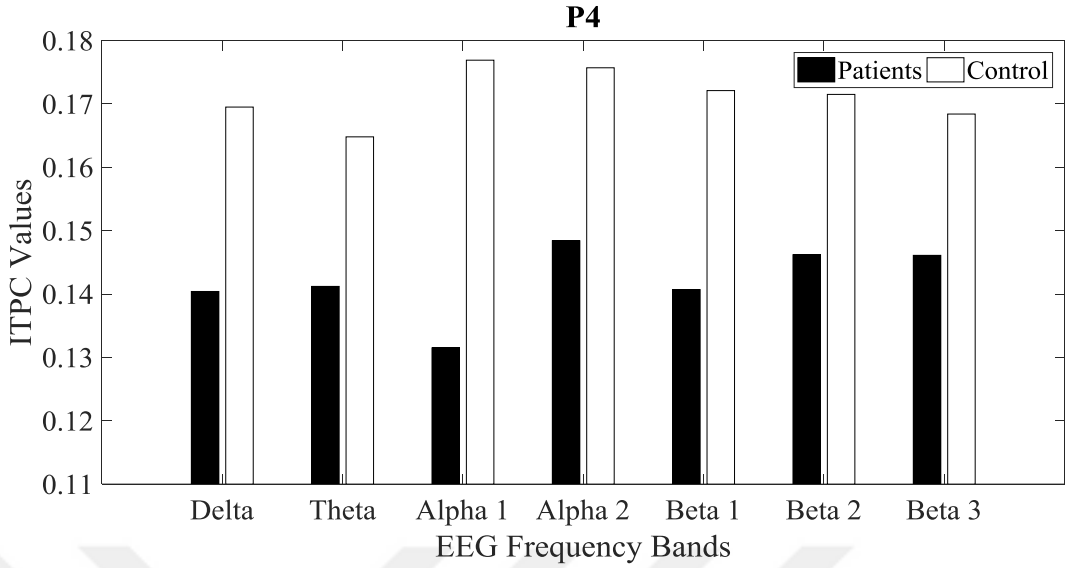

Figure 3.14: Illustration of ITPC analysis results for P4 channel.

Several parameters such as average and standard deviation values of ITPC values was found for every EEG band for O2 channel. Analysis results of OCD patients' data and HCs' data compared between using independent sample t-test. Significantly difference between OCD and HC data was found in all EEG bands ($p<0.01$). The results were shown in Table 3.15. Graphical illustration of results can be shown in Figure 3.15.

Table 3.15: ITPC synchronization analysis results of O2 channel.

Frequency bands	**Delta**	**Theta**	**Alpha 1**	**Alpha 2**	**Beta 1**	**Beta 2**	**Beta 3**
Frequency range in Hz	0.0-4.0	4.0-7.0	8.0-10.0	10.0-12.0	12.0-18.0	18.0-21.0	21.0-30.0
Patients' ITPC value	0.1412	0.1389	0.1405	0.1407	0.1465	0.1418	0.1438
Standart Deviation	0.01698	0.01436	0.02225	0.02212	0.01614	0.01217	0.01468
Control Group's ITPC value	0.1687	0.1660	0.1724	0.1726	0.1668	0.1710	0.1656
Standart Deviation	0.03773	0.03692	0.02851	0.03678	0.03509	0.03658	0.03178
p value (2-tailed t test)	**0.002**	**0.001**	**0.0001**	**0.001**	**0.014**	**0.0001**	**0.003**
p value (1-tailed t test)	**0.001**	**0.0005**	**0.00005**	**0.0005**	**0.007**	**0.00005**	**0.0015**

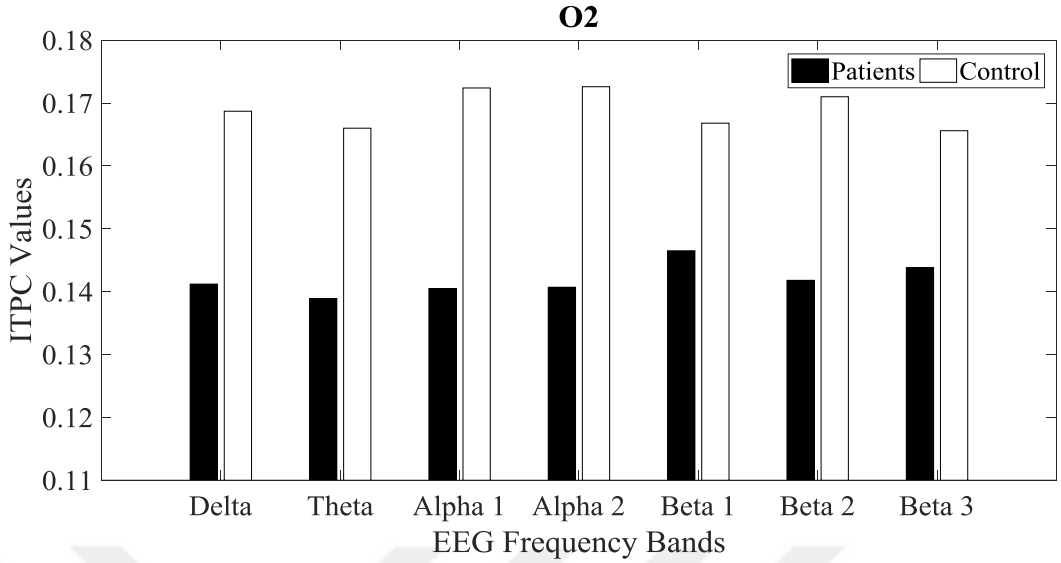

Figure 3.15: Illustration of ITPC analysis results for O2 channel.

Several parameters such as average and standard deviation values of ITPC values was found for every EEG band for F8 channel. Analysis results of OCD patients' data and HCs' data compared between using independent sample t-test. Significantly difference between OCD and HC data was found in all EEG bands ($p<0.01$). The results were shown in Table 3.16. Graphical illustration of results can be shown in Figure 3.16.

Table 3.16: ITPC synchronization analysis results of F8 channel.

Frequency bands	**Delta**	**Theta**	**Alpha 1**	**Alpha 2**	**Beta 1**	**Beta 2**	**Beta 3**
Frequency range in Hz	0.0-4.0	4.0-7.0	8.0-10.0	10.0-12.0	12.0-18.0	18.0-21.0	21.0-30.0
Patients' ITPC value	0.1387	0.1419	0.1489	0.1403	0.1460	0.1491	0.1463
Standart Deviation	0.01244	0.01988	0.03023	0.02448	0.01944	0.02318	0.01553
Control Group's ITPC value	0.1753	0.1672	0.1649	0.1590	0.1688	0.1708	0.1672
Standart Deviation	0.03862	0.03504	0.03035	0.02991	0.03041	0.03543	0.03370
p value (2-tailed t test)	**0.0001**	**0.03**	**0.03**	**0.017**	**0.002**	**0.008**	**0.005**
p value (1-tailed t test)	**0.00005**	**0.015**	**0.015**	**0.0085**	**0.001**	**0.004**	**0.0025**

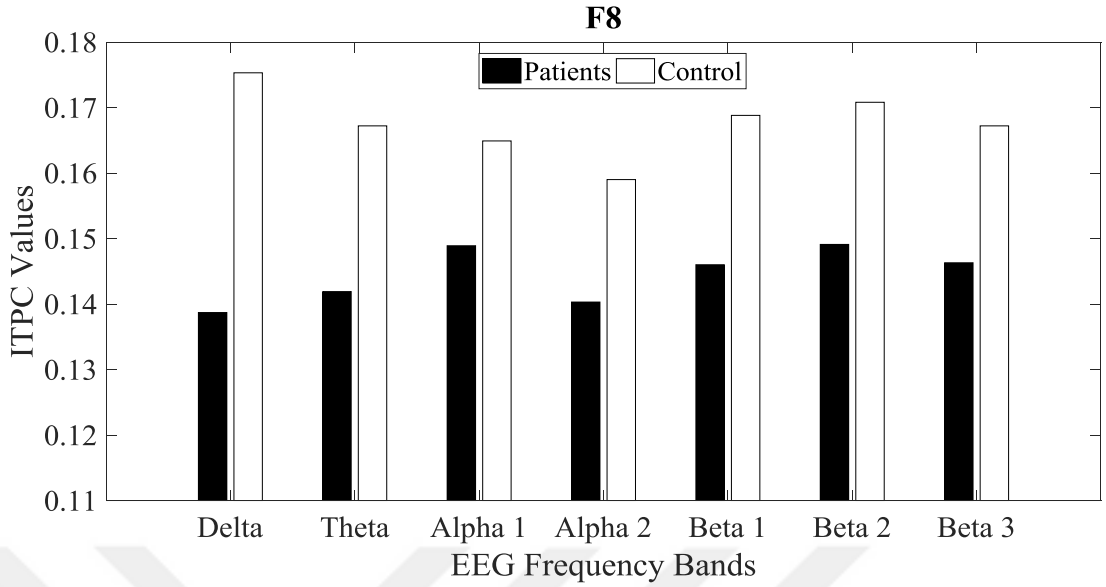

Figure 3.16: Illustration of ITPC analysis results for F8 channel.

Several parameters such as average and standard deviation values of ITPC values was found for every EEG band for T4 channel. Analysis results of OCD patients' data and HCs' data compared between using independent sample t-test. Significantly difference between OCD and HC data was found in all EEG bands ($p<0.01$). The results were shown in Table 3.17. Graphical illustration of results can be shown in Figure 3.17.

Table 3.17: ITPC synchronization analysis results of T4 channel.

Frequency bands	**Delta**	**Theta**	**Alpha 1**	**Alpha 2**	**Beta 1**	**Beta 2**	**Beta 3**
Frequency range in Hz	0.0-4.0	4.0-7.0	8.0-10.0	10.0-12.0	12.0-18.0	18.0-21.0	21.0-30.0
Patients' ITPC value	0.1396	0.1413	0.1411	0.1359	0.1391	0.1407	0.1419
Standart Deviation	0.01880	0.01520	0.2158	0.01854	0.01594	0.01587	0.01686
Control Group's ITPC value	0.1723	0.1692	0.1714	0.1644	0.1686	0.1680	0.1642
Standart Deviation	0.03936	0.03403	0.03250	0.02972	0.02690	0.02863	0.03275
p value (2-tailed t test)	**0.0001**	**0.001**	**0.0001**	**0.0001**	**0.0001**	**0.0001**	**0.003**
p value (1-tailed t test)	**0.00005**	**0.0005**	**0.00005**	**0.00005**	**0.00005**	**0.00005**	**0.0015**

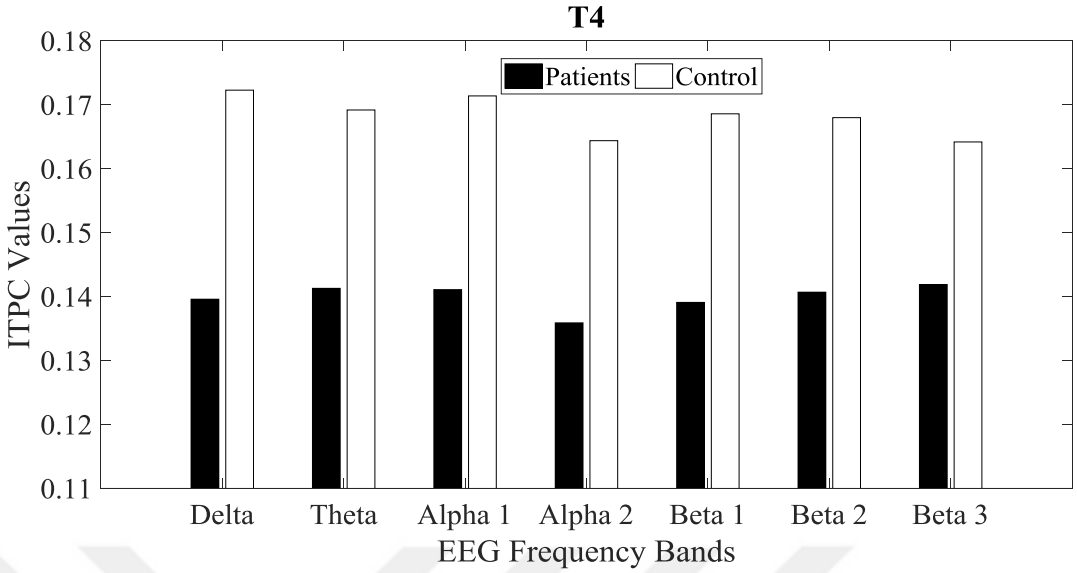

Figure 3.17: Illustration of ITPC analysis results for T4 channel.

Several parameters such as average and standard deviation values of ITPC values was found for every EEG band for T6 channel. Analysis results of OCD patients' data and HCs' data compared between using independent sample t-test. Significantly difference between OCD and HC data was found in delta, alpha1, alpha2, beta1, beta2 and beta 3 EEG bands ($p<0.01$). The results were shown in Table 3.18. Graphical illustration of results can be shown in Figure 3.18

Table 3.18: ITPC synchronization analysis results of T6 channel.

Frequency bands	**Delta**	**Theta**	**Alpha 1**	**Alpha 2**	**Beta 1**	**Beta 2**	**Beta 3**
Frequency range in Hz	0.0-4.0	4.0-7.0	8.0-10.0	10.0-12.0	12.0-18.0	18.0-21.0	21.0-30.0
Patients' ITPC value	0.1400	0.1460	0.1420	0.1449	0.1480	0.1490	0.1466
Standart Deviation	0.02480	0.02568	0.02139	0.02156	0.01725	0.02072	0.01678
Control Group's ITPC value	0.1695	0.1610	0.1682	0.1677	0.1682	0.1672	0.1637
Standart Deviation	0.03527	0.03843	0.02509	0.02953	0.03731	0.1490	0.3395
p value (2-tailed t test)	**0.001**	0.102	**0.0001**	**0.003**	**0.013**	**0.025**	**0.023**
p value (1-tailed t test)	**0.0005**	0.051	**0.00005**	**0.0015**	**0.0065**	**0.0125**	**0.0115**

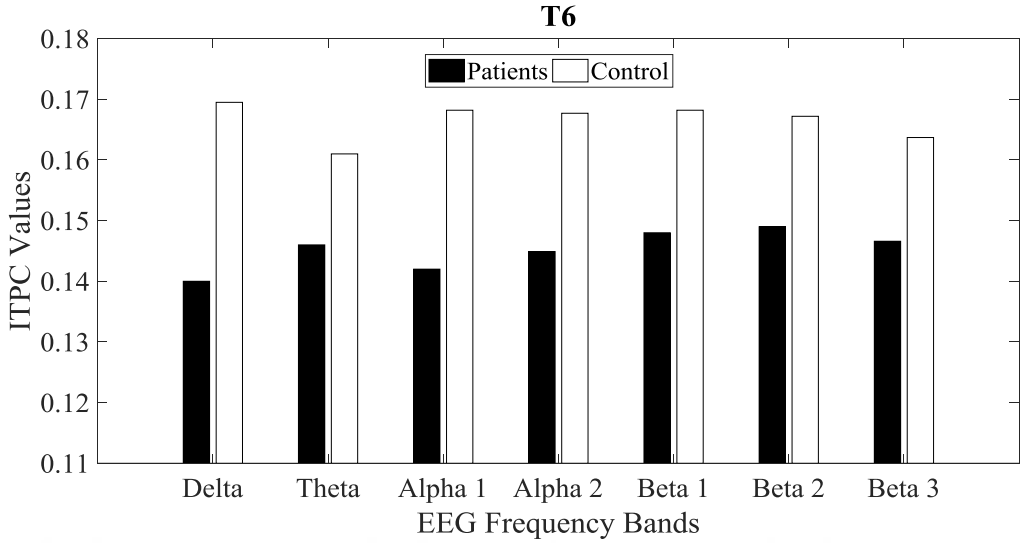

Figure 3.18: Illustration of ITPC analysis results for T6 channel.

Several parameters such as average and standard deviation values of ITPC values was found for every EEG band for Fz channel. Analysis results of OCD patients' data and HCs' data compared between using independent sample t-test. Significantly difference between OCD and HC data was found in all EEG bands ($p<0.01$). The results were shown in Table 3.19. Graphical illustration of results can be shown in Figure 3.19.

Table 3.19: ITPC synchronization analysis results of Fz channel.

Frequency bands	**Delta**	**Theta**	**Alpha 1**	**Alpha 2**	**Beta 1**	**Beta 2**	**Beta 3**
Frequency range in Hz	0.0-4.0	4.0-7.0	8.0-10.0	10.0-12.0	12.0-18.0	18.0-21.0	21.0-30.0
Patients' ITPC value	0.1530	0.1463	0.1391	0.1371	0.1367	0.1443	0.1468
Standart Deviation	0.02179	0.01784	0.01934	0.03097	0.01496	0.01815	0.01522
Control Group's ITPC value	0.1785	0.1629	0.1674	0.1665	0.1626	0.1676	0.1622
Standart Deviation	0.04405	0.03181	0.03014	0.02944	0.02768	0.03093	0.03590
p value (2-tailed t test)	**0.005**	**0.023**	**0.0001**	**0.001**	**0.0001**	**0.001**	**0.030**
p value (1-tailed t test)	**0.0025**	**0.0115**	**0.00005**	**0.0005**	**0.00005**	**0.0005**	**0.015**

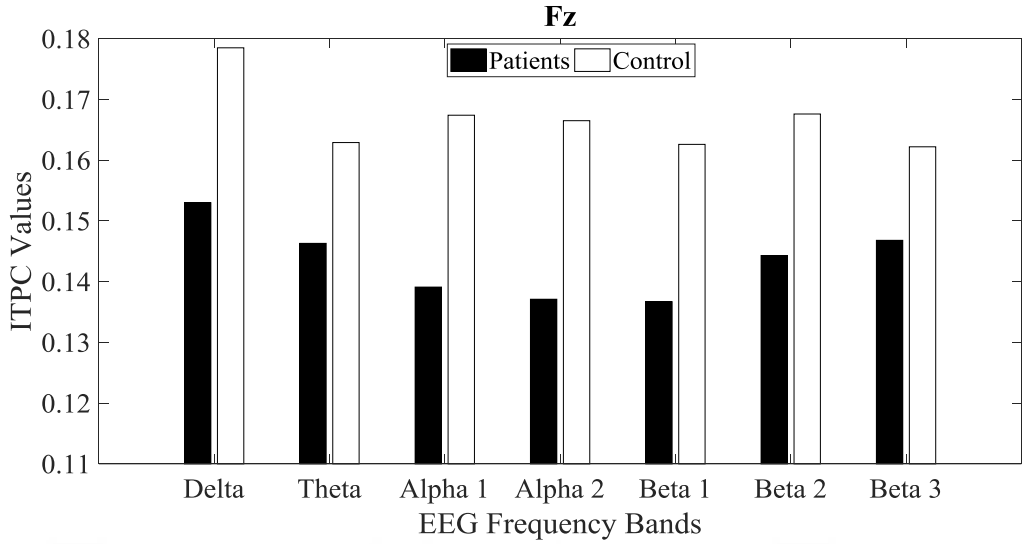

Figure 3.19: Illustration of ITPC analysis results for Fz channel.

Several parameters such as average and standard deviation values of ITPC values was found for every EEG band for Cz channel. Analysis results of OCD patients' data and HCs' data compared between using independent sample t-test. Significantly difference between OCD and HC data was found in all EEG bands ($p<0.01$). The results were shown in Table 3.20. Graphical illustration of results can be shown in Figure 3.20.

Table 3.20: ITPC synchronization analysis results of Cz channel.

Frequency bands	**Delta**	**Theta**	**Alpha 1**	**Alpha 2**	**Beta 1**	**Beta 2**	**Beta 3**
Frequency range in Hz	0.0-4.0	4.0-7.0	8.0-10.0	10.0-12.0	12.0-18.0	18.0-21.0	21.0-30.0
Patients' ITPC value	0.1387	0.1386	0.1396	0.1351	0.1352	0.01440	0.1444
Standart Deviation	0.01706	0.01926	0.02335	0.01696	0.01342	0.01440	0.01342
Control Group's ITPC value	0.1761	0.1573	0.1658	0.1621	0.1519	0.1630	0.1641
Standart Deviation	0.04090	0.02631	0.03357	0.04111	0.03080	0.03174	0.03101
p value (2-tailed t test)	**0.0001**	**0.011**	**0.002**	**0.004**	**0.019**	**0.003**	**0.004**
p value (1-tailed t test)	**0.00005**	**0.0055**	**0.001**	**0.002**	**0.0095**	**0.0015**	**0.002**

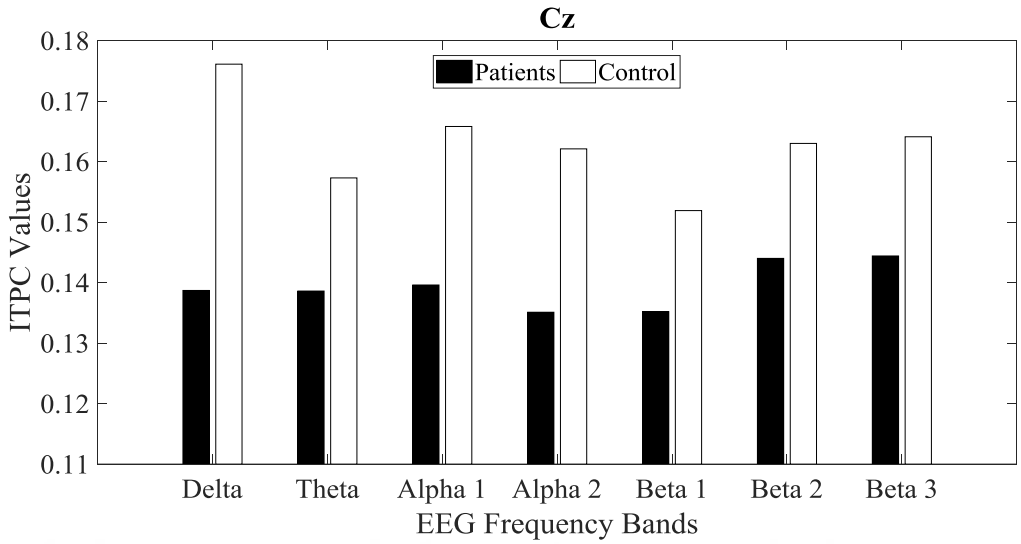

Figure 3.20: Illustration of ITPC analysis results for Cz channel.

Several parameters such as average and standard deviation values of ITPC values was found for every EEG band for Pz channel. Analysis results of OCD patients' data and HCs' data compared between using independent sample t-test. Significantly difference between OCD and HCs data was found in all EEG bands ($p<0.01$). The results were shown in Table 3.21. Graphical illustration of results can be shown in Figure 3.21.

Table 3.21: ITPC synchronization analysis results of Pz channel.

Frequency bands	**Delta**	**Theta**	**Alpha 1**	**Alpha 2**	**Beta 1**	**Beta 2**	**Beta 3**
Frequency range in Hz	0.0-4.0	4.0-7.0	8.0-10.0	10.0-12.0	12.0-18.0	18.0-21.0	21.0-30.0
Patients' ITPC value	0.1462	0.1436	0.1401	0.1406	0.1406	0.1402	0.1444
Standart Deviation	0.01996	0.01926	0.01982	0.02080	0.01683	0.01302	0.01773
Control Group's ITPC value	0.1673	0.1665	0.1697	0.1717	0.1635	0.1630	0.1651
Standart Deviation	0.03363	0.03588	0.03306	0.03320	0.03775	0.03580	0.03219
p value (2-tailed t test)	**0.006**	**0.007**	**0.0001**	**0.0001**	**0.007**	**0.004**	**0.005**
p value (1-tailed t test)	**0.003**	**0.0035**	**0.00005**	**0.00005**	**0.0035**	**0.002**	**0.0025**

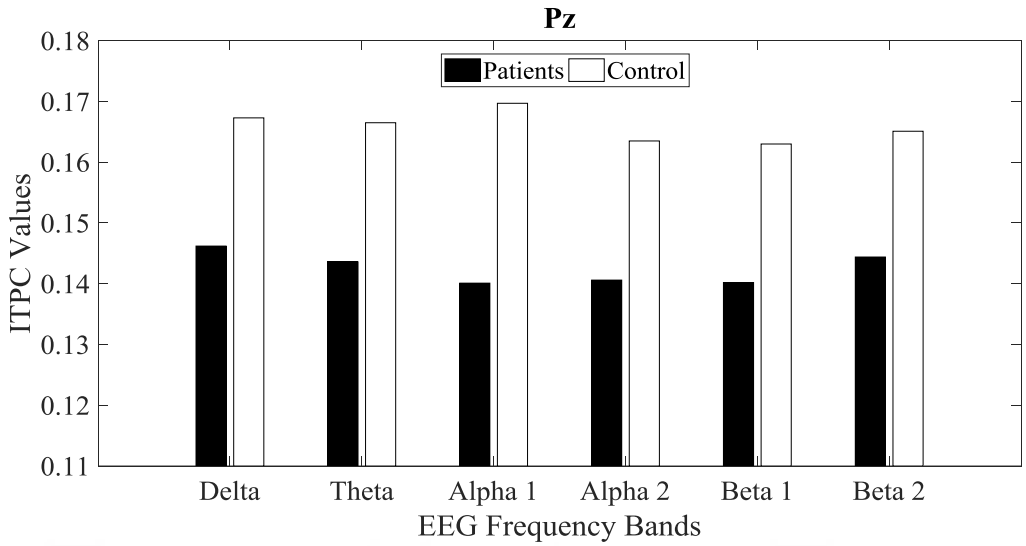

Figure 3.21: Illustration of ITPC analysis results for Pz channel.

3.3. CLASSIFICATION PERFORMANCE OF FEATURES

Classification algorithms have been used for identifying to which set of values belongs, based on a training set of data containing observations whose group membership is known. Classification results was used to support the reliability of the results. SVM method that is one of the most convenient and efficient classification method was used for classifying the synchronization values and setting auto-detection and auto-tracking system.

In the classification process, the leave one out cross-validation method was employed for determining the training and testing features. In every iteration process, one of the features was used for test data and the others were used for training data. Thus, each data sample was used for both training and testing, so that the training and testing data selection process was done objectively. In order to robustly evaluate the estimation quality, classification was performed using five different parameters that will be explained in the following lines;

- Sensitivity can be determined as a ratio of number of correctly classified as patient and total patients.

- Specificity is determined as a ratio of number of correctly classified HCs and total HCs.

- Accuracy shows the correctly classified data in the complete labelled dataset (both true and false).

- Precision is the ratio of successfully labelled patients in the total samples that were detected as an OCD patient to those that were not detected.

- The F score is determined as a sub-contrary means of recall besides that of precision.

The GFS values of frontal channels that were computed for all epochs. The number of features was used for SVM classification computed as following:

Firstly, 3 minutes EEG data divided to 4 seconds epochs (trials) for facilitating the analysis. Synchronization values (GFS and ITPC) was computed for each epoch separately. Thus 45 features were obtained by only one subject (OCD or HCs). The analysis repeated for every band with as many as the number of subjects (45x64=2880). Some of these features were used as training set and the others used as prediction values.

3.3.1. Classification Performance of Frontal GFS Analysis Results with SVM

Synchronization degree of frontal lobe was calculated by GFS method for only 6 electrodes that placed on frontal site such as Fp1, Fp2, F7, F3, F4 and F8. As a result of statistical analysis, significantly difference was found between HCs and OCD patients in delta ($p<0.001$) and beta 3 ($p<0.005$). Therefore, only synchronization values of these two band (Delta and Beta3) were classified by SVM. Classification parameters of feature values is given in Table 3.22. Receiver Operating Characteristic Curve (ROC) graphic analysis of the classification results are demonstrated in Figure 3.22.

Table 3.22: The values of statistical parameters for frontal GFS analysis.

Frequency Bands	Sensitivity	Specificity	Precision	F-Score	Accuracy
Delta	97.66	93.29	92.95	95.42	95.37
Beta 3	95.93	94.94	95.28	95.43	95.48

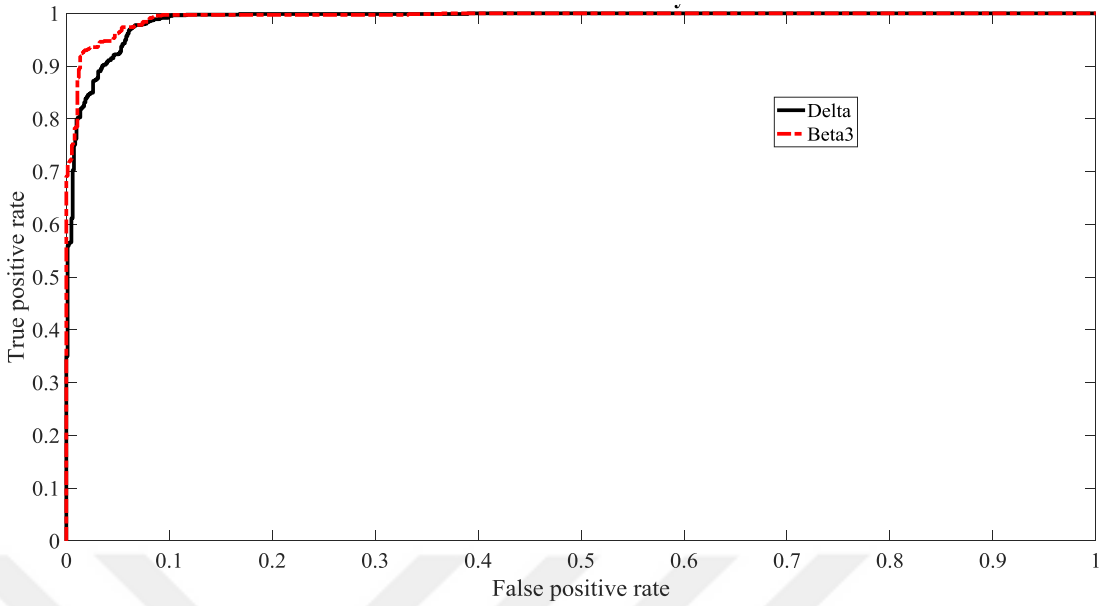

Figure 3.22: ROC curve of classifiers for frontal GFS analysis.

The Area Under Curve (AUC) value is determined as the area under the ROC curve. The AUC value always lies between '0' and '1'. If the value is close to '1', this is interpreted as the excellent classifier system but in the other case where the AUC value is near zero this is interpreted as a bad classifier system.

3.3.2. Classification Performance of Whole Brain GFS Analysis Results with SVM

Synchronization power of whole brain was computed by GFS method for all electrodes that placed on skull. At the end of the statistical analysis, statistical reduction was found in OCD patients for delta ($p<0.01$) and beta 2 ($p<0.005$). Therefore, only synchronization values of these two band (delta and beta 2) were classified by SVM. Classification parameters of feature values is given in Table 3.23. ROC graphic analysis of the classification results are demonstrated in Figure 3.23.

Table 3.23: The values of statistical parameters for GFS analysis.

Frequency Bands	Sensitivity	Specificity	Precision	F-Score	Accuracy
Delta	96.32	93.05	92.32	94.67	94.57
Beta 2	94.05	94.82	94.45	94.43	94.44

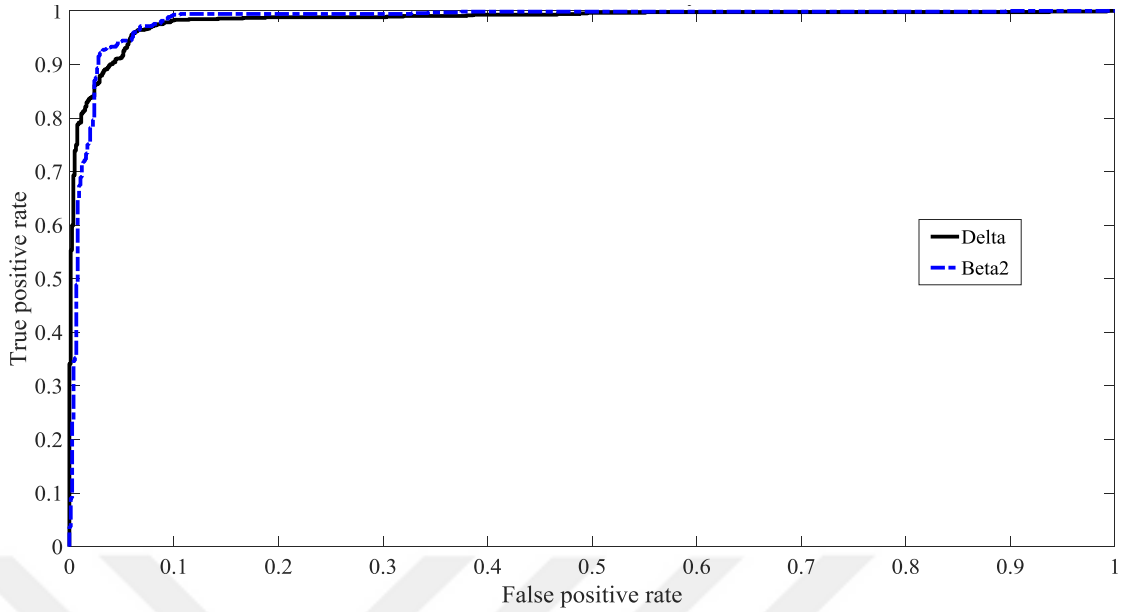

Figure 3.23: ROC curve of classifiers for GFS analysis.

3.3.3. Classification Performance of All Channels Synchronization Values with SVM

Synchronization power of Fp1 channel was calculated with ITPC method and statistically decreased phase coupling was found in OCD patients for all EEG band. These results were classified with SVM method. Training and testing data was determined by using Leave-subject-out CVM. It is reached to very successful parameters as a result of the classification process. Main statistical parameters of classification were given in Table 3.24 and ROC curve of the results was illustrated in Figure 3.24.

Table 3.24: The values of statistical parameters for Fp1 channel.

Frequency Bands	Sensitivity	Specificity	Precision	F-Score	Accuracy
Delta	95.78	91.36	91.11	93.52	93.48
Theta	90.63	84.44	84.26	87.43	87.40
Alpha 1	82.26	96.83	96.25	88.95	89.58
Alpha 2	93.85	95.98	95.82	94.91	94.93
Beta 1	95.74	93.88	91.52	94.80	94.64
Beta 2	95.80	96.94	98.09	96.37	96.23
Beta 3	88.30	92.55	92.07	90.37	90.44

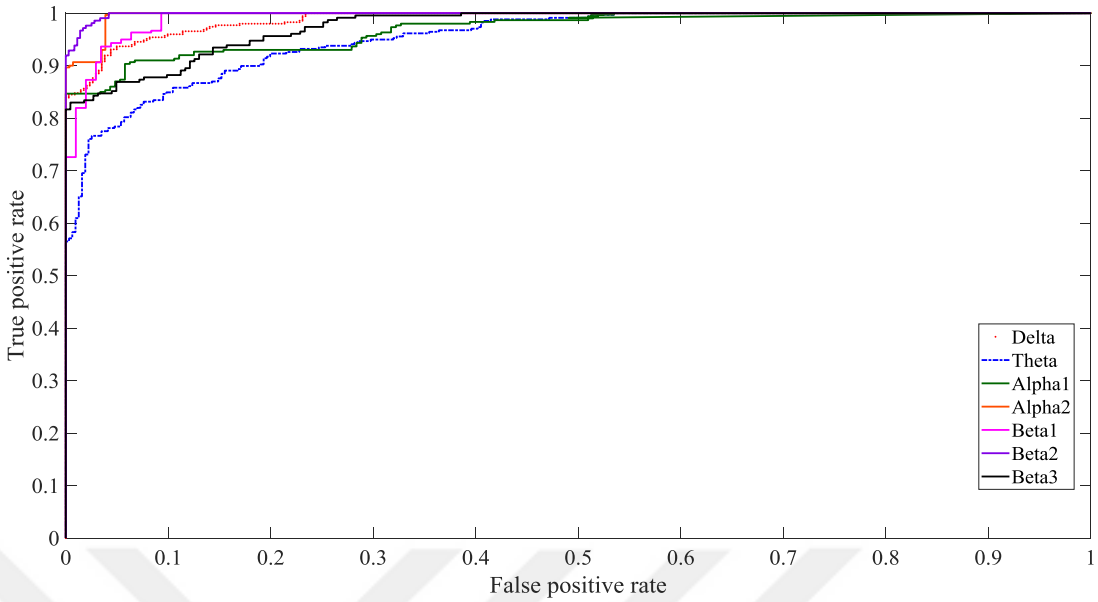

Figure 3.24: ROC curves of classifier for Fp1 band.

Synchronization power of F3 channel was calculated with ITPC method and statistically decreased phase coupling was found in OCD patients for all EEG band. These results were classified with SVM method. Training and testing data was determined by using Leave-subject-out CVM. It is reached to very successful parameters as a result of the classification process. Main statistical parameters of classification were given in Table 3.25 and ROC curve of the results was illustrated in Figure 3.25.

Table 3.25: The values of statistical parameters for F3 band.

Frequency Bands	Sensitivity	Specificity	Precision	F-Score	Accuracy
Delta	97.77	92.20	95.65	94.91	95.75
Theta	100	90.58	88.11	95.06	94.45
Alpha 1	97.43	88.44	90.83	92.72	93.30
Alpha 2	89.95	99.10	98.94	94.30	94.68
Beta 1	100	90.94	90.54	95.25	95.15
Beta 2	97.93	98.45	96.59	98.19	98.29
Beta 3	100	98.41	98.19	99.20	99.14

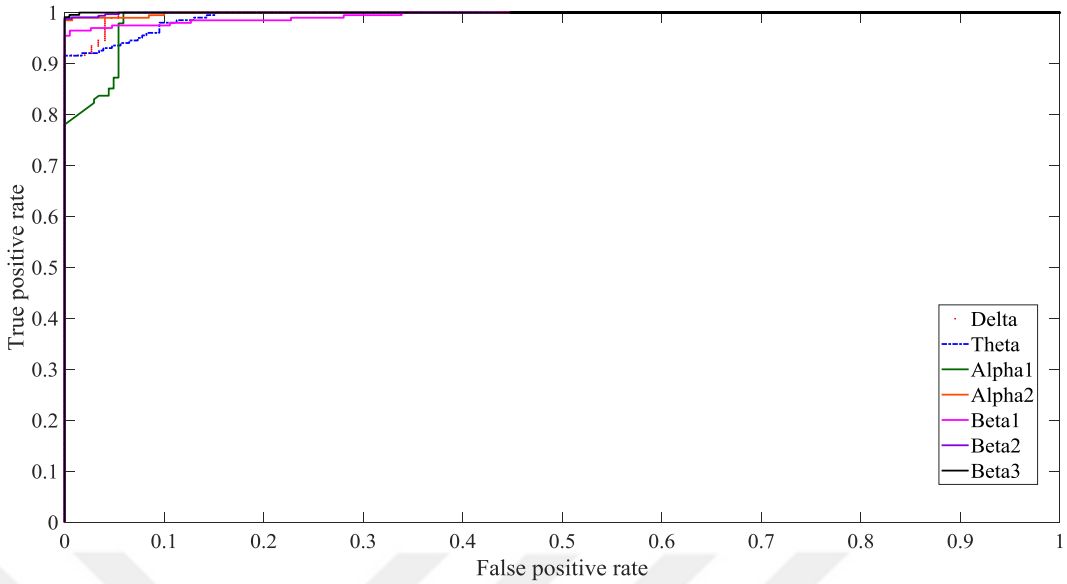

Figure 3.25: ROC curves of classifier for F3 band.

Synchronization power of C3 channel was calculated with ITPC method and statistically decreased phase coupling was found in OCD patients for all EEG band. These results were classified with SVM method. Training and testing data was determined by using Leave-subject-out CVM. It is reached to very successful parameters as a result of the classification process. Main statistical parameters of classification were given in Table 3.26 and ROC curve of the results was illustrated in Figure 3.26.

Table 3.26: The values of statistical parameters for C3 channel.

Frequency Bands	Sensitivity	Specificity	Precision	F-Score	Accuracy
Delta	96.89	100	100	98.42	98.29
Theta	99.4	92.83	94.63	96.01	96.51
Alpha 1	95.70	96.61	96.53	96.15	96.16
Alpha 2	97.62	100	100	98.79	98.58
Beta 1	98.92	90.94	91.39	94.76	94.87
Beta 2	99.13	94.57	96.61	96.79	97.34
Beta 3	98.07	94.95	96.74	96.49	96.84

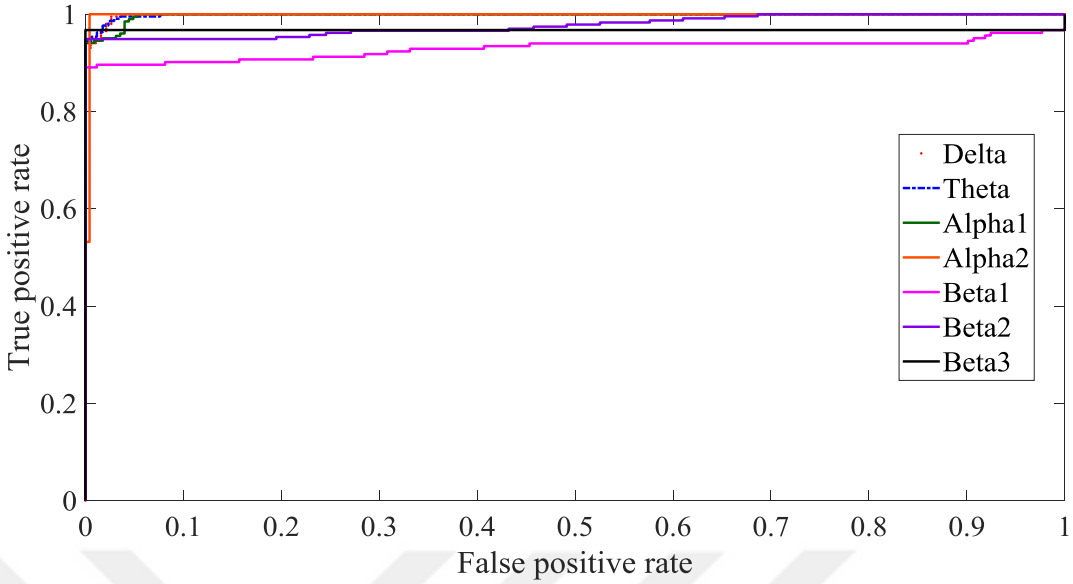

Figure 3.26: The values of statistical parameters for C3 channel.

Synchronization power of P3 channel was calculated with ITPC method and statistically decreased phase coupling was found in OCD patients for all EEG band. These results were classified with SVM method. Training and testing data was determined by using Leave-subject-out CVM. It is reached to very successful parameters as a result of the classification process. Main statistical parameters of classification were given in Table 3.27 and ROC curve of the results was illustrated in Figure 3.27.

Table 3.27: The values of statistical parameters for P3 channel.

Frequency Bands	Sensitivity	Specificity	Precision	F-Score	Accuracy
Delta	99.75	98.01	99.00	98.87	99.16
Theta	92.89	97.08	98.44	94.94	94.29
Alpha 1	97.04	97.82	98.20	97.43	97.39
Alpha 2	97.46	95.89	97.71	96.67	96.90
Beta 1	96.19	99.18	99.43	97.66	97.39
Beta 2	97.60	97.24	96.07	97.42	97.40
Beta 3	95.40	93.20	93.26	94.29	94.30

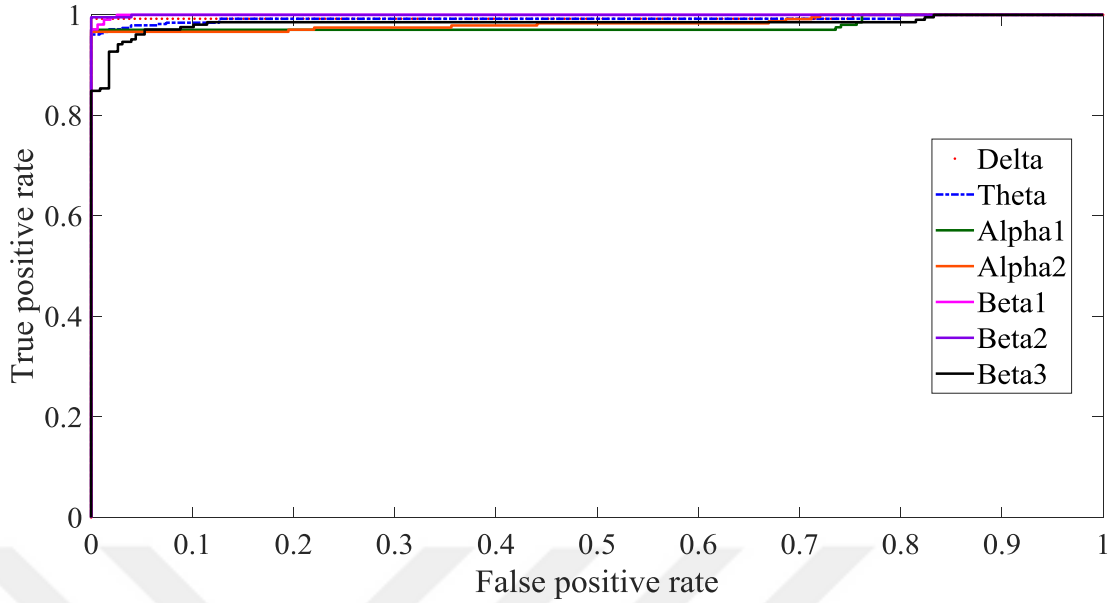

Figure 3.27: ROC curves of classifier for P3 channel.

Synchronization power of O1 channel was calculated with ITPC method and statistically decreased phase coupling was found in OCD patients for delta, theta, alfa1, alfa2, beta1, beta3 EEG bands. These results were classified with SVM method. Training and testing data was determined by using Leave-subject-out CVM. It is reached to very successful parameters as a result of the classification process. Main statistical parameters of classification were given in Table 3.28 and ROC curve of the results was illustrated in Figure 3.28.

Table 3.28: The values of statistical parameters for O1 channel.

Frequency Bands	Sensitivity	Specificity	Precision	F-Score	Accuracy
Delta	95.72	100	100	97.81	97.17
Theta	100	94.75	90.78	97.30	96.54
Alpha 1	99.26	96.72	96.07	97.97	97.85
Alpha 2	96.93	100	100	98.44	98.18
Beta 1	97.19	98.68	98.57	97.93	97.96
Beta 3	99.28	96.54	97.41	97.89	98.09

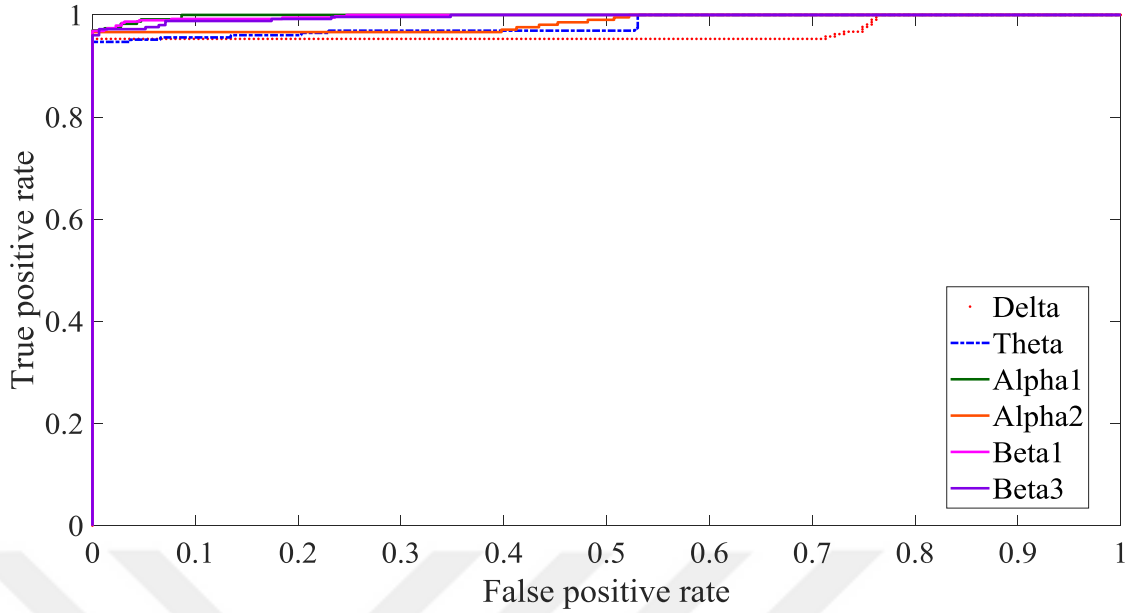

Figure 3.28: ROC curves of classifier for O1 channel.

Synchronization power of F7 channel was calculated with ITPC method and statistically decreased phase coupling was found in all EEG band. These results were classified with SVM method. Training and testing data was determined by using Leave-subject-out CVM. It is reached to very successful parameters as a result of the classification process. Main statistical parameters of classification were given in Table 3.29 and ROC curve of the results was illustrated in Figure 3.29.

Table 3.29: The values of statistical parameters for F7 channel.

Frequency Bands	Sensitivity	Specificity	Precision	F-Score	Accuracy
Delta	97.76	92.5	97.21	95.05	96.33
Theta	94.45	98.40	98.27	96.38	96.46
Alpha 1	99.47	96.06	96.42	97.74	97.82
Alpha 2	90.13	99.72	99.70	94.68	94.83
Beta 1	96.59	99.15	99.19	97.85	97.82
Beta 2	97.96	94.44	95.30	96.17	96.33
Beta 3	93.45	99.03	98.68	96.16	96.60

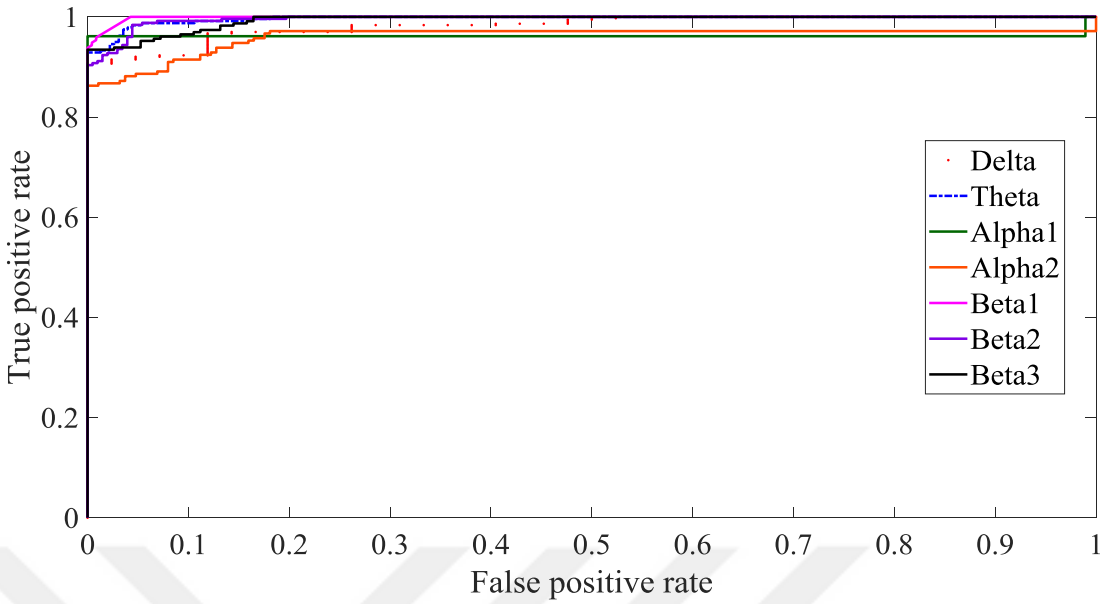

Figure 3.29: ROC curves of classifier for F7 channel.

Synchronization power of T3 channel was calculated with ITPC method and statistically decreased phase coupling was found in all EEG band. These results were classified with SVM method. Training and testing data was determined by using Leave-subject-out CVM. It is reached to very successful parameters as a result of the classification process. Main statistical parameters of classification were given in Table 3.30 and ROC curve of the results was illustrated in Figure 3.30.

Table 3.30: The values of statistical parameters for T3 channel.

Frequency Bands	Sensitivity	Specificity	Precision	F-Score	Accuracy
Delta	93.35	99.63	99.66	96.39	96.26
Theta	99.63	91.37	91.05	95.32	95.24
Alpha 1	91.02	98.12	98.32	94.43	94.22
Alpha 2	98.06	90.63	89.08	94.20	93.88
Beta 1	89.02	98.51	98.61	93.53	93.37
Beta 2	88.88	98.17	98.24	93.30	93.20
Beta 3	97.41	89.93	89.18	93.52	93.37

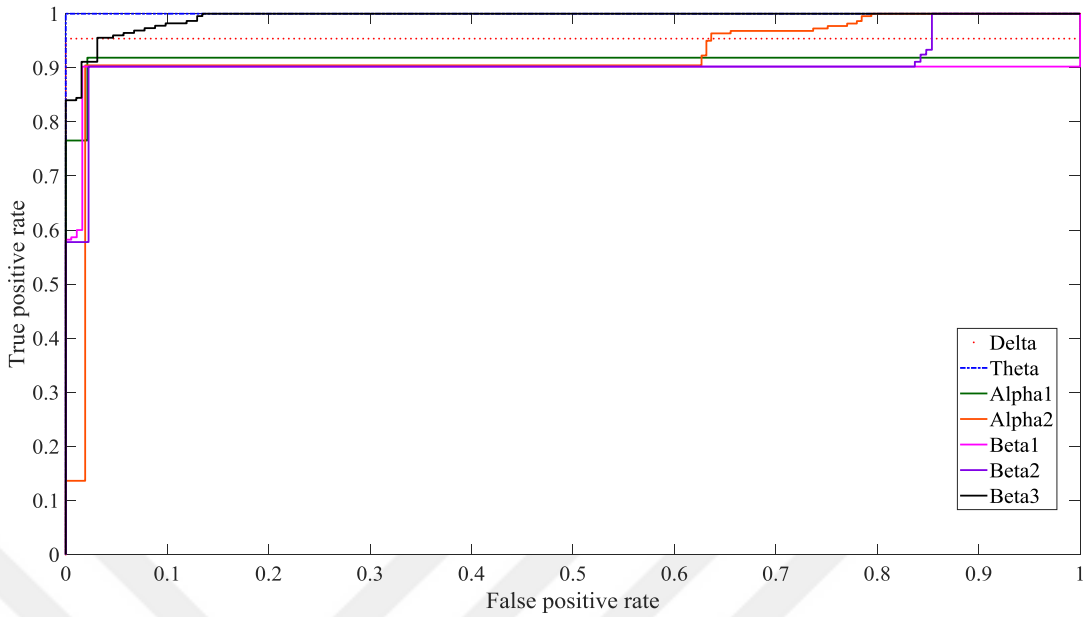

Figure 3.30: ROC curves of classifier for T3 channel.

Synchronization power of T5 channel was calculated with ITPC method and statistically decreased phase coupling was found in OCD patients for all EEG band. These results were classified with SVM method. Training and testing data was determined by using Leave-subject-out CVM. It is reached to very successful parameters as a result of the classification process. Main statistical parameters of classification were given in Table 3.31 and ROC curve of the results was illustrated in Figure 3.31.

Table 3.31: The values of statistical parameters for T5 channel.

Frequency Bands	Sensitivity	Specificity	Precision	F-Score	Accuracy
Delta	94.97	100	100	97.42	97.49
Theta	97.51	88.05	89.09	92.54	92.78
Alpha 1	99.54	91.75	93.58	95.49	96.01
Alpha 2	94.81	99.50	99.50	97.10	97.10
Beta 1	95.14	100	100	97.51	97.58
Beta 2	98.55	95.16	95.32	96.83	96.85
Beta 3	92.70	100	100	96.21	95.89

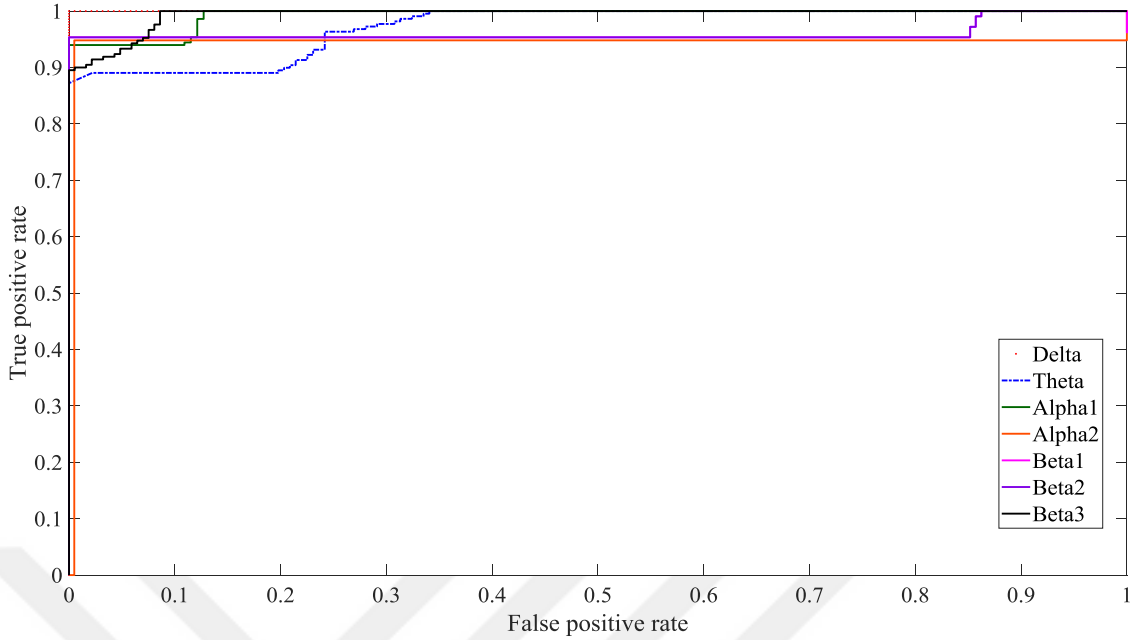

Figure 3.31: ROC curves of classifier for T5 channel.

Synchronization power of Fp2 channel was calculated with ITPC method and statistically decreased phase coupling was found in OCD patients for all EEG band. These results were classified with SVM method. Training and testing data was determined by using Leave-subject-out CVM. It is reached to very successful parameters as a result of the classification process. Main statistical parameters of classification were given in Table 3.32 and ROC curve of the results was illustrated in Figure 3.32.

Table 3.32: The values of statistical parameters for Fp2 channel.

Frequency Bands	Sensitivity	Specificity	Precision	F-Score	Accuracy
Delta	92.70	100	100	96.21	95.89
Theta	100	94.13	94.62	96.98	97.11
Alpha 1	90.77	84.33	75.70	87.43	86.58
Alpha 2	91.46	98.32	99.20	94.76	93.54
Beta 1	99.62	93.20	92.30	96.30	96.09
Beta 2	98.09	92.35	91.13	95.13	94.90
Beta 3	96.82	93.79	94.72	95.28	95.41

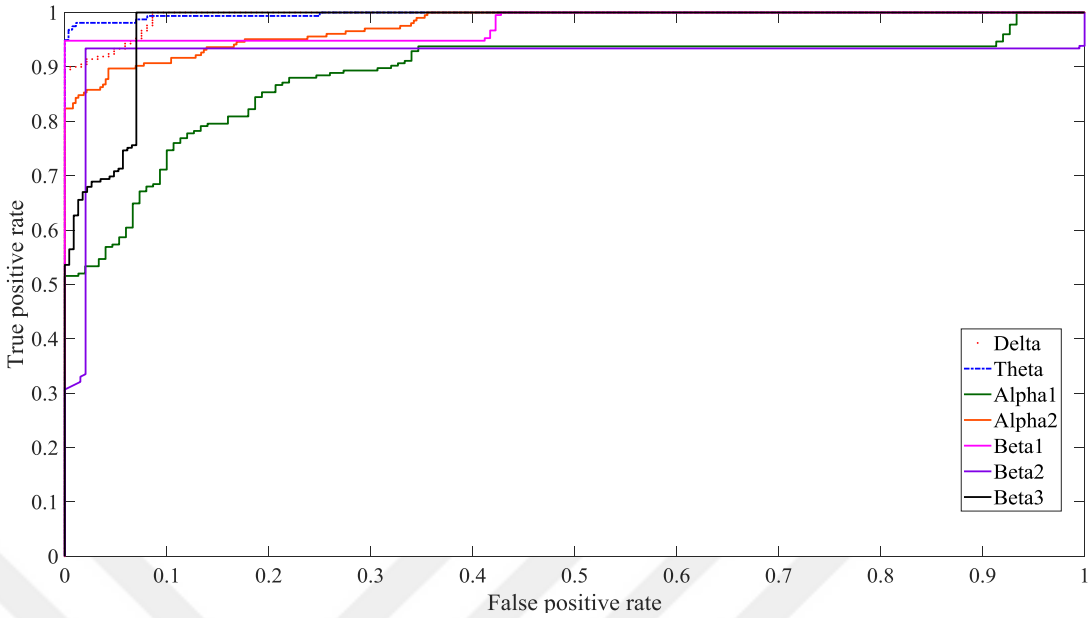

Figure 3.32: ROC curves of classifier for Fp2 channel.

Synchronization power of F4 channel was calculated with ITPC method and statistically decreased phase coupling was found in OCD patients for all EEG band. These results were classified with SVM method. Training and testing data was determined by using Leave-subject-out CVM. It is reached to very successful parameters as a result of the classification process. Main statistical parameters of classification were given in Table 3.33 and ROC curve of the results was illustrated in Figure 3.33.

Table 3.33: The values of statistical parameters for F4 channel.

Frequency Bands	Sensitivity	Specificity	Precision	F-Score	Accuracy
Delta	94.09	89.36	89.43	91.67	91.68
Theta	96.93	98.09	98.44	97.51	97.45
Alpha 1	98.14	96.25	95.65	97.18	97.11
Alpha 2	99.63	96.21	95.75	97.89	97.79
Beta 1	99.67	95.10	95.56	97.33	97.45
Beta 2	99.64	96.06	95.93	97.82	97.79
Beta 3	95.70	99.65	99.66	97.64	97.62

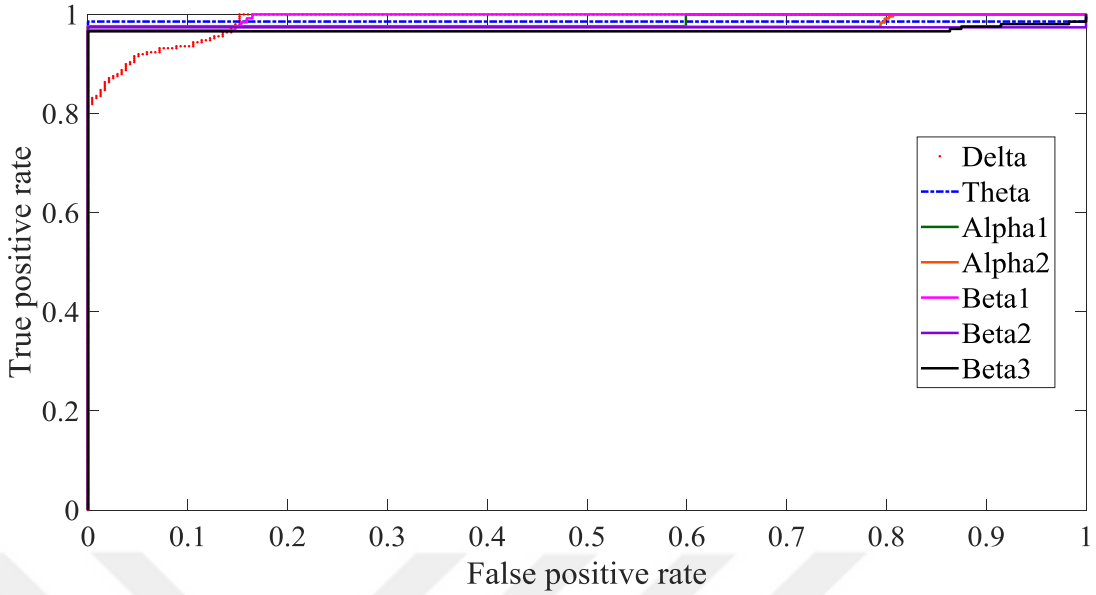

Figure 3.33: ROC curves of classifier for F4 channel.

Synchronization power of C4 channel was calculated with ITPC method and statistically decreased phase coupling was found in OCD patients for all EEG band. These results were classified with SVM method. Training and testing data was determined by using Leave-subject-out CVM. It is reached to very successful parameters as a result of the classification process. Main statistical parameters of classification were given in Table 3.34 and ROC curve of the results was illustrated in Figure 3.34.

Table 3.34: The values of statistical parameters for C4 channel.

Frequency Bands	Sensitivity	Specificity	Precision	F-Score	Accuracy
Delta	93.51	99.67	99.63	96.49	96.60
Theta	99.70	94.56	93.15	94.56	95.58
Alpha 1	99.71	91.73	94.53	95.55	96.43
Alpha 2	99.63	91.40	91.02	95.34	95.25
Beta 1	99.66	92.83	93.35	96.12	96.26
Beta 2	93.94	99.63	99.66	96.70	96.60
Beta 3	85.92	91.79	84.23	88.76	89.81

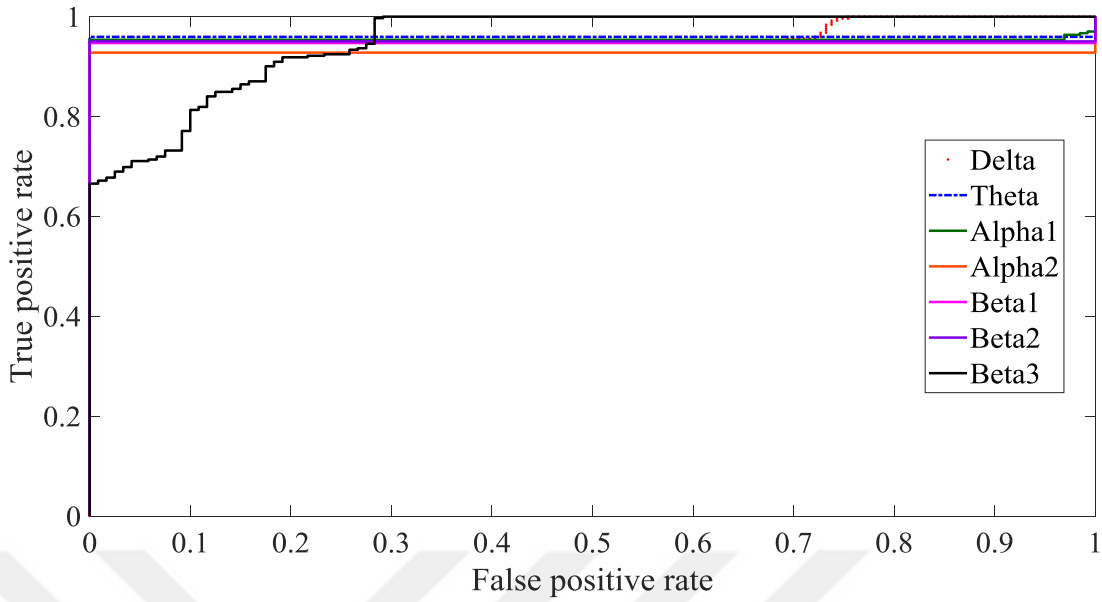

Figure 3.34: ROC curves of classifier for C4 channel.

Synchronization power of P4 channel was calculated with ITPC method and statistically decreased phase coupling was found in all EEG band. These results were classified with SVM method. Training and testing data was determined by using Leave-subject-out CVM. It is reached to very successful parameters as a result of the classification process. Main statistical parameters of classification were given in Table 3.35 and ROC curve of the results was illustrated in Figure 3.35.

Table 3.35: The values of statistical parameters for P4 channel.

Frequency Bands	Sensitivity	Specificity	Precision	F-Score	Accuracy
Delta	98.16	99.23	99.38	98.69	98.64
Theta	93.52	99.64	99.65	96.48	96.43
Alpha 1	100	98.14	98.53	99.06	99.14
Alpha 2	96.98	100	100	98.47	98.34
Beta 1	100	98.47	98.85	99.23	99.39
Beta 2	96.86	100	100	98.40	98.34
Beta 3	91.70	100	100	95.67	94.05

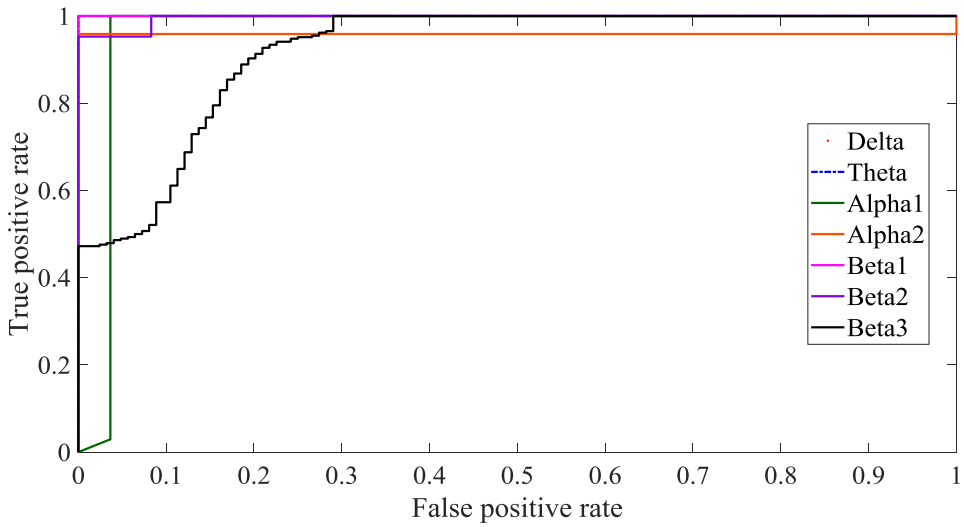

Figure 3.35: ROC curves of classifier for P4 channel.

Synchronization power of O2 channel was calculated with ITPC method and statistically decreased phase coupling was found in OCD patients for all EEG band. These results were classified with SVM method. Training and testing data was determined by using Leave-subject-out CVM. It is reached to very successful parameters as a result of the classification process. Main statistical parameters of classification were given in Table 3.36 and ROC curve of the results was illustrated in Figure 3.36.

Table 3.36: The values of statistical parameters for O2 channel.

Frequency Bands	Sensitivity	Specificity	Precision	F-Score	Accuracy
Delta	98.97	80.28	69.92	88.65	86.20
Theta	96.32	99.05	98.96	97.66	97.72
Alpha 1	95.93	97.05	97.63	96.49	96.42
Alpha 2	99.55	96.41	94.11	97.96	97.54
Beta 1	77.89	99.29	99.73	87.30	82.79
Beta 2	88.05	94.30	94.85	91.07	90.90
Beta 3	99.62	88.15	86.78	93.53	93.18

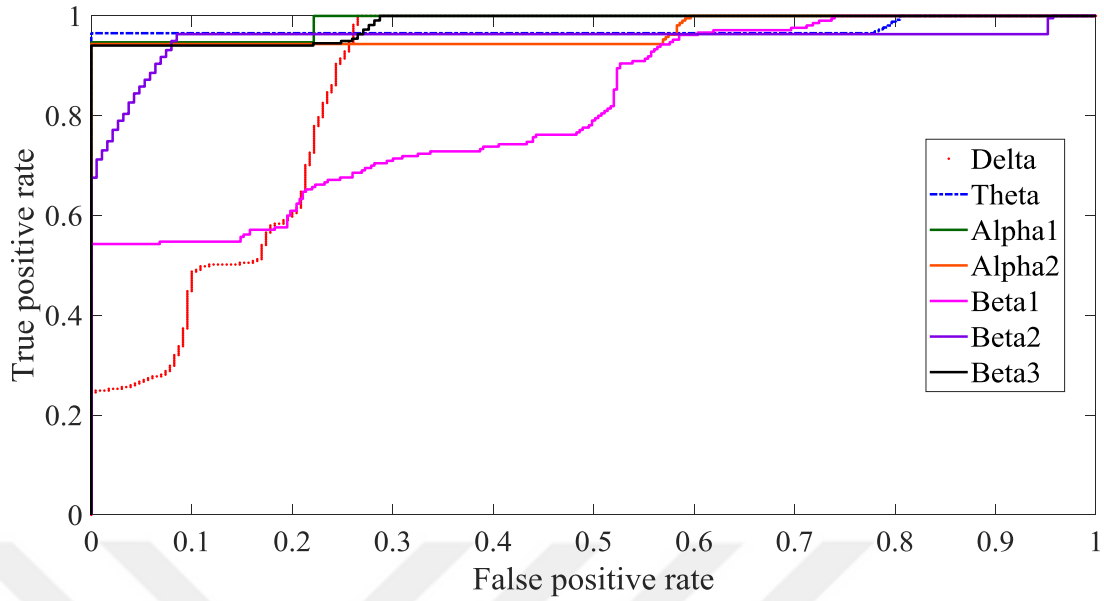

Figure 3.36: ROC curves of classifier for O2 channel.

Synchronization power of F8 channel was calculated with ITPC method and statistically decreased phase coupling was found in OCD patients for all EEG band. These results were classified with SVM method. Training and testing data was determined by using Leave-subject-out CVM. It is reached to very successful parameters as a result of the classification process. Main statistical parameters of classification were given in Table 3.37 and ROC curve of the results was illustrated in Figure 3.37.

Table 3.37: The values of statistical parameters for F8 channel.

Frequency Bands	Sensitivity	Specificity	Precision	F-Score	Accuracy
Delta	93.29	97.11	98.02	95.17	94.80
Theta	85.24	98.59	98.60	91.43	91.39
Alpha 1	94.94	99.58	99.72	97.20	96.75
Alpha 2	99.64	91.64	90.90	95.47	95.29
Beta 1	99.60	89.16	86.73	94.09	93.50
Beta 2	91.59	99.64	99.67	95.44	95.29
Beta 3	93.46	89.64	88.27	91.51	91.38

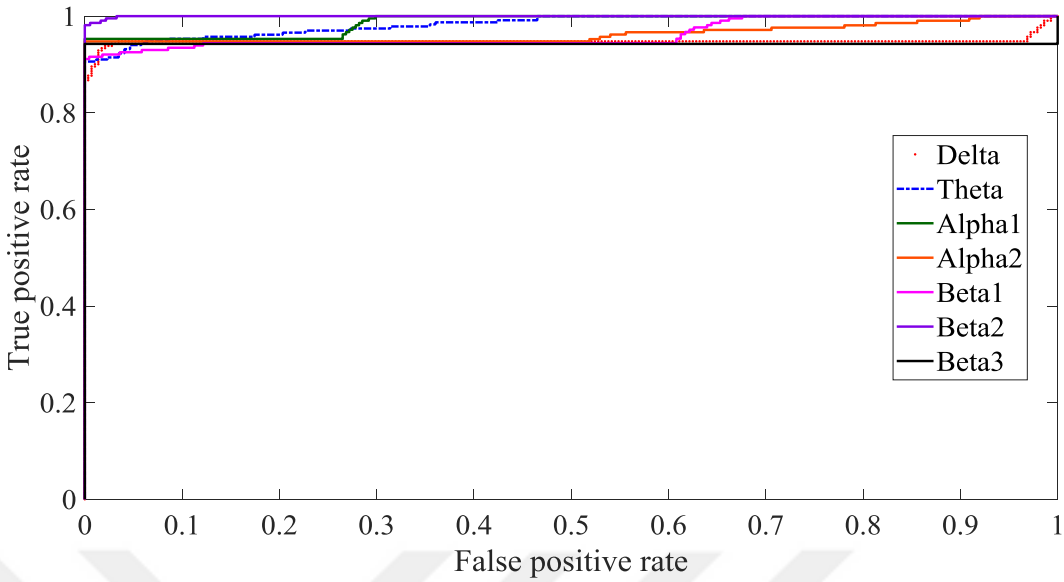

Figure 3.37: ROC curves of classifier for F8 channel.

Synchronization power of T4 channel was calculated with ITPC method and statistically decreased phase coupling was found in OCD patients for all EEG band. These results were classified with SVM method. Training and testing data was determined by using Leave-subject-out CVM. It is reached to very successful parameters as a result of the classification process. Main statistical parameters of classification were given in Table 3.38 and ROC curve of the results was illustrated in Figure 3.38.

Table 3.38: The values of statistical parameters for T4 channel.

Frequency Bands	Sensitivity	Specificity	Precision	F-Score	Accuracy
Delta	100	95.05	95.08	97.46	97.47
Theta	100	97.46	97.24	98.71	98.67
Alpha 1	95.91	90.70	90.23	93.23	93.16
Alpha 2	97.03	96.72	96.74	96.88	96.87
Beta 1	97.38	93.92	94.36	95.62	95.69
Beta 2	93.49	97.42	97.10	95.42	95.54
Beta 3	94.62	97.33	97.23	95.96	95.98

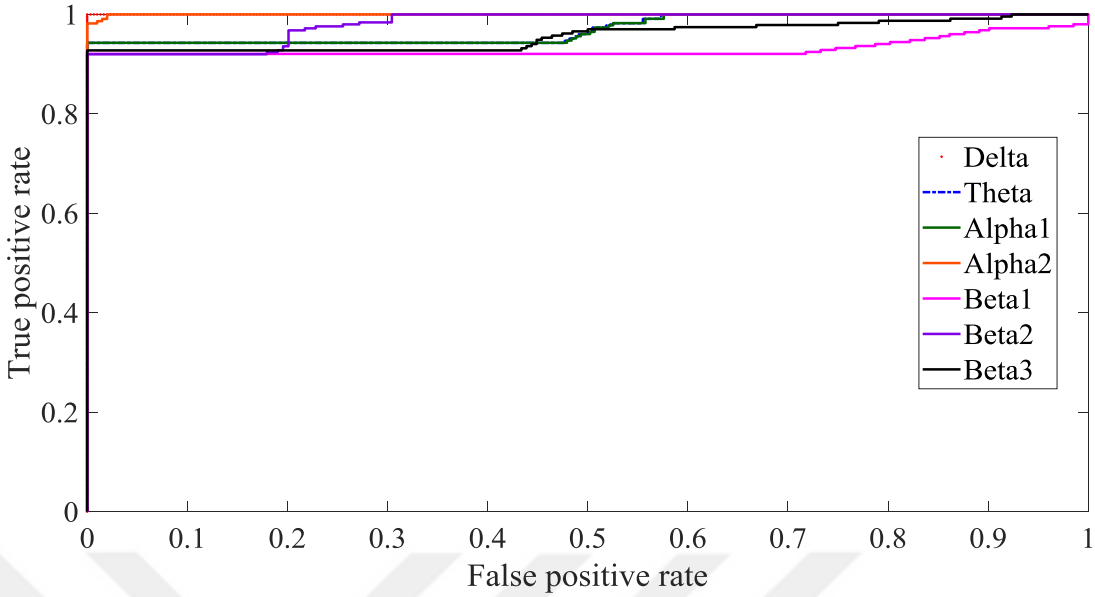

Figure 3.38: ROC curves of classifier for T4 channel.

Synchronization power of T6 channel was calculated with ITPC method and statistically decreased phase coupling was found in delta, alpha 1, alpha 2, beta 1, beta 2 and beta 3 EEG bands. These results were classified with SVM method. Training and testing data was determined by using Leave-subject-out CVM. It is reached to very successful parameters as a result of the classification process. Main statistical parameters of classification were given in Table 3.39 and ROC curve of the results was illustrated in Figure 3.39.

Table 3.39: The values of statistical parameters for T6 channel.

Frequency Bands	Sensitivity	Specificity	Precision	F-Score	Accuracy
Delta	95.81	100	100	97.86	97.08
Alpha 1	93.66	100	100	96.72	96.27
Alpha 2	98.65	100	100	99.32	99.18
Beta 1	98.21	97.03	96.49	97.61	97.56
Beta 2	91.25	86.53	87.95	88.82	88.97
Beta 3	94.79	100	100	97.32	95.74

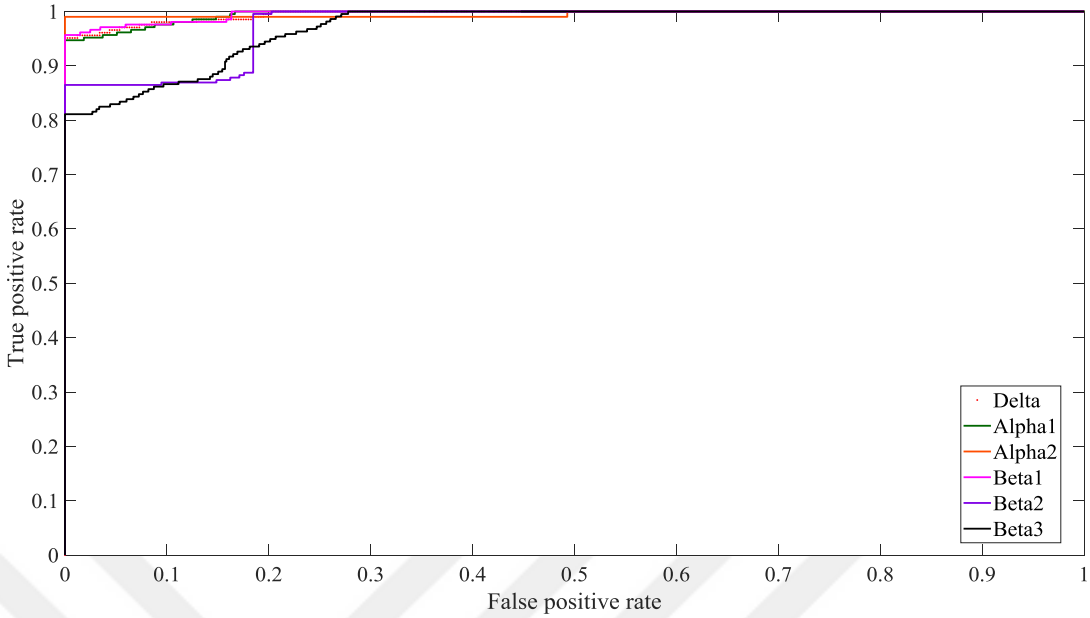

Figure 3.39: ROC curves of classifier for T6 channel.

Synchronization power of Fz channel was calculated with ITPC method and statistically decreased phase coupling was found in OCD patients for all EEG band. These results were classified with SVM method. Training and testing data was determined by using Leave-subject-out CVM. It is reached to very successful parameters as a result of the classification process. Main statistical parameters of classification were given in Table 3.40 and ROC curve of the results was illustrated in Figure 3.40.

Table 3.40: The values of statistical parameters for Fz channel.

Frequency Bands	Sensitivity	Specificity	Precision	F-Score	Accuracy
Delta	100	95.84	96.69	97.88	98.12
Theta	100	95.08	95.56	97.48	97.61
Alpha 1	91.43	74.78	70.62	82.28	81.43
Alpha 2	100	96.27	96.36	98.10	98.12
Beta 1	80.23	73.12	79.76	76.51	77.12
Beta 2	100	95.31	95.36	97.60	97.61
Beta 3	94.31	86.68	85.27	90.34	90.11

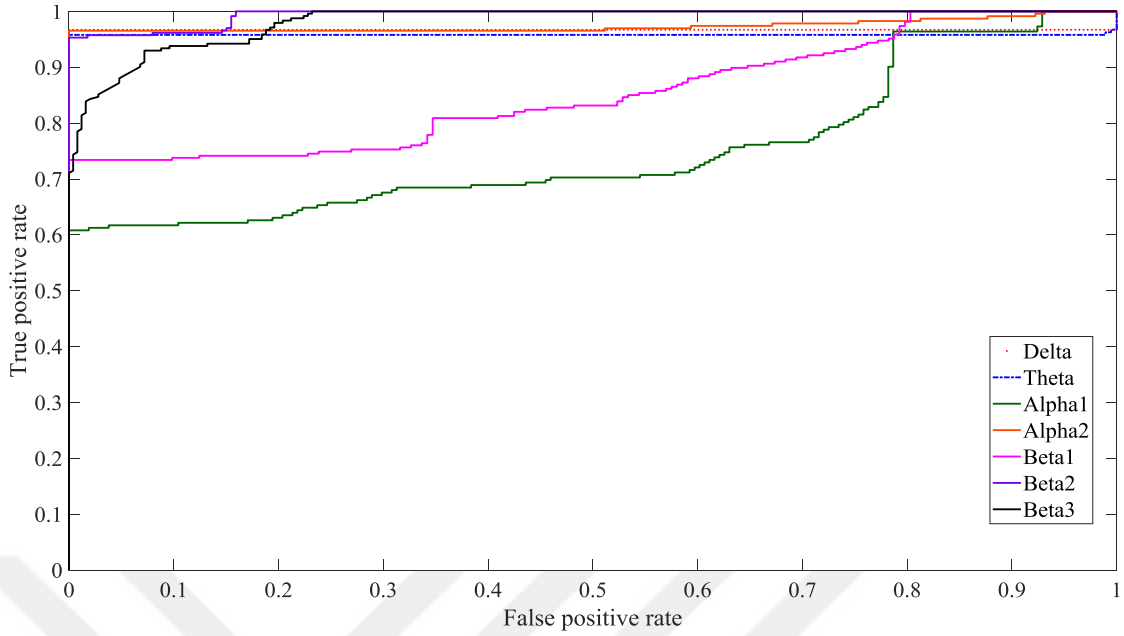

Figure 3.40: ROC curves of classifier for Fz channel.

Synchronization power of Cz channel was calculated with ITPC method and statistically decreased phase coupling was found in OCD patients for all EEG band. These results were classified with SVM method. Training and testing data was determined by using Leave-subject-out CVM. It is reached to very successful parameters as a result of the classification process. Main statistical parameters of classification were given in Table 3.41 and ROC curve of the results was illustrated in Figure 3.41.

Table 3.41: The values of statistical parameters for Cz channel.

Frequency Bands	Sensitivity	Specificity	Precision	F-Score	Accuracy
Delta	97.65	80.57	75.52	88.29	87.07
Theta	88.00	98.14	98.08	92.79	92.86
Alpha 1	96.19	95.16	95.36	95.67	95.69
Alpha 2	98.74	95.48	95.16	97.08	97.02
Beta 1	94.89	98.82	98.75	96.81	96.87
Beta 2	94.76	95.13	95.32	94.95	94.94
Beta 3	98.46	94.54	94.39	96.46	96.43

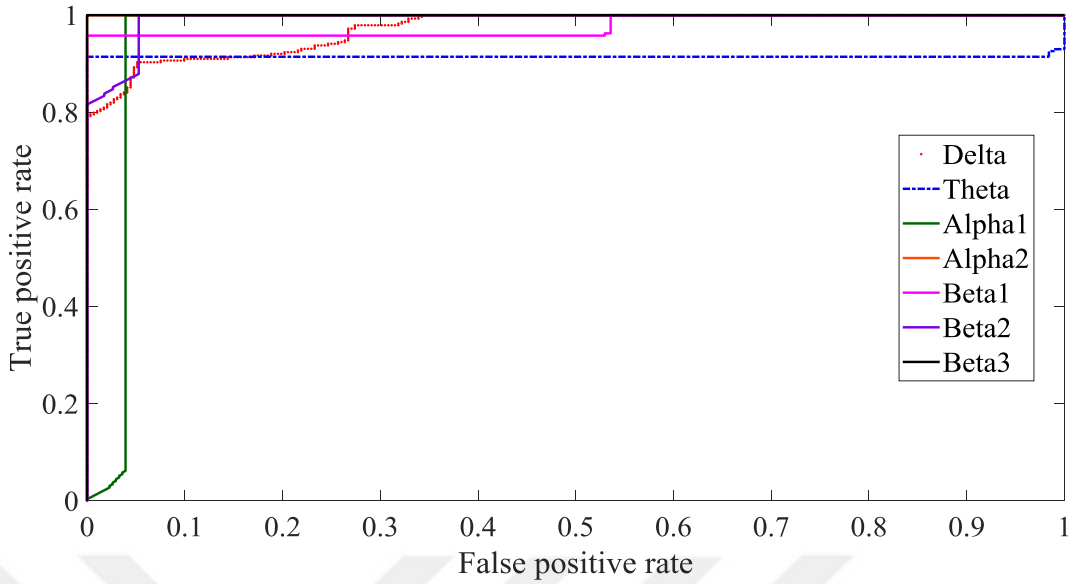

Figure 3.41: ROC curves of classifier for Cz channel.

Synchronization power of Pz channel was calculated with ITPC method and statistically decreased phase coupling was found in OCD patients for all EEG band. These results were classified with SVM method. Training and testing data was determined by using Leave-subject-out CVM. It is reached to very successful parameters as a result of the classification process. Main statistical parameters of classification were given in Table 3.42 and ROC curve of the results was illustrated in Figure 3.42.

Table 3.42: The values of statistical parameters for Pz channel.

Frequency Bands	Sensitivity	Specificity	Precision	F-Score	Accuracy
Delta	93.86	90.95	92.45	92.38	92.53
Theta	92.96	92.92	93.70	92.94	92.96
Alpha 1	93.95	95.31	95.49	94.64	94.61
Alpha 2	87.16	100	100	93.14	90.85
Beta 1	94.89	86.58	90.00	90.54	91.23
Beta 2	92.23	93.77	94.58	93.00	92.95
Beta 3	89.73	92.64	91.90	91.16	91.23

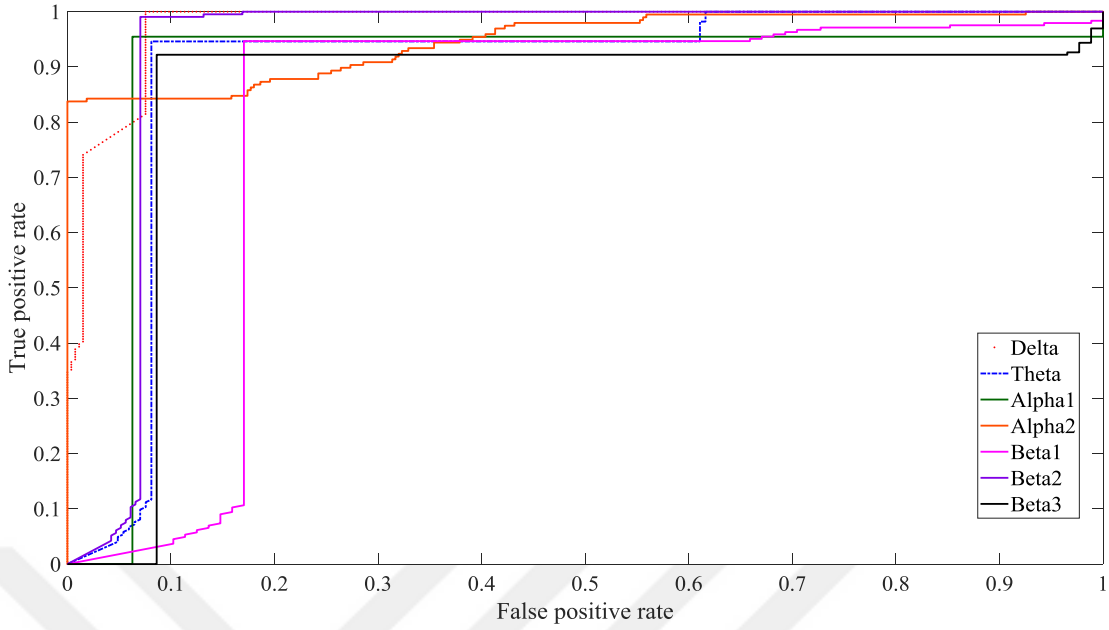

Figure 3.42: ROC curves of classifier for Pz channel.

4. DISCUSSION

In this thesis study, the OCD, which is one of the major neuropsychiatric diseases was investigated using electrophysiological signals. Our motivational goals are to suggest more objective criteria in clinical diagnosis, treatment, tracking of treatment stages and to reveal how OCD effects on functional connectivity, neurophysiological biomarkers, neural networks and cognitive processes.

Neuropsychiatric diseases increased awfully and these threatens public health (Organization, 2001). OCD is one of the most common neuropsychiatric diseases. OCD is characterised by DSM-V (Association, 2013) and ICD 10 (World Health Organization) (Organization, 1993). At the present time several neuropsychological tests are used for diagnosing and detecting severity of symptom in OCD. These are; Y-BOCs, HDRS-17 and BAI (Gohle et al., 2008). In clinical practice, the EEG methods such as synchronization, complexity analysis etc., is used only for exclusion of the comorbid disease (for instance depression with OCD), which may cause obsessive compulsive symptoms. In treatment or therapeutic use of EEG methods is very limited. Our study was shown that GFS and ITPC values may be used as biomarker for OCD and it can be used also for monitoring course of disease and treatment. GFS studies is shown that synchronization power is important marker for diagnosis of neuropsychiatric disease. These results indicate that GFS can be a clinically useful and important method for diagnosis of OCD and other disorders comorbid with OCD.

4.1. DISCUSSION OF THE RESULTS

As a result of synchronization analysis with GFS technique for only frontal site, decreased synchronization degrees were detected for OCD patients in delta, theta, beta1 and beta 3 band. Independent sample t-test was used for statistical analysis of the results. Significantly difference was found in delta band ($p=0.00005$) and beta 3 band ($p<0.013$). SVM classification method was applied on these results in order to classification and consolidation. Train and test data were selected by leave-subject-out CVM. Accuracy rate

was found for delta is 95.37% and for beta 3 is 95.48%. These are high accuracy values. In the second stage of the analysis, GFS was computed for all channels (19 electrodes or channels). Decreased synchronization degrees for OCD patients was computed in delta, theta, beta 2 and beta 3 bands. Significantly difference between OCD and HCs data was calculated in delta band ($p=0.001$) and beta2 band ($p=0.014$). These results were classified and delta band 94.57% accuracy rate for delta band and 94.44% rate was found for beta 2 band. In the last stage of synchronization, ITPC techniques also called as Phase Amplitude Coupling and Inter-Trial Phase Coherence etc., was used for detecting of phase synchronization. Unlike GFS, ITPC can compute phase coupling degree between EEG trials, separately for each channel. ITPC values were computed for every channel and synchronization degree of HCs and OCD patients were compared. According to ITPC analysis results, loss of phase coupling was observed in all bands and all channels. Significantly difference was found in most of the channels such as; it was found as $p=0.00005$ for Fp1, F3, T3, F4, C4 channels and $p<0.05$ for C3, P3, O1 (only except beta 2 band), P4, O2, F8, T4, T6 (only except theta band), Fz, Pz and Cz channels. The values that was found in statistically important, were classified with SVM. Train and test values also defined with Leave-subject out CVM. Most of these values have been successfully classified in accuracy rate greater than 85%. These results were compared and discussed with previous investigations.

Our results are similar to previous OCD research's results: Loss of inter hemispheric coherence in several EEG bands was detected (Velikova et al., 2010), Phase Preservation Index (PPI) was used to phase stability and as a results of analysis, reduction of phase coupling was observed (Index et al., 2013), decreased nonlinear coherence was found in beta 2 band (Olbrich et al., 2013), decreased GFS synchronization in slow bands was computed (Özçoban et al., 2017b) and significantly lower phase synchrony was observed in OCD patients (Koh et al., 2017).

4.1.1. Neurophysiological Discussion of Results

In this section our findings will compare with previous medical outcomes that obtained with neuroimaging studies, electrophysiological investigations and neuropsychological tests. Because, it is known that synchronization, coherence or phase coupling level degrees are related to functional connectivity, brain networks and cognitive functions, we

can interpret our results with abnormality or dysfunction of anatomic origin of neurophysiological oscillations and mental dysfunctions.

According to our results decreased synchronization on frontal GFS values and frontal channels of ITPC values were detected. These findings are consistent with previous studies. Neuroimaging studies of neurophysiology such as positron emission tomography (PET), single photon emission computer tomography (SPECT), functional magnetic resonance imaging (fMRI) used to examine, how OCD effect on brain functions and which regions are affected by this. Strong evidence was found dysfunction of frontal, orbitofrontal-subcortical circuitry (Baxter Jr et al., 1988, Machlin and Harris, 1991, Hollander et al., 1995) , impairment of orbitofrontal cortex (Cavedini et al., 1998), significantly decreased bilateral orbital frontal and amygdala volumes compared with HCs was detected (Szeszko et al., 1999).

Loss of phase synchronization can have interpreted as functional dysconnectivity. Several researches in past found strong evidence about relation among functional connectivity and desynchronization. Decreased functional connectivity and synchronization was explored in slow bands for neuroleptic-naïve schizophrenia (Koenig et al., 2005), loss of functional connectivity and phase coupling was reported for Alzheimer disease (König et al., 2001), reduced functional connectivity was explored in the cingulate network by (Weber et al., 2014). These electrophysiological studies that related to functional connectivity, have been supported by other studies that were carried out with neuroimaging methods. It was reported that OCD caused functional dysconnectivity in the default mode network (Jang et al., 2010) and functional connectivity alterations was detected in OCD (Hou et al., 2013).

Decreased synchronization also found in slow frequency band (delta, theta) with GFS and ITPC method. Studies to determine source of slow frequency bands reported that deep cortical centers generating slow band activities in medial prefrontal cortex and orbitofrontal cortex (Knyazev, 2012, Leung and Yim, 1993, Murphy et al., 2009, Knyazev, 2007, Anderer et al., 2002). This means that our findings that explored slow band desynchronization is consistent with EEG band source localization studies.

Results of current study can give us information about cognitive functions. Delta activities oscillated by thalamo-cortical networks (Steriade, 2005) so it is significant for cognitive functions that attentional and language processes (Devrim et al., 1999, Schürmann et al., 2001, Roehm et al., 2004, Sauseng and Klimesch, 2008). Theta oscillations were created by hippocampus so that it is known that hippocampus is related to memory processes. In an experiment a memory encoding memory found a similar frontal-temporo-parietal network. Theta coherence plays important role for successful episodic encoding and memory span (Klimesch et al., 2008) global theta desynchronization has associated with short term memory (Koenig et al., 2001). Alpha and beta waves are generated by cortical activities (Salenius and Hari, 2003, Klimesch, 1996, Jensen et al., 2002) and strong evidence was found that alpha band effects attentional (Von Stein and Sarnthein, 2000, Rihs et al., 2007, Thut et al., 2006, Worden et al., 2000, Sauseng et al., 2005) and memory functions (Klimesch, 1996, Klimesch et al., 2007), beta band also play important role in attention (Wróbel et al., 2007, Gross et al., 2004) and higher cognitive processes (Razumnikova, 2004).

In previous studies reported that OCD patients showed memory impairments such as deficits in spatial memory (Purcell et al., 1998a, Purcell et al., 1998b), impairment in metamemory (Tuna et al., 2005, McNally and Kohlbeck, 1993, Tolin et al., 2001), memory deficits in verbal information (Boone et al., 1991, Christensen et al., 1992, Dirson et al., 1995, Radomsky and Rachman, 1999) and impairment of attentional processes (Muller and Roberts, 2005).

Results of this thesis provide extra information and evidence about OCD effects on functional connectivity, spatial influences, brain networks and cognitive functions. Our results show that OCD causes dysfunction and impairment on some site such as; orbitofrontal cortex, medial prefrontal cortex, hippocampus and several brain networks that are thalamo-cortical networks, orbito-frontal-striatal circuits (Menzies et al., 2008). The findings also demonstrate that OCD causes strong disruptive effects on cognitive functions such as; memory, learning and attention.

4.1.2. Discussion of Classification Results

The synchronization values that were computed by GFS and ITPC methods, were classified by SVM algorithms. The classification scores are compared with some of

previous researches. Patterns that were produced by Fractional Anisotropy (FA) method for discriminate between OCD and HCs. This method uses white matter differences. The highest accuracy score was calculated as 84% (Li et al., 2014). An auto-diagnose system was designed for OCD. The system was used brain images as patterns. Accuracy score was computed as 99.11% (Zhang et al., 2015). EEG complexity and interhemispheric dependency measurements features were classified for OCD patients. Train and test data were determined using k-fold cross validated method and the highest classification accuracy was computed as 85% (Aydin et al., 2015). Many classification algorithms were used for distinguishing between Trichotillomania (TTM) disorder and OCD. The most successful classification accuracy was computed as 81.04% (Erguzel et al., 2015).

The classification scores that were obtained by GFS and ITPC values, seem to be very successful when compared to previous similar studies for auto-diagnosing the OCD.

5. CONCLUSION AND RECOMMENDATIONS

We measured EEG phase synchronization using the GFS and ITPC method and classified these patterns of OCD and HCs for selected frequency bands. The high synchronization values (those close to '1') were interpreted as representing a considerable number of neurons becoming active at common time simultaneously. According to the frontal GFS analysis, statistical significantly differences were obtained for slow delta and beta 3 band. Same analysis was repeated for whole brain GFS, decreased synchronization was detected in delta and beta 2 band. Because the ITPC method compute phase coupling degree among data segments, this can give us synchronization degree for which channel we want. As a result, this analysis, significantly reduced phase coupling difference in OCD patients was found for all channels-only except for O1 channel in beta-2 band and T6 channel in theta band-in all EEG band and These results were interpreted as indicating that OCD cases have disrupted synchronization between the whole-brain oscillations in the low frequency bands. These results were compared with results of other similar researches in previous section. In this section the outcomes will be concluded, summarized and contributions of results to literature will be explained in following items.

- Result of the thesis hypothesized that OCD cause desynchronization in brain waves. In this way; EEG technique can be used for OCD diagnose and it can provide clinical usage to EEG techniques. Several techniques (for example, deep brain stimulation technique) can be used for effect these desynchronizations for novel treatment in future.

- Because the loss of synchronization is indication of functional dysconnectivity, our results support and constitute with previous neuroimaging studies on OCD.

- Our results constitute and supported to findings that OCD is underpinned by functional and structural abnormalities in some brain networks and structures such as orbito-frontal-striatal circuits, thalamo-cortical networks. Contribution in literature of this finding that the results were obtained by neuroimaging studies,

have been proved also electrophysiological data and using it can be interpreted as electrophysiological methods may aid our understanding of OCD.

- Because to our knowledge this is the first application of the ITPC on neuropsychiatric data, it will encourage the scientist for using the ITPC their own investigations about other disease. This is the other contribution to literature for future researches.

- Some of the past neuroimaging investigations show that OCD caused impairment on cognitive functions such as memory and attention. This finding may new approach for diagnosis and treatment methods of OCD.

- One of our findings is successful classification scores belongs to synchronization values. To our knowledge, these scores is one of the most successful results when compared to our autodetection system for OCD. This classification results may be used for auto-detection system.

REFERENCES

web [Online]. Available: http://cogsci.stackexchange.com/questions/1553/do-the-jungian-cognitive-functions-processes-really-exist.

Abramowitz, J. S., Taylor, S. & Mckay, D. 2009. Obsessive-compulsive disorder. *The Lancet,* 374**,** 491-499.

Achermann, P., Rusterholz, T., Dürr, R., König, T. & Tarokh, L. 2016. Global field synchronization reveals rapid eye movement sleep as most synchronized brain state in the human EEG. *Royal Society open science,* 3**,** 160201.

Alexander, G. E., Delong, M. R. & Strick, P. L. 1986. Parallel organization of functionally segregated circuits linking basal ganglia and cortex. *Annual review of neuroscience,* 9**,** 357-381.

Alper, K., Günther, W., Prichep, L. S., John, E. R. & Brodie, J. 1998. Correlation of qEEG with PET in schizophrenia. *Neuropsychobiology,* 38**,** 50-56.

Anderer, P., Gruber, G., Saletu, B., Klösch, G., Zeitlhofer, J. & Pascual-Marqui, R. Non-invasive electrophysiological neuroimaging of sleep. International Congress Series, 2002. Elsevier, 795-800.

Association, A. P. 2013. *DSM 5,* American Psychiatric Association.

Aydin, S., Arica, N., Ergul, E. & Tan, O. 2015. Classification of obsessive compulsive disorder by EEG complexity and hemispheric dependency measurements. *International journal of neural systems,* 25**,** 1550010.

Baxter JR, L. R., Schwartz, J. M., Mazziotta, J. C., Phelps, M. E. & Pahl, J. J. 1988. Cerebral glucose metabolic rates in nondepressed patients with obsessive-compulsive disorder. *The American journal of psychiatry,* 145**,** 1560.

Bear, M. F., Connors, B. W. & Paradiso, M. A. 2007. *Neuroscience*, Lippincott Williams & Wilkins.

Beck, A. T., Epstein, N., Brown, G. & Steer, R. A. 1988. An inventory for measuring clinical anxiety: psychometric properties. *Journal of consulting and clinical psychology,* 56**,** 893.

Ben-hur, A. & Weston, J. 2010. A user's guide to support vector machines. *Data mining techniques for the life sciences***,** 223-239.

Bishop, C. M. 2006. *Pattern recognition and machine learning,* Springer.

Boone, K. B., Ananth, J., Philpott, L., Kaur, A. & Djenderedjian, A. 1991. Neuropsychological characteristics of nondepressed adults with obsessive-compulsive disorder. *Cognitive and Behavioral Neurology,* 4**,** 96-109.

Boser, B. E., Guyon, I. M. & Vapnik, V. N. A training algorithm for optimal margin classifiers. Proceedings of the fifth annual workshop on Computational learning theory, 1992. ACM, 144-152.

Browne, M. W. 2000. Cross-validation methods. *Journal of mathematical psychology,* 44**,** 108-132.

Burges, C. J. 1998. A tutorial on support vector machines for pattern recognition. *Data mining and knowledge discovery,* 2**,** 121-167.

Cavanagh, J. F., Cohen, M. X. & Allen, J. J. 2009. Prelude to and resolution of an error: EEG phase synchrony reveals cognitive control dynamics during action monitoring. *Journal of Neuroscience,* 29**,** 98-105.

Cavedini, P., Ferri, S., Scarone, S. & Bellodi, L. 1998. Frontal lobe dysfunction in obsessive-compulsive disorder and major depression: a clinical-neuropsychological study. *Psychiatry research,* 78**,** 21-28.

Christensen, K. J., Kim, S. W., Dysken, M. W. & Hoover, K. M. 1992. Neuropyschological performance in obsessive-compulsive disorder. *Biological psychiatry,* 31**,** 4-18.

Clark, L., Cools, R. & Robbins, T. 2004. The neuropsychology of ventral prefrontal cortex: decision-making and reversal learning. *Brain and cognition,* 55**,** 41-53.

Cohen, M. X. 2014. *Analyzing neural time series data: theory and practice,* MIT Press.

Cohen, M. X. 2017. *MATLAB for Brain and Cognitive Scientists,* MIT Press.

Cummings, J. L. 1993. Frontal-subcortical circuits and human behavior. *Archives of neurology,* 50**,** 873-880.

Da Silva, F. L., Vos, J., Mooibroek, J. & Van Rotterdam, A. 1980. Relative contributions of intracortical and thalamo-cortical processes in the generation of alpha rhythms, revealed by partial coherence analysis. *Electroencephalography and clinical neurophysiology,* 50**,** 449-456.

Dauwels, J., Vialatte, F., Musha, T. & Cichocki, A. 2010. A comparative study of synchrony measures for the early diagnosis of Alzheimer's disease based on EEG. *NeuroImage,* 49**,** 668-693.

De Hemptinne, C., Ryapolova-webb, E. S., Air, E. L., Garcia, P. A., Miller, K. J., Ojemann, J. G., Ostrem, J. L., Galifianakis, N. B. & Starr, P. A. 2013. Exaggerated phase–amplitude coupling in the primary motor cortex in Parkinson disease. *Proceedings of the National Academy of Sciences,* 110**,** 4780-4785.

Devrim, M., Demiralp, T., Ademoglu, A. & Kurt, A. 1999. A model for P300 generation based on responses to near-threshold visual stimuli. *Cognitive brain research,* 8**,** 37-43.

Dirson, S., Bouvard, M., Cottraux, J. & Martin, R. 1995. Visual memory impairment in patients with obsessive-compulsive disorder: a controlled study. *Psychotherapy and Psychosomatics,* 63**,** 22-31.

Elliott, R. & Deakin, B. 2005. Role of the orbitofrontal cortex in reinforcement processing and inhibitory control: evidence from functional magnetic resonance imaging studies in healthy human subjects. *International review of neurobiology,* 65**,** 89-116.

Erguzel, T. T., Ozekes, S., Sayar, G. H., Tan, O. & Tarhan, N. 2015. A hybrid artificial intelligence method to classify trichotillomania and obsessive compulsive disorder. *Neurocomputing,* 161**,** 220-228.

First, M. B. & Gibbon, M. 2004. The Structured Clinical Interview for DSM-IV Axis I Disorders (SCID-I) and the Structured Clinical Interview for DSM-IV Axis II Disorders (SCID-II).

Frankel, M., Cummings, J. L., Robertson, M. M., Trimble, M. R., Hill, M. A. & Benson, D. F. 1986. Obsessions and compulsions in Gilles de la Tourette's syndrome. *Neurology,* 36**,** 378-378.

Friedman, J., Hastie, T. & Tibshirani, R. 2001. *The elements of statistical learning,* Springer series in statistics New York.

Gohle, D., Juckel, G., Mavrogiorgou, P., Pogarell, O., Mulert, C., Rujescu, D., Giegling, I., Zaudig, M. & Hegerl, U. 2008. Electrophysiological evidence for cortical abnormalities in obsessive–compulsive disorder–A replication study using auditory event-related P300 subcomponents. *Journal of psychiatric research,* 42**,** 297-303.

Goldberg, D. E. & Holland, J. H. 1988. Genetic algorithms and machine learning. *Machine learning,* 3**,** 95-99.

Goodman, W. K., Price, L. H., Rasmussen, S. A., Mazure, C., Delgado, P., Heninger, G. R. & Charney, D. S. 1989. The yale-brown obsessive compulsive scale: II. Validity. *Archives of general psychiatry,* 46**,** 1012-1016.

Greenberg, B. D., Benjamin, J., Martin, J. D., Keuler, D., Huang, S.-J., Altemus, M. & Murphy, D. L. 1998. Delayed obsessive-compulsive disorder symptom exacerbation after a single dose of a serotonin antagonist in fluoxetine-treated but not untreated patients. *Psychopharmacology,* 140**,** 434-444.

Gross, J., Schmitz, F., Schnitzler, I., Kessler, K., Shapiro, K., Hommel, B. & Schnitzler, A. 2004. Modulation of long-range neural synchrony reflects temporal limitations

of visual attention in humans. *Proceedings of the National Academy of Sciences of the United States of America,* 101**,** 13050-13055.

Gutierrez-Osuna, R. 2006. Lecture 13: Validation. *Retrieved February,* 28**,** 2007.

Hayashi, H., Iijima, S., Sugita, Y., Teshima, Y., Tashiro, T., Matsuo, R., Yasoshima, A., Hishikawa, Y. & Ishihara, T. 1987. Appearance of frontal mid-line theta rhythm during sleep and its relation to mental activity. *Electroencephalography and clinical neurophysiology,* 66**,** 66-70.

Heyman, I., Mataix-Cols, D. & Fineberg, N. 2006. Obsessive-compulsive disorder. *BMJ: British Medical Journal,* 333**,** 424.

Hofmann, T. 2001. Unsupervised learning by probabilistic latent semantic analysis. *Machine learning,* 42**,** 177-196.

Hollander, E., Prohovnik, I. & Stein, D. J. 1995. Increased cerebral blood flow during m-CPP exacerbation of obsessive-compulsive disorder. *The Journal of neuropsychiatry and clinical neurosciences,* 7**,** 485-490.

Hou, J., Song, L., Zhang, W., Wu, W., Wang, J., Zhou, D., QU, W., GUO, J., GU, S. & HE, M. 2013. Morphologic and functional connectivity alterations of corticostriatal and default mode network in treatment-naïve patients with obsessive-compulsive disorder. *PloS one,* 8**,** e83931.

Hughes, S. W., Lörincz, M., Cope, D. W., Blethyn, K. L., Kékesi, K. A., Parri, H. R., Juhász, G. & Crunelli, V. 2004. Synchronized oscillations at α and θ frequencies in the lateral geniculate nucleus. *Neuron,* 42**,** 253-268.

Index, P. P., Off, D. & On, D. 2013. Deep brain stimulation targeted at the nucleus accumbens decreases the potential for pathologic network communication. *Arch Gen Psychiatry,* 67**,** 1061-1068.

Jang, J. H., Kim, J.-H., Jung, W. H., CHOI, J.-S., Jung, M. H., Lee, J.-M., Choi, C.-H., Kang, D.-H. & Kwon, J. S. 2010. Functional connectivity in fronto-subcortical circuitry during the resting state in obsessive-compulsive disorder. *Neuroscience letters,* 474**,** 158- 162.

Jefferson, J. W., Kobak, K. A., Katzelnick, D. J. & Serlin, R. C. 1995. Efficacy and tolerability of serotonin transport inhibitors in obsessive-compulsive disorder: a meta-analysis. *Archives of General psychiatry,* 52**,** 53-60.

Jensen, O. 2005. Reading the hippocampal code by theta phase-locking. *Trends in cognitive sciences,* 9**,** 551-553.

Jensen, O., Gelfand, J., Kounios, J. & Lisman, J. E. 2002. Oscillations in the alpha band (9–12 Hz) increase with memory load during retention in a short-term memory task. *Cerebral cortex,* 12**,** 877-882.

Jones, B. & Mishkin, M. 1972. Limbic lesions and the problem of stimulus—reinforcement associations. *Experimental neurology,* 36**,** 362-377.

Klimesch, W. 1996. Memory processes, brain oscillations and EEG synchronization. *International Journal of Psychophysiology,* 24**,** 61-100.

Klimesch, W., Freunberger, R., Sauseng, P. & Gruber, W. 2008. A short review of slow phase synchronization and memory: evidence for control processes in different memory systems? *Brain research,* 1235**,** 31-44.

Klimesch, W., Sauseng, P. & Hanslmayr, S. 2007. EEG alpha oscillations: the inhibition–timing hypothesis. *Brain research reviews,* 53**,** 63-88.

Knyazev, G. G. 2007. Motivation, emotion, and their inhibitory control mirrored in brain oscillations. *Neuroscience & Biobehavioral Reviews,* 31**,** 377-395.

Knyazev, G. G. 2012. EEG delta oscillations as a correlate of basic homeostatic and motivational processes. *Neuroscience & Biobehavioral Reviews,* 36**,** 677-695.

Koenig, T., Lehmann, D., Saito, N., Kuginuki, T. & Kinoshita, T. 2001. Decreased functional connectivity of EEG theta-frequency activity in first-episode, neuroleptic-naive patients with schizophrenia:preliminary results. *Schizophr Research,* 50**,** 55-60.

Koenig, T., Prichep, L., Dierks, T., Hubl, D., Wahlund, L. O., John, E. R. & Jelic, V. 2005. Decreased EEG synchronization in Alzheimer's disease and mild cognitive impairment. *Neurobiol Aging,* 26**,** 165-71.

Koh, M. J., Seol, J., Kang, J. I., Kim, B. S., Namkoong, K., Chang, J. W. & Kim, S. J. 2017. Altered resting-state functional connectivity in patients with obsessive–compulsive disorder: A magnetoencephalography study. *International Journal of Psychophysiology*.

König, T., Lehmann, D., Saito, N., Kuginuki, T., Kinoshita, T. & KOUKKOU, M. 2001. Decreased functional connectivity of EEG theta-frequency activity in first-episode, neuroleptic-naıve patients with schizophrenia: preliminary results. *Schizophrenia research,* 50**,** 55-60.

Lambertz, M. & Langhorst, P. 1998. Simultaneous changes of rhythmic organization in brainstem neurons, respiration, cardiovascular system and EEG between 0.05 Hz and 0.5 Hz. *Journal of the autonomic nervous system,* 68**,** 58-77.

Lavin, A. & GRACE, A. A. 1996. Physiological properties of rat ventral pallidal neurons recorded intracellularly in vivo. *Journal of neurophysiology,* 75**,** 1432-1443.

Lehmann, D. & C., M. 1990. Intracerebral dipole source localization for FFT power maps *Electroencephalography and Clinical Neurophystology*, 76**,** 271-276.

Leung, L. S. & Yim, C. C. 1993. Rhythmic delta-frequency activities in the nucleus accumbens of anesthetized and freely moving rats. *Canadian journal of physiology and pharmacology,* 71**,** 311-320.

LI, F., Huang, X., Tang, W., Yang, Y., LI, B., Kemp, G. J., Mechelli, A. & GONG, Q. 2014. Multivariate pattern analysis of DTI reveals differential white matter in individuals with obsessive-compulsive disorder. *Human brain mapping,* 35**,** 2643-2651.

Lőrincz, M. L., Kékesi, K. A., Juhász, G., Crunelli, V. & Hughes, S. W. 2009. Temporal framing of thalamic relay-mode firing by phasic inhibition during the alpha rhythm. *Neuron,* 63**,** 683-696.

Lotte, F. 2008. *Study of electroencephalographic signal processing and classification techniques towards the use of brain-computer interfaces in virtual reality applications.* INSA de Rennes.

Machlin, S. R. & Harris, G. J. 1991. Elevated medial-frontal cerebral blood flow in obsessive-compulsive patients: a SPECT study. *The American journal of psychiatry,* 148**,** 1240.

McnallY, R. J. & Kohlbeck, P. A. 1993. Reality monitoring in obsessive-compulsive disorder. *Behaviour Research and Therapy,* 31**,** 249-253.

Menzies, L., Chamberlain, S. R., Laird, A. R., Thelen, S. M., Sahakian, B. J. & Bullmore, E. T. 2008. Integrating evidence from neuroimaging and neuropsychological studies of obsessive-compulsive disorder: the orbitofronto-striatal model revisited. *Neuroscience & Biobehavioral Reviews,* 32**,** 525-549.

Millon, T. & Davis, R. O. 1996. *Disorders of personality: DSM-IV and beyond,* John Wiley & Sons.

Mizuki, Y., Tanaka, M., Isozaki, H., Nishijima, H. & Inanaga, K. 1980. Periodic appearance of theta rhythm in the frontal midline area during performance of a mental task. *Electroencephalography and clinical neurophysiology,* 49**,** 345-351.

Molina, G. N. G., Ebrahimi, T. & Vesin, J.-M. 2003. Joint time-frequency-space classification of EEG in a brain-computer interface application. *EURASIP Journal on Advances in Signal Processing,* 2003**,** 253269.

Mosier, C. I. 1951. I. Problems and designs of cross-validation 1. *Educational and Psychological Measurement,* 11**,** 5-11.

Muller, J. & Roberts, J. E. 2005. Memory and attention in obsessive–compulsive disorder: a review. *Journal of anxiety disorders,* 19**,** 1-28.

Murphy, M., Riedner, B. A., Huber, R., Massimini, M., Ferrarelli, F. & Tononi, G. 2009. Source modeling sleep slow waves. *Proceedings of the National Academy of Sciences,* 106**,** 1608-1613.

Nicolaou, N. & Georgiou, J. 2013. Global field synchrony during general anaesthesia. *British journal of anaesthesia,* 112**,** 529-539.

Olbrich, S., Olbrich, H., Adamaszek, M., Jahn, I., Hegerl, U. & Stengler, K. 2013. Altered EEG lagged coherence during rest in obsessive–compulsive disorder. *Clinical Neurophysiology,* 124**,** 2421-2430.

Organization, W. H. 1993. *The ICD-10 classification of mental and behavioural disorders: diagnostic criteria for research,* World Health Organization.

Organization, W. H. 2001. *The World Health Report 2001: Mental health: new understanding, new hope,* World Health Organization.

Osowski, S., Siwek, K. & Markiewicz, T. Mlp and svm networks-a comparative study. Signal Processing Symposium, 2004. NORSIG 2004. Proceedings of the 6th Nordic, 2004. IEEE, 37-40.

Özçoban, M. A., Aydın, A., Oğuz, T. & Aydin, S. 2017a. Obsesif Kompulsif Bozukluk Hastalarında Klinik Değerlendirme Ölçekleri ile EEG Senkronizasyonu Arasındaki Korelasyon. *Süleyman Demirel Üniversitesi Fen Bilimleri Enstitüsü Dergisi***,** DOI: 10.19113/sdufbed. 47821-Online Yayınlanma: 09.10.2017.

Özçoban, M. A., Tan, O., Aydin, S. & Akan, A. 2017b. Decreased global field synchronization of multichannel frontal EEG measurements in obsessive-compulsive disorders. *Medical & Biological Engineering & Computing***,** 1-8.

Park, Y. M., Che, H. J., Im, C. H., Jung, H. T., Bae, S. M. & Lee, S. H. 2008. Decreased EEG synchronization and its correlation with symptom severity in Alzheimer's disease. *Neurosci Res,* 62**,** 112-7.

Purcell, R., Maruff, P., Kyrios, M. & Pantelis, C. 1998a. Cognitive deficits in obsessive-compulsive disorder on tests of frontal-striatal function. *Biological psychiatry,* 43**,** 348-357.

Purcell, R., Maruff, P., Kyrios, M. & Pantelis, C. 1998b. Neuropsychological deficits in obsessive-compulsive disorder: a comparison with unipolar depression, panic disorder, and normal controls. *Archives of General Psychiatry,* 55**,** 415-423.

Radomsky, A. S. & Rachman, S. 1999. Memory bias in obsessive–compulsive disorder (OCD). *Behaviour Research and Therapy,* 37**,** 605-618.

Rauch, S. L. & Jenike, M. A. 1993. Neurobiological models of obsessive-compulsive disorder. *Psychosomatics,* 34**,** 20-32.

Razumnikova, O. M. 2004. Gender differences in hemispheric organization during divergent thinking: an EEG investigation in human subjects. *Neuroscience Letters,* 362**,** 193-195.

Rihs, T. A., Michel, C. M. & Thut, G. 2007. Mechanisms of selective inhibition in visual spatial attention are indexed by α-band EEG synchronization. *European Journal of Neuroscience,* 25**,** 603-610.

Roehm, D., Schlesewsky, M., Bornkessel, I., Frisch, S. & Haider, H. 2004. Fractionating language comprehension via frequency characteristics of the human EEG. *Neuroreport,* 15**,** 409-412.

Rolls, E. T. 2004. The functions of the orbitofrontal cortex. *Brain and cognition,* 55**,** 11-29.

Rolls, E. T., Hornak, J., Wade, D. & Mcgrath, J. 1994. Emotion-related learning in patients with social and emotional changes associated with frontal lobe damage. *Journal of Neurology, Neurosurgery & Psychiatry,* 57**,** 1518-1524.

Salenius, S. & Hari, R. 2003. Synchronous cortical oscillatory activity during motor action. *Current opinion in neurobiology,* 13**,** 678-684.

Sauseng, P. & Klimesch, W. 2008. What does phase information of oscillatory brain activity tell us about cognitive processes? *Neuroscience & Biobehavioral Reviews,* 32**,** 1001-1013.

Sauseng, P., Klimesch, W., Stadler, W., Schabus, M., Doppelmayr, M., Hanslmayr, S., Gruber, W. R. & Birbaumer, N. 2005. A shift of visual spatial attention is selectively associated with human EEG alpha activity. *European Journal of Neuroscience,* 22**,** 2917-2926.

Saxena, S., Brody, A. L., Ho, M. L., Zohrabi, N., Maidment, K. M. & Baxter JR, L. R. 2003. Differential brain metabolic predictors of response to paroxetine in obsessive-compulsive disorder versus major depression. *American Journal of Psychiatry,* 160**,** 522-532.

Saxena, S. & Rauch, S. L. 2000. Functional neuroimaging and the neuroanatomy of obsessive-compulsive disorder. *Psychiatric Clinics of North America,* 23**,** 563-586.

Schürmann, M., Başar-Eroglu, C., Kolev, V. & Başar, E. 2001. Delta responses and cognitive processing: single-trial evaluations of human visual P300. *International Journal of Psychophysiology,* 39**,** 229-239.

Shipp, M. A., Ross, K. N., Tamayo, P., Weng, A. P., Kutok, J. L., Aguiar, R. C., Gaasenbeek, M., Angelo, M., Reich, M. & Pinkus, G. S. 2002. Diffuse large B-cell lymphoma outcome prediction by gene-expression profiling and supervised machine learning. *Nature medicine,* 8**,** 68-74.

Siapas, A. G., Lubenov, E. V. & Wilson, M. A. 2005. Prefrontal phase locking to hippocampal theta oscillations. *Neuron,* 46**,** 141-151.

Smailovic, U., Koenig, T., Kåreholt, I., Andersson, T., Kramberger, M. G., WINBLAD, B. & JELIC, V. 2018. Quantitative EEG power and synchronization correlate with Alzheimer's disease CSF biomarkers. *Neurobiology of aging,* 63**,** 88-95.

Smith, S.W. (1997) 'The scientist and engineer's guide to digital signal processing'.

Soman, K., Loganathan, R. & Ajay, V. 2009. *Machine learning with SVM and other kernel methods*, PHI Learning Pvt. Ltd.

Steriade, M. 2005. Cellular substrates of brain rhythms. *Electroencephalography: Basic principles, clinical applications, and related fields,* 5**,** 31-83.

Szeszko, P. R., Robinson, D., Alvir, J. M. J., Bilder, R. M., Lencz, T., Ashtari, M., Wu, H. & Bogerts, B. 1999. Orbital frontal and amygdala volume reductions in obsessive-compulsive disorder. *Archives of general psychiatry,* 56**,** 913-919.

Thut, G., Nietzel, A., Brandt, S. A. & Pascual-Leone, A. 2006. α-Band electroencephalographic activity over occipital cortex indexes visuospatial attention bias and predicts visual target detection. *Journal of Neuroscience,* 26**,** 9494-9502.

Tolin, D. F., Abramowitz, J. S., Brigidi, B. D., Amir, N., Street, G. P. & Foa, E. B. 2001. Memory and memory confidence in obsessive–compulsive disorder. *Behaviour research and therapy,* 39**,** 913-927.

Tuna, Ş., Tekcan, A. I. & Topçuoğlu, V. 2005. Memory and metamemory in obsessive–compulsive disorder. *Behaviour Research and Therapy,* 43**,** 15-27.

Valencia, M., Alegre, M., Iriarte, J. & Artieda, J. 2006. High frequency oscillations in the somatosensory evoked potentials (SSEP's) are mainly due to phase-resetting phenomena. *Journal of neuroscience methods,* 154**,** 142-148.

Van Noordt, S., Wu, J., Venkataraman, A., Larson, M. J., South, M. & Crowley, M. J. 2017. Inter-trial coherence of medial frontal theta oscillations linked to differential feedback processing in youth and young adults with autism. *Research in Autism Spectrum Disorders,* 37**,** 1-10.

Vapnik, V. N. & Vapnik, V. 1998. *Statistical learning theory*, Wiley New York.

Velikova, S., Locatelli, M., Insacco, C., Smeraldi, E., Comi, G. & Leocani, L. 2010. Dysfunctional brain circuitry in obsessive–compulsive disorder: source and coherence analysis of EEG rhythms. *Neuroimage,* 49**,** 977-983.

Von Stein, A. & Sarnthein, J. 2000. Different frequencies for different scales of cortical integration: from local gamma to long range alpha/theta synchronization. *International Journal of Psychophysiology,* 38**,** 301-313.

Waxman, S. G. 2010. *Clinical neuroanatomy*, McGraw Hill.

Weber, A. M., Soreni, N. & Noseworthy, M. D. 2014. A preliminary study of functional connectivity of medication naïve children with obsessive–compulsive disorder. *Progress in Neuro-Psychopharmacology and Biological Psychiatry,* 53**,** 129-136.

Whiteside, S. P., Port, J. D. & Abramowitz, J. S. 2004. A meta–analysis of functional neuroimaging in obsessive–compulsive disorder. *Psychiatry Research: Neuroimaging,* 132**,** 69-79.

Williams, J. B. 1988. A structured interview guide for the Hamilton Depression Rating Scale. *Archives of general psychiatry,* 45**,** 742-747.

Wise, S. P. & Rapoport, J. L. 1989. Obsessive-compulsive disorder: is it basal ganglia dysfunction. *Obsessive-compulsive disorder in children and adolescents***,** 327-44.

Worden, M. S., Foxe, J. J., Wang, N. & Simpson, G. V. 2000. Anticipatory biasing of visuospatial attention indexed by retinotopically specific-band electroencephalography increases over occipital cortex. *J Neurosci,* 20**,** 1-6.

Wróbel, A., Ghazaryan, A., Bekisz, M., Bogdan, W. & Kamiński, J. 2007. Two streams of attention-dependent β activity in the striate recipient zone of cat's lateral posterior–pulvinar complex. *Journal of Neuroscience,* 27**,** 2230-2240.

Zhang, Y. D., Chen, S., Wang, S. H., Yang, J. F. & Phillips, P. 2015. Magnetic resonance brain image classification based on weighted-type fractional Fourier transform and nonparallel support vector machine. *International Journal of Imaging Systems and Technology,* 25**,** 317-327.

CURRICULUM VITAE

Personal Information	
Name Surname	Mehmet Akif ÖZÇOBAN
Place of Birth	Gaziantep
Date of Birth	December 1983
Nationality	☑ T.C. ❒ Other:
Phone Number	02165958717
Email	mehmetakifozcoban@gmail.com
Web Page	

Educational Information	
B. Sc.	
University	Erciyes University
Faculty	Engineering
Department	Electrical and Electronic
Graduation Year	2007

M. Sc.	
University	Erciyes University
Institute	Institute of Graduate Studies in Science and Engineering
Department	Department of Biomedical Engineering
Programme	Biomedical Engineering Programme
Graduation Year	2010

Ph. D.	
University	İstanbul University
Institute	Institute of Graduate Studies in Science and Engineering
Department	Department of Biomedical Engineering
Programme	Biomedical Engineering Programme
Graduation Year	2018

Publications
Özçoban, M. A., Aydın, A., Oğuz, T. & Aydin, S. 2017a. Obsesif Kompulsif Bozukluk Hastalarında Klinik Değerlendirme Ölçekleri ile EEG Senkronizasyonu Arasındaki Korelasyon. *Süleyman Demirel Üniversitesi Fen Bilimleri Enstitüsü Dergisi***,** DOI: 10.19113/sdufbed. 47821-Online Yayınlanma: 09.10. 2017.

Özçoban, M. A., Tan, O., Aydin, S. & Akan, A. 2017b. Decreased global field synchronization of multichannel frontal EEG measurements in obsessive-compulsive disorders. *Medical & Biological Engineering & Computing***,** 1-8.

Ozcoban, M. A., Kara, S., Tan, O. & Aydin, S. Investigation the level of neural synchronization by using global field synchronization method in Obsessive Compulsive Disorder. *Biomedical Engineering Meeting* (BIYOMUT), 2014 18th National, 2014. IEEE, 1-3.

Özçoban, M. A., Aydın, S., KARA, S. & TAN, O. 2015. Obsesif Kompülsif Bozukluğun EEG Ölçümüne Dayalı Fourier Dipol Yaklaşımı Yöntemi ile İncelenmesi Investigation of Obsessive Compulsive Disorder with FFT Dipol Approximation by Means of EEG. *Vogue,* 15.

Özçoban, M. A., Latifoglu, F., Ülgen, A. & Asyalı, M. H. Monitoring the body water exchange using dielectric permeability method. *Biomedical Engineering Meeting* (BIYOMUT), 2010 15th National, 2010. IEEE, 1-3.

Tan, O., Özçoban, M. A. & Aydın, S. 1. Nöropsikiyatri Sağlık, Uygulama ve Araştırma Hastanesi, Üsküdar Üniversitesi, İstanbul, Türkiye.